

**The author(s) shown below used Federal funds provided by the U.S. Department of Justice and prepared the following final report:**

**Document Title: Validation of Forensic Characterization and Chemical Identification of Dyes Extracted from Millimeter-length Fibers**

**Author(s): Stephen L. Morgan, Ph.D.**

**Document No.: 248579**

**Date Received: January 2015**

**Award Number: 2010-DN-BX-K245**

**This report has not been published by the U.S. Department of Justice. To provide better customer service, NCJRS has made this Federally-funded grant report available electronically.**

**Opinions or points of view expressed are those of the author(s) and do not necessarily reflect the official position or policies of the U.S. Department of Justice.**

## FINAL REPORT

**Federal Agency and Organization Element to Which Report is Submitted:**

U. S. Department of Justice, National Institute of Justice

**Federal Grant or Other Identifying Number Assigned by Agency:**

NIJ award number NIJ Award 2010-DN-BX-K245

**Project Title:**

Validation of Forensic Characterization and Chemical Identification  
of Dyes Extracted from Millimeter-length Fibers

**PI Name, Title and Contact Information (e-mail address and phone number):**

Dr. Stephen L. Morgan, Professor  
Department of Chemistry and Biochemistry, 631 Sumter Street,  
University of South Carolina, Columbia, SC 29208  
Voice: 803.777.2461, FAX: 803.777.9521  
Email: [morgansl@mailbox.sc.edu](mailto:morgansl@mailbox.sc.edu)

**Administrative Point Of Contact:**

Lumi Bakos, Administrator  
Sponsored Awards Management  
1600 Hampton Street, 4<sup>th</sup> Floor  
Columbia, SC 29208 University of South Carolina, Columbia, SC 29208  
Voice: 803.777.2274, FAX: 803.777.4136  
Email: [bakos@mailbox.sc.edu](mailto:bakos@mailbox.sc.edu)

**Submission Date:**

29 September 2014

**DUNS and EIN Numbers:**

DUNS number 11-131-0249  
EIN number 57-0967350

**Recipient Organization (Name and Address):**

South Carolina Research Foundation,  
1600 Hampton Street, Columbia, SC 29208

**Project/Grant Period (Start Date, End Date):**

1 October 2007-30 June 2014

## Abstract

The objective of the research described here the development and validation of methods for the forensic chemical characterization of dyes extracted from trace evidence fibers. If the chemical composition of dye formulations on trace fibers can be reliably profiled by liquid chromatography, match exclusions can be made with higher reliability, and results will have a solid scientific basis and increased practical significance. Separation and detection of individual dye components provides a qualitative and semi-quantitative fiber dye 'fingerprint' that characterizes the number and relative amounts of dyes present. Chemical identity of extracted dyes can be inferred from liquid chromatography (LC) retention time matching of dye peaks, comparison of UV/visible spectra of the separated dye components, and from molecular weight determination and structural analysis by mass spectrometry. A significant challenge is that such analyses are destructive to the fiber evidence. We have achieved lower limits of detection (low ppb levels) for reliable analysis of single fibers that are 15-25  $\mu\text{m}$  and 0.5 mm, respectively in diameter and length. Larger samples allow multiple for validation or independent analysis

We have developed extraction protocols for (basic) dyes on acrylic, (direct, reactive, and vat) dyes on cotton, (acid) dyes on nylon, and disperse dyes on polyester that are compatible with subsequent liquid chromatographic analysis. Because these dye types adhere to different polymers by varying mechanisms, methods must be individually designed to disrupt those mechanisms and provide efficient extraction. A single gradient-based ultra-performance UPLC method has been developed for simultaneous separation of basic dyes on acrylic fibers, acidic dyes on nylon fibers, and disperse dyes on polyester fibers; this method avoids using different chromatographic conditions for these dyes and increases sample throughput. Due to cotton's high prevalence in casework, improved extraction methods for the analysis of direct, and reactive dyes on cotton were also developed. We also report the detection of fiber dyes and finishing agents extracted from fibers taken from fabrics subjected to outdoor weathering conditions for up to 12 months.

Microextraction, followed by ultra-performance liquid chromatography, can distinguish similar fibers containing different, but similar, dyes with the combination of retention time matching, UV/visible spectral comparison, and structural analysis by mass spectrometry. The analysis of cotton fibers is challenging because they can be dyed with three different classes of dye, each requiring a different method for extraction and analysis. This work focuses on the chemistries of direct dyes and indigo and their optimum extraction conditions and chromatographic methods. We have successfully extracted direct dyes from cotton fibers as small as 1 mm in length and have quantitated dye amounts by UPLC with UV/visible detection. Analytical figures of merit and validation statistics, including extraction reproducibility, linearity, limits of detection and quantitation, and precision, are reported.

Validation practices for calibration based on forensic and international standards have been employed in this work. Issues that have been addressed with respect to estimation of limits of detection (LOD) include: (a) rational choices of measurement uncertainty are important for valid estimates of LOD ; (b) reporting a range of multiple types of decision limits (limit of detection, minimum consistently detectable amount, limit of detection based on statistical tolerance intervals) provides a stronger statistical basis for specification and control of false positive and false negative detection probabilities; (c) use of Mandel sensitivity, which is independent of the scale in which measurements are expressed, and thus is a useful tool for comparisons of variability between different analytical methods.

## Table of contents

Title page, technical contact and administrative contact information	page 1
Abstract	2
Table of contents	3
Executive summary	4
Technical report	14
A. Comprehensive screening of acid, basic, and disperse dyes extracted from millimeter-length trace evidence fibers by ultra-performance liquid chromatography: methodology and figures of merit	14
B. Extraction of direct dyes and indigo vat dye from trace cotton fibers for forensic characterization by ultra-performance liquid chromatography	42
C. Extraction and characterization of reactive dyes and their hydrolysis products from trace cotton fibers by ultra-performance liquid chromatography	57
D. Forensic analysis of fluorescent brighteners, dyes and textile fiber degradation by capillary electrophoresis, liquid chromatography/mass spectrometry, and ultra performance liquid chromatography	78
E. Mandel sensitivity applied to analytical method performance comparisons and limits of detection	95
F. Limits of detection from the viewpoint of statistical hypothesis testing	106
Overall Results	133
Conclusions	134
1. Discussion of findings	134
2. Implications for policy and practice	135
3. Implications for further research	137
4. Dissemination of research findings	138

## EXECUTIVE SUMMARY

The research objective of this project was to develop and validate analytical chemical methods using ultra performance liquid chromatography (UPLC) for the comprehensive analysis of textile dyes on the four most common types of textile fibers found in practice: acrylic, cotton, polyester, and nylon.

Forensic fiber examinations involve comparison of questioned fibers with one or more known fibers to determine possible associations between victims, suspects, and crime scenes. Initial steps in fiber comparison involve microscopic examination. Polymer type can be established by refractive index measurements or by infrared (IR) spectroscopy and UV/visible or fluorescence micro spectrophotometry may show differences or confirm similarities among questioned and known fibers. However, trace evidence fibers, as well as the dyes that produce color on fibers, are class evidence; because these items mass produced, they may share common characteristics. Establishing a scientific basis for unique matches among questioned and known fibers is difficult.

Trace fiber evidence has been probative in cases ranging from the 1963 JFK assassination,<sup>1</sup> to the Atlanta Child murders<sup>2</sup> of the early 1980s, and the 2002 Washington, DC, sniper case.<sup>3</sup> The fiber examiner typically performs a series of comparisons of the questioned fiber to a known fiber in an attempt to exclude the possibility that a ‘questioned’ fiber and ‘known’ fiber could have originated from a common source. If the two fibers can be shown to be substantially different, then the hypothesis that the two fibers originated from a common source can be discounted. The comparison of an ‘unknown’ to a ‘known’ fiber is illustrated by the testimony of FBI fiber examiner Paul Stombaugh before the Warren Commission.<sup>1</sup> A tuft of fibers that appeared to match fibers from Oswald’s shirt was found caught on a jagged edge of Oswald’s rifle stock. Stombaugh testified “there is no doubt in my mind that these fibers could have come from this shirt. There is no way, however, to eliminate the possibility of the fibers having come from another identical shirt.” Whenever the hypothesis of a common source for two fibers cannot be rejected, evidence may have probative value, and investigative leads could evolve from the suggested association between victim and suspect. The history of fiber examinations is characterized by a search for increased discrimination to render trace evidence more specific and discriminating. Significance of fiber evidence and discrimination are expanded by combinatorial possibilities of fiber types and dyes.<sup>4-9</sup> If dye formulations on trace fibers can be reliably profiled at trace levels, match exclusions can be made with higher reliability, and “results consistent with” will have increased significance. Separation and detection of individual dye components provides a qualitative and semi-quantitative fiber dye ‘fingerprint.’ Determining the number and relative amounts of dyes present, and characterizing those dyes at the molecular level by UV/visible absorbance and MS, offers an entirely new level of discrimination. Such information may also open the possibility of tracing specific dye formulations to the dye manufacturer.

Our work has focused on manufactured fibers (nylon, acrylic, and polyester), and the natural fiber, cotton, because of their prevalence in case work.<sup>10,11</sup> Understanding the chemistry and industrial processes involving fibers and dyes is a starting point for design of extraction methods, for developing improved analysis methods, and for correct data interpretation.<sup>4,12</sup> In manufacturing, raw fibers are treated to remove contaminants and lubricants, or to change morphology; fabrics may be bleached; cotton is mercerized to change its morphology and increase dye uptake; nylon and polyester are heat-set to stabilize distortion and to improve

dyeability. Fabrics may be flame-treated to remove surface fuzz, or desized by enzymes to remove weaving aids (*e.g.*, lubricants). Fibers are dyed with processes appropriate for their chemistry (acid dyes, basic dyes, direct dyes, azoic dyes, mordant dyes, sulfur dyes, vat dyes, reactive dyes, disperse dyes, and pigments). Dyes may be loosely associated with fibers (direct dyes on cotton are held by Van der Waals forces and hydrogen bonding), bound by salt linkages (acid dyes on nylon, basic dyes on acrylic), or covalently bonded (reactive dyes on cotton). Dyes may be dispersed through the fiber (*e.g.*, on polyester), mechanically trapped through redox processes (vat dyes on cotton), applied during melt spinning (pigment coloration of nylon, polyolefins, and polyester), or adhered to surfaces with adhesives (pigment dyeing of bedding and apparel fabrics). Fabrics are often finished to impart aesthetic and performance properties, such as stay-press finishing and water-proofing. Preprocessing, dyeing, and finishing all may leave residues on fibers that are useful for discrimination.

Dyes are conjugated molecules, generally consisting of aromatic and/or unsaturated compounds that are either derived from natural sources or are made synthetically. Dyes are often classified according to their application method (*e.g.*, reactive, disperse, and vat) and their chemical constitution (*e.g.*, azo, anthraquinone, metal complex azo). Knowledge of the chemistry of both fibers and dyes is relevant to the extraction of dyes from fibers and to development of appropriate methods of analysis. To extract dye from fiber, the dye's substantivity for the fiber (affinity via intermolecular interactions) must be reduced, then the dye is solvated and transported from the fiber into the extractant. Wiggins<sup>13</sup> summarized solvents for dye extraction. Thin layer chromatography (TLC) of dyes has been widely used in forensic labs.<sup>4-6,13-27</sup> Gaudette<sup>14</sup> mentions that some dyes on 2 mm fibers can be analyzed by TLC, but light-colored fibers may require more than 100× that length. Of 64 fibers listed by polymers, dyes, and color intensities, only 17% of those fibers could be analyzed at 2 mm lengths, 30% at 5 mm, and 61% at 10 mm. For applicability to casework relevant sample sizes, optimizing extraction protocols is critical.

Stefan, *et al.* and Dockery, *et al.* employed experimental design<sup>30-33</sup> to optimize extraction of acid dyes on nylon, basic dyes on acrylic, disperse dyes on polyester, and direct, reactive, and indigo vat dyes on cotton. As an example, with acid dyes on nylon, 10 mixtures of water:pyridine:aqueous ammonia were prepared in duplicate by a laboratory robot, in vials on a 96-well plate. Identical 10-cm fibers were extracted and the absorbance of extracts were measured by a plate reader.<sup>30</sup> In the fitted model, a diagonal ridge of high extraction response runs across the surface from 50:50 pyridine:water to 50 :50 pyridine/ammonia. Of the pure solvents, water gives the best extraction, although the amount of dye extracted is low. Pyridine does not dissolve the dye completely; the solubility of the dye in water is four times higher than that in pyridine. However, pure water is not sufficiently basic to deprotonate the nylon amine end groups and to release acid dyes completely from nylon. Although aqueous ammonia dissolves acid dyes better than does pure pyridine, aqueous ammonia lacks the organic content necessary to fully extract the organic anions of acid dyes. The diagonal ridge runs across the ternary solvent triangle at constant pyridine content of about 45-50%. For extraction of the anthraquinone Acid Blue 45 dye from nylon, the predicted optimum is at a solvent composition of 42% pyridine/58% water. These extraction conditions were confirmed for two other subclasses of acid dyes (azo, and metal complex azo dyes) and produce complete extraction of the tested dyes.<sup>30</sup> All extraction protocols that we have developed can be done in reasonable times (30-60 min, even if done manually).

Liquid chromatography (LC), capillary electrophoresis (CE), and mass spectrometry (MS) are established in applications from drug identification to DNA analysis and forensic toxicology. CE and LC methods offer efficiency, selectivity, short analysis time, low organic solvent consumption, low required sample, and relatively low running costs. CE is well suited for dye analysis because many dyes are ionized, depending on their  $pK_a$  and buffer solution pH, however a comprehensive separation method by CE is problematic due to a number of non-ionizable dyes (disperse dyes on polyester, vat dyes on cotton). Modern LC is theoretically superior to CE because dye species need not be ionic or ionizable, and offers mobile and stationary phase tunability. Sirén and Sulkava<sup>34</sup> used CE and UV/visible diode array detection (DAD) for analysis of black dyes from cotton and wool fibers. Xu, *et al.*<sup>35</sup> employed CE to separate reactive, acid, direct, azoic and metal complex dyes extracted from cotton, wool, polyacrylic, polyester, and polyamide fibers; sample stacking was used to improve detection limits. Environmental or industrial applications dominate the dye extract analysis literature.<sup>36-47</sup>

Minor peaks are often observed in separations of dye extracts using any separation technique. These contaminants in the “pure” dyestuffs and side products from incomplete dye synthesis may be signatures of the manufacturing process. Purified component dyes are neither required nor economically feasible on a commercial scale as long as the dyes possess the desired properties. Whether patterns of trace contaminants can be related to manufacturing processes is worth investigating in discussions with industrial manufacturers. However, whether such trace patterns can be reliably used to associate a fiber with a manufacturer is unlikely. The relative amounts of dyes can be correlated with the quantitative dye formulation from the manufacturer might be of forensic significance, if such information were obtainable. Additionally, environmental changes associated with a questioned fiber could affect the quality of such information for comparative purposes.

Ultra-violet (UV) and/or visible detection of dyes from short single fiber lengths can be difficult. One cm of nylon fiber dyed with commercial levels of an acid dye was extracted with 60:40 water:pyridine and the extract was dried down and reconstituted with 190  $\mu$ L of water prior to CE injection. The absorbance of 3 mAU at the peak maximum produced unreliable spectra. Wheals, *et al.*<sup>49</sup> reported HPLC detection limits of 200 pg/dye, but also found that extracts of short fibers of light shades often yielded insufficient dye. Minor dye components sometimes discriminated fibers even when major components were indistinguishable. Laing, *et al.*<sup>50</sup> analyzed acid dyes by LC with UV/visible detection, but did not show analysis of very short fibers. The target size for forensically relevant fibers derives in part from fiber examinations and population studies reporting that recovered fibers are often as small as 2 mm in length, depending on the degree of dyeing.<sup>50-52</sup> Clearly, methods for the analysis of dyes extracted from fibers require high sensitivity for applicability to forensic casework. Other studies have also reported that UV/visible detection provides neither sufficient sensitivity, nor discrimination, for analysis of trace fiber extracts from structurally-related dyes.<sup>53-58</sup>

LC-MS, and more often LC-MS/MS, is the benchmark analytical approach for chemical quantitation in virtually all biological fluids. Analysis of dye extracted from single fibers of 2-10 mm in length has been achieved by Xu, *et al.*<sup>55</sup> by sample-induced isotachopheresis with micellar electrokinetic capillary chromatography, by Tuinman, *et al.*<sup>56</sup> who directly infused dyes into electrospray MS, and by other researchers with LC or CE coupled to MS.<sup>30-33,48,53-58</sup> Huang, *et al.*<sup>57</sup> demonstrated LC-MS identification of dyes with 22 reference dyes and 10 dyes extracted from fibers. Significantly, this paper showed MS discrimination of dyes that were not reliably

identified by high performance LC (HPLC) with UV/visible detection.<sup>58</sup> Pawlak, *et al.* used HPLC-MS to successfully identify several natural blue dye compounds from a tapestry fiber and concluded that several compounds exhibited complex fragmentation patterns due to chromatographic conditions using electrospray ionization (ESI)-MS.<sup>59</sup> Zhang, *et al.* investigated alternative methods to HCl extraction for six flavonoid and mordant dyes on silk and used HPLC/ESI-MS to identify and quantify extracts for comparison.<sup>60</sup> ESI appears to be the ionization method of choice for most dye classes, however Szostek, *et al.* reported difficulty in ionizing indigotin and brominated indigotin dyes by ESI but demonstrated successful ionization using atmospheric pressure chemical ionization) APCI.<sup>61</sup> Several wool dyes were extracted from historic textiles and analyzed using HPLC and tandem ESI-MS (ion trap MS-MS) by Petroviciu, *et al.* who also noted that most MS literature on dyes focuses on molecular ion identification, and highlighted the importance of the availability of standards to build databases for unambiguous dye identification.<sup>62</sup> The importance of method optimization for fiber extract analysis was highlighted by Rafaëly, *et al.* who cited the challenges of small extract quantities and commercial availability of dyestuff standards. They concluded that the superior sensitivity and structural elucidation properties of MS were sufficient to overcome low concentrations of extracts.<sup>63</sup>

Conventional HPLC uses 4-5 mm ID columns of 10-25 cm length; injected dyes are diluted by band broadening and relatively large samples are needed. Only a small number of papers in the forensic literature have applied HPLC to dye extracts. Laing, *et al.* used diode array detection for LC analysis of acid dyes.<sup>64</sup> Ultra-performance liquid chromatography (UPLC), introduced commercially in 2004-2005, uses high pressures (>10,000 psi), smaller column particles (<2 µm), short columns (~5 cm), and minimal sample (~100 µL) to obtain high speed, resolution, and sensitivity. UPLC has rapidly become an established, especially in areas requiring sample throughput (speed of analysis) and high resolution. Decreasing column particle size allows for columns to be packed tighter and more uniformly, resulting in reduced band broadening due to eddy diffusion. Smaller particles also provide a shorter pathway into and out of the stationary phase, yielding less band broadening due to mass transfer. Using small particle columns of shorter column length reduces band broadening due to longitudinal diffusion within the column. Together, these three factors produce increased plate count and flatten the van Deemter curve at high flow rates. As a result, UPLC chromatographic peaks are narrower, and flow rates can be effectively doubled over that in HPLC columns by using particles 1-5 µ in size without incurring band broadening and decreased resolution, thus achieving faster separation times. Use of small UPLC particle sizes requires the high pressures to achieve flow through packed columns.

Compared to HPLC separations, UPLC separations produce a narrower, and more concentrated, analyte band allowing for lower limit of detection (LD) by UV/visible analysis. A comparison of detection limits of several food dyes characterized by HPLC and UPLC (both with UV/visible detection shows similar detection limits at first glance, however the required injection volume to achieve these levels by HPLC was 20 µL versus 3 µL for UPLC.<sup>65,66</sup> These results are summarized in Table 1.1.

The HPLC UV/visible literature for dye analysis is abundant with refined analysis techniques, but literature for UPLC-DAD of dyes is underdeveloped at the moment. Achieving comparable limits of detection at lower injection volumes by UPLC suggests the possibility of lowering those limits through higher volume injections and method optimization. UPLC-DAD limits of detection for food dyes were reported by Ji, *et al.* to range from 88 to 21 pg. They also reported

that LD values using UPLC-MS/MS for Tartrazine, Amaranth, Indigo Carmine, Allura Red AC, and Sunset Yellow FCF are high than LDs determined by UV/visible detection.<sup>65</sup>

A search on *Science Direct* (only Elsevier journals) found 1,334 articles on UPLC, most of which involved biomedical and environmental applications; forensic applications of UPLC were targeted mostly in toxicology and drug identification. These applications typically report UPLC/MS analysis times of 30 s to 1-3 min, and detection limits in the range of pg of analyte injected. For example, UPLC (time-of-flight) TOF-MS was used to analyze liver blood from a poisoning case involving Bromo-Dragonfly drug.<sup>67</sup> Another forensic application involved post-mortem analysis of ethyl glucuronide (EtG) as an alcohol metabolite in hair; with an evaporative light scattering detector, levels of EtG at just above 30 pg/mg were detected.<sup>68</sup> A review of applications of LC/MS, including some UPLC discussion, was published by Wood, *et al.*<sup>69</sup>

The development and validation of reliable microextraction protocols followed by sensitive trace analyses by chromatography and mass spectrometry is the subject of the research presented in this report. The main body of the technical report documents accomplishments, methodology, and data from the project. In summary, methodology for the microextraction of basic dyes on acrylic, acid dyes on nylon, disperse dyes on polyester, and reactive dyes, direct dyes, and indigo on cotton textile fibers is reported. The analysis of cotton fibers is challenging because they can be dyed with three different classes of dye, each requiring a different method for extraction and analysis. Reactive dyes present a unique challenge because they are chemically bound to the cellulose structure of the fiber. Release of these dyes from cotton requires breaking of the covalent bond using hot sodium hydroxide. The resulting hydrolysis reactions can also cleave amide bonds and possibly other chemical bonds in the dye molecule. The various structural changes that can take place leads, in many cases, to production of multiple reaction products from a single dye. We demonstrate successful extraction of reactive dyes from single 1 mm cotton fibers with detection limits as low as 3.3 pg. Systematic experiments at varying reaction conditions, with product analysis by MS, were also performed to characterize the degradation of reactive dyes under hydrolysis, and to facilitate interpretation of reactive dye extractions.

Extraction methods developed for basic dyes on acrylic, acid dyes on nylon, and disperse dyes on polyester fibers involve extraction with solvents that do not affect the chemical composition of the polymer, and thus do not impose limitations on use of the fiber for further examinations. With these fibers, IR can be conducted on previously extracted samples if needed. Reactive dye extraction from cotton requires base hydrolysis with sodium hydroxide which can change the chemical form of the dye and modify the fiber polymer chemistry; strongly alkaline solutions are also not compatible with C18 stationary phases for liquid chromatography. Previous research employed 1.5% NaOH which does cause damage. In this work, 0.1875 M sodium hydroxide was employed and the resulting chromatograms showed no evidence of chemical products from cellulose.

Although these processes are destructive to the fiber evidence, the ability to analyze dye extracts from sub-millimeter fiber lengths of single fibers, coupled with detection limits in the hundred picogram range by ultra-performance liquid chromatography (UPLC) with both diode array detection (DAD) and tandem mass spectrometry (MS-MS) makes routine forensic characterization feasible. Microextraction, followed by UPLC, can often distinguish similar fibers containing different, but similar, dyes with the combination of retention time matching, UV/visible spectral comparison, and structural analysis by mass spectrometry. This work focuses on determining the optimum extraction conditions for each dye class and developing

chromatographic methods with suitable resolution and sensitivity for trace analysis. Analysis of fibers as small as 1 mm in length is the target sample size to minimize destruction of fiber evidence. Analytical figures of merit and validation statistics, including extraction reproducibility, measures of calibration performance, linearity, limits of detection and quantitation, and precision, are reported. Modern instrumental analysis of separated dye components can increase the reliability of fiber examinations by providing discriminating information on dye characterization and possibly identification of dyes at the molecular level from trace evidence fibers as small as 0.5 mm.

## REFERENCES

- (1) *The Warren Commission Report*. St. Martin's Press, New York, 1964; p. 592.
- (2) Deadman, H. *Fiber evidence and the Wayne Williams trial*, US Government Document J1.14/8a:F44, Federal Bureau of Investigation, US Department of Justice, FBI Law Enforcement Bulletin, March and May, 1984.
- (3) Oien, C. T. *Case management issues from crime scene to courtroom*. Trace Evidence Symposium, Clearwater, FL, 2007 [URL: <http://nfstc.org/projects/trace/>].
- (4) Robertson J.; Grieve, M., Eds., *Forensic Examination of Fibres*. 2nd edition. London: Taylor & Francis: 1999.
- (5) Eyring, M. B.; Gaudette, B. D. An introduction to the forensic aspects of textile fiber examinations. Chapter 6 in: *Forensic Science Handbook*, vol. 2, R. Saferstein, Ed.; Prentice Hall: Englewood Cliffs, NJ, 2005.
- (6) Grieve, M. Interpretation of fibres evidence. Chapter 13 in: *Forensic Examination of Fibres*, 2nd edition, Robertson J.; Grieve, M., Eds.; Taylor & Francis: London, 1999.
- (7) Wiggins, K.G.; Cook, R.; Turner, Y.J. Dye batch variation in textile fibers. *J. Forensic Sci.* **1988**, *33*, 998-1007.
- (8) Wiggins, K.; Holness, J. A further study of dye batch variation in textile and carpet fibres. *Science & Justice* **2005**, *45*, 93-96.
- (9) National Research Council of the National Academies. *Forensic Analysis: Weighing Bullet Lead Evidence*. The National Academies Press: Washington, DC, 2004.
- (10) Rendle, D. F.; Wiggins, K. G. Forensic analysis of textile fibre dyes. *Review of Progress in Coloration and Related Topics* **1995**, *25*, 29-34.
- (11) Webb-Salter, M.; Wiggins, K. G. Aids to Interpretation, in: *Forensic Examination of Fibres*. 2nd edition, J. Robertson, M. Grieve, Eds., Taylor & Francis: London, 1999; pp. 364-378.
- (12) Needles, H. L. *Textile Fibers, Dyes, Finishes, and Processes: A Concise Guide*. Noyes Publications: Park Ridge, NJ, 1986.
- (13) Wiggins, K. G. Thin layer chromatographic analysis for fibre dyes. Chapter 11 in: *Forensic Examination of Fibres*, 2nd edition, Robertson J.; Grieve, M., Eds.; Taylor & Francis: London, 1999.
- (14) Gaudette, B. D. The forensic aspects of textile fiber examination. Chapter 5 in: *Forensic Science Handbook*, vol. 2, R. Saferstein, Ed.; Prentice Hall: Englewood Cliffs, NJ, 1988.
- (15) Macrae, R.; Dudley, R. J.; Smalldon, K. W. The characterization of dyestuffs on wool fibers with special reference to microspectrophotometry. *J. Forensic Sci.* **1979**, *24*, 117-129.
- (16) Resua, R. A semi-micro technique for the extraction and comparison of dyes in textile fibers. *J. Forensic Sci.* **1980**, *25*, 168-173.
- (17) Shaw, I. C. Micro-scale thin-layer chromatographic method for the comparison of dyes stripped from wool fibers. *Analyst* **1980**, *105*, 729-730.

- (18) Home, J. M.; Dudley, R. J. Thin-layer chromatography of dyes extracted from cellulosic fibers. *Forensic Sci.Int.* **1981**, *17*, 71-78.
- (19) Beattie, B.; Roberts, H.; Dudley, R. J. The extraction and classification of dyes from cellulose acetate fibers. *J. Forensic Sci. Soc.* **1981**, *21*, 233-237.
- (20) Hartshorne, A. W.; Laing, D. K. The dye classification and discrimination of colored polypropylene fibers. *Forensic Sci.Int.* **1984**, *25*, 133-141.
- (21) Wiggins, K. G.; Crabtree, S. R.; March, B. M. The importance of thin layer chromatography in the analysis of reactive dyes released from wool fibers. *J. Forensic Sci.* **1996**, *41*, 1042-1045.
- (22) Laing, D. K.; Boughey, L.; Hartshorne, A. W. The standardization of thin layer chromatographic systems for comparison of fiber dyes. *J. Forensic Sci. Soc.* **1990**, *30*, 299-307.
- (23) Laing, D. K.; Hartshorne, A. W.; Bennett, D. C. Thin layer chromatography of azoic dyes extracted from cotton fibers. *J. Forensic Sci. Soc.* **1990**, *30*, 309-315.
- (24) Rendle, D. F.; Wiggins, K. G. Forensic analysis of textile fibre dyes. *Review of Progress in Coloration and Related Topics* **1995**, *25*, 29-34.
- (25) Rendle, D. F.; Crabtree, S. R.; Wiggins, K. G.; Salter, M. T. Cellulase Digestion of Cotton Dyed with Reactive Dyes and Analysis of the Products by Thin-Layer Chromatography. *J. Soc. Dye. Colour* **1994**, *110*, 338-341.
- (26) Crabtree, S. R.; Rendle, D. F.; Wiggins, K. G.; Salter, M. T. The Release of Reactive Dyes from Wool Fibers by Alkaline- Hydrolysis and Their Analysis by Thin-Layer Chromatography. *J. Soc. Dye. Colour* **1995**, *111*, 100-102.
- (27) Beattie, I.B.; Dudley, R.J.; Smalldon, K.W. The extraction and classification of dyes on single nylon, polyacrylonitrile and polyester fibers. *J. Soc. Dye. Colour* **1979**, *95*, 295-302.
- (28) Smith, W. F. *Experimental Design for Formulation*. Cambridge University Press: New York, 2005.
- (29) Deming, S. N.; Morgan, S. L. *Experimental Design: A Chemometric Approach*, 2nd ed. Elsevier Science Publishers: Amsterdam, 1993.
- (30) Stefan, A. R., Dockery C. R., Nieuwland, A. A., Roberson, S. N., Baguley, B. M., Hendrix, J. E., Morgan, S. L. Forensic analysis of anthraquinone, azo, and metal complex acid dyes from nylon fibers by micro-extraction and capillary electrophoresis. *Anal. Bioanal. Chem.* **2009**, *394*, 2077-2085.
- (31) Stefan, A. R., Dockery, C. R., Baguley, B.M., Vann, B. C., Nieuwland, A. A., Hendrix, J. E., Morgan, S. L. Microextraction, capillary electrophoresis, and mass spectrometry for forensic analysis of azo and methine basic dyes from acrylic fibers. *Anal. Bioanal. Chem.* **2009**, *394*, 2087-2094.
- (32) Hartzell-Baguley, B.; Stefan, A. R.; Dockery, C. R.; Hendrix, J. E.; Morgan, S. L. Non-aqueous capillary electrophoresis of azo and anthraquinone disperse dyes extracted from polyester fibers for forensic analysis. *Anal. Bioanal. Chem.*, **2009**, unpublished manuscript.
- (33) Dockery C. R., Stefan, A. R., Nieuwland, A. A., Roberson, S. N., Baguley, B.M., Hendrix, J. E., Morgan, S. L. Automated extraction of direct, reactive, and vat dyes from cellulosic fibers for forensic analysis by capillary electrophoresis. *Anal. Bioanal. Chem.* **2009**, *394*, 2095-2103.
- (34) Sirén, H.; Sulkava, R. Determination of black dyes from cotton and wool fibers by capillary zone electrophoresis with UV detection: application of marker technique. *J. Chromatogr. A* **1995**, *717*, 149-155.

- (35) Xu, X.; Leijenhorst, H.; Van den Hoven, P.; De Koeijer, J.A.; Logtenberg, H. Analysis of single textile fibres by sample-induced isotachopheresis-micellar electrokinetic capillary chromatography. *Sci. Justice* **2001**, *41*, 93-105.
- (36) Croft, S.N.; Lewis, D.M. Analysis of reactive dyes and related derivatives using high-performance capillary electrophoresis. *Dyes and Pigm.* **1992**, *18*, 309-317.
- (37) Croft, S.N.; Hinks, D. Analysis of dyes by capillary electrophoresis. *Textile Chemist and Colorist* **1993**, *25*, 47-51.
- (38) Burkinshaw, S.M.; Hinks, D.; Lewis, D.M. Capillary zone electrophoresis in the analysis of dyes and other compounds employed in the dye-manufacturing and dye-using industries. *J. Chromatogr. A* **1993**, *640*, 413-417.
- (39) Burkinshaw, S.M.; Hinks, D.; Lewis, D.M. The use of capillary electrophoresis for the analysis of several dye classes. In: Special Publication - *Royal Society of Chemistry* **1993**, *122*, 93-100.
- (40) Croft, S.N.; Hinks, D. Analysis of dyes by capillary electrophoresis. *J. Soc. Dye. Colour* **1992**, *108*, 546-551.
- (41) Takeda, S.; Tanaka, Y.; Nishimura, Y.; Yamane, M.; Siroma, Z.; Wakida, S. Analysis of dyestuff degradation products by capillary electrophoresis. *J. Chromatogr. A* **1999**, *853*, 503-509.
- (42) Borros, S.; Barbera, G.; Biada, J.; Agullo, N. The use of capillary electrophoresis to study the formation of carcinogenic aryl amines in azo dyes. *Dyes and Pigm.* **1999**, *43*, 189-196.
- (43) Burkinshaw, S.M.; Graham, C. Capillary zone electrophoresis analysis of chlorotriazinyl reactive dyes in dyebath effluent. *Dyes and Pigm.* **1997**, *34*, 307-319.
- (44) Riu, J.; Schonsee, I.; Barcelo, D. Determination of sulfonated azo dyes in groundwater and industrial effluents by automated solid-phase extraction followed by capillary electrophoresis mass spectrometry. *J. Mass Spectrom.* **1998**, *33*, 653-663.
- (45) Riu, J.; Eichhorn, P.; Guerrero, J.A.; Knepper, T.P.; Barcelo, D. Determination of linear alkylbenzenesulfonates in wastewater treatment plants and coastal waters by automated solid-phase extraction followed by capillary electrophoresis-UV detection and confirmation by capillary electrophoresis-mass spectrometry. *J. Chromatogr. A* **2000**, *889*, 221-229.
- (46) Riu, J.; Barcelo, D. Determination of linear alkylbenzene sulfonates and their polar carboxylic degradation products in sewage treatment plants by automated solid-phase extraction followed by capillary electrophoresis-mass spectrometry. *Analyst* **2001**, *126*, 825-828.
- (47) Robertson, J.; Wells, R.J.; Pailthorpe, M.T.; David, S.; Aumatell, A.; Clark, R. *An assessment of the use of capillary electrophoresis for the analysis of acid dyes in wool fibers.* Advances in Forensic Sciences, Proceedings of the Meeting of the International Association of Forensic Sciences, 13th, Duesseldorf, Aug. 22-28, 1995, 4, 247-249.
- (48) Morgan, S. L.; Vann, B. C.; Baguley, B. M.; Stefan, A. R. *Advances in discrimination of dyed textile fibers using capillary electrophoresis/mass spectrometry.* Trace Evidence Symposium, Clearwater, FL, 2007
- (49) Wheals, B.B.; White, P.C.; Paterson, M.D. High-performance liquid chromatographic method utilizing single or multi-wavelength detection for the comparison of disperse dyes extracted from polyester fibers. *J. Chromatogr.* **1985**, *350*, 205-215.
- (50) Macrae, R.; Smalldon, K.W. The characterization of dyestuffs on wool fibers with special reference to microspectrophotometry. *J. Forensic Sci.* **1979**, *24*, 109-116.
- (51) Roux, C.; Margot, P. The population of textile fibres on car seats. *Sci Justice* **1997**, *37*, 25-30.

- (52) Watt, R.; Roux, C.; Robertson, “The population of coloured textile fibres in domestic washing machines. *J. Sci Justice* **2005**, *45*,75-83.
- (53) Petrick, L.M.; Wilson, T. A.; Fawcett, W. R. High-performance Liquid Chromatography-Ultraviolet-Visible Spectroscopy-Electrospray Ionization Mass Spectrometry Method for Acrylic and Polyester Forensic Fiber Dye Analysis. *J. Forensic Sci.* **2006**, *51*, 771-779
- (54) Yinon, J.; Saar, J. Analysis of dyes extracted from textile fibers by thermospray high-performance liquid chromatography-mass spectrometry. *J. Chromatogr. A* **1991**, *586*, 73-84.
- (55) Xu, X.; Leijenhurst, H.; Van den Hoven, P.; De Koeijer, J. A.; Logtenberg, H. Analysis of single textile fibres by sample-induced isotachopheresis-micellar eletrokinetic capillary chromatography. *Sci. Justice* **2001**, *41*, 93-105.
- (56) Tuinman, A. A.; Lewis, L. A.; Lewis, S. A. Trace-fiber color discrimination by electrospray ionization mass spectrometry: A tool for the analysis of dyes extracted from submillimeter nylon fibers. *Anal. Chem.* **2003**, *75*, 2753-2760.
- (57) Huang, M.; Yinon, J.; Sigman, M. E. Forensic identification of dyes extracted from textile fibers by liquid chromatography mass spectrometry (LC-MS). *J. Forensic Sci.* **2004**, *49*, 238-249.
- (58) Huang, M.; Russo, R.; Fookes, B. G.; Sigman, M. E. Analysis of Fiber Dyes by Liquid Chromatography Mass Spectrometry (LC-MS) with Electrospray Ionization: Discriminating Between Dyes with Indistinguishable UV-Visible Absorption Spectra. *J. Forensic Sci.* **2005**, *50*, 526-534.
- (59) Pawlak, K.; Puchalska, M.; Miszczak, A.; Rosloniec, E.; Jarosz, M. Blue natural organic dyestuffs – from textile dyeing to mural painting. Separation and characterization of coloring matters present in elderberry, longwood and indigo. *J. Mass Spectrom.* **2006**, *41*, 613-622.
- (60) Zhang, X.; Laursen, R. Development of Mild Extraction Methods for the Analysis of Natural Dyes in Textiles of Historical Interest Using LC-Diode Array Detector-MS. *Anal. Chem.* **2005**, *77*, 2022-2025.
- (61) Szostek, B.; Orska-Gawrys, J.; Surowiec, I.; Trojanowicz, M. Investigation of natural dyes occurring in historical Coptic textiles by high-performance liquid chromatography with UV-Vis and mass spectrometric detection. *J. Chromatogr. A* **2003**, *1012*, 179-192.
- (62) Petroviciu, I.; Albu, F.; Medvedovici, A. LC/MS and LC/MS/MS based protocol for identification of dyes in historic textiles.” *Microchemical Journal*, **2010**, *95*, 247-254.
- (63) Rafaëly, L.; Héron, S.; Nowik, W.; Tchaplà, A. Optimization of ESI-MS detection for the HPLC of anthraquinone dyes. *Dyes and Pigm.* **2008**, *77*, 191-203.
- (64) Laing, D. K.; Gill, R.; Blacklaws, C.; Bickley, H.M. Characterization of acid dyes in forensic fiber analysis by high-performance liquid chromatography using narrow-bore columns and diode array detection. *J. Chromatogr.* **1988**, *442*, 187-208.
- (65) Minioti, K.; Sakellariou, C.; Thomaidis, N. Determination of 13 synthetic food colorants in water-soluble foods by reversed-phase high-performance liquid chromatography coupled with diode-array detector. *Anal. Chim. Acta*, **2007**, *583*, 103-110.
- (66) Ji, C.; Feng, F.; Chen, Z.; Chu, X. Highly sensitive determination of 10 dyes in food with complex matrices using SPE followed by UPLC-DAD-Tandem mass spectrometry. *J. Liq. Chromatogr. & Relat. Technol.* **2011**, *34*, 93-105.
- (67) Andreasen, M. F.; Telving, R.; Birkler, R.I.D.; Schumacher, B.; Johannsen, M. A fatal poisoning involving Bromo-Drögonfly. *Forensic Sci. Int.* **2009**, *183*, 91–96.

- (68) Bendroth, P.; Kronstrand, R.; Helander, A.; Greby, J.; Stephanson, N.; Krantz, P. Comparison of ethyl glucuronide in hair with phosphatidylethanol in whole blood as post-mortem markers of alcohol abuse. *Forensic Sci. Int.* **2008**, *176*, 76-81.
- (69) Wood, M.; Laloup, M.; Samync, N.; del Mar Ramirez Fernandez, M.; de Bruijn, E. A.; Maes, R A.A.; De Boeck, G. Recent applications of liquid chromatography-mass spectrometry in forensic science. *J. Chromatogr. A* **2006**, *1130*, 3–15.

## TECHNICAL REPORT

### A. Comprehensive screening of acid, basic, and disperse dyes extracted from millimeter-length trace evidence fibers by ultra-performance liquid chromatography: methodology and figures of merit

Scott J. Hoy, Molly R. Burnip, Kaylee R. McDonald, Oscar G. Cabrices, Andrew Green, and Stephen L. Morgan, Department of Chemistry and Biochemistry, University of South Carolina, Columbia, SC 29208

#### ABSTRACT

Methodology for the microextraction of basic dyes on acrylic, acid dyes on nylon, and disperse dyes on polyester textile fibers is reported. A single ultra-performance liquid chromatography method suited for qualitative and semi-quantitative analysis of all three dye types has also been developed. Although our approach is destructive to the fiber evidence, the ability to analyze sub-millimeter fiber lengths of single fibers, coupled with limits of detection in the 2-40 ppb range by both UV/visible and tandem mass spectrometric detection make routine forensic characterization feasible.

#### INTRODUCTION

The ubiquitous nature of textile fibers provides an information-rich evidence source for crime scene investigations, however in cases of similarly dyed fibers current fiber analysis techniques do not provide adequate chemical information for unambiguous match determinations to be made. The standard procedure for analyzing forensic textile fibers involves measurement of physical and optical properties in an attempt to exclude matches of known and questioned fibers, followed by visual color matching and infrared (IR) spectroscopy and UV/visible spectral comparisons.<sup>1</sup> These techniques are efficient, non-destructive, and most often able to discriminate fiber evidence. However, fibers are class evidence and often share properties or characteristics due to common or similar sources, manufacturing methods, or treatments. The conclusion that the questioned fiber exhibits the same physical, optical and chemical properties as the known sample and could have originated from the same source as the known sample or another fiber source composed of fibers with the same properties may not be convincing in the courtroom. Fibers often are multiply dyed. Reliable quantitative extraction of those dyes from a trace evidence fiber can enhance forensic decision-making by distinguishing fibers containing different, but similar, dyes with the combination of retention time matching, UV/visible spectral comparison, and structural analysis by mass spectrometry.

The challenge of analyzing dye extracts from forensic fibers stems from the need to preserve the evidence as much as possible. Extraction of dyes is destructive to the fiber, and recovered trace evidence fibers are often as small as 2 mm in length and contain as little as 2 ng of dye<sup>2</sup>, thus very sensitive analysis techniques are needed. Previous research into dye extract analysis has used thin layer chromatography (TLC) as a classification technique, however issues of reproducibility and large required sample size plague the conclusions.<sup>3-13</sup> More advanced techniques have been applied such as capillary electrophoresis (CE), and while CE excels at separating ionized dyes, dye classes such as disperse dyes on polyester and vat dyes on cotton are difficult to ionize.<sup>14-16</sup>

Liquid chromatography has the added benefit of both stationary phase and mobile phase tuning to achieve a separation. Because many dyes have acid or base character, control of the mobile phase pH permits adjustment of retention for improved resolution and tuning of retention times for faster analysis speed. The numerous combinations of mobile and stationary phases offer a universal separation system for small organic molecules such as dyes. HPLC has been previously used to separate mixtures of acid, basic, and disperse dyes.<sup>17,18,20</sup> Where HPLC with UV/visible detection was not sufficient to differentiate between some similarly colored dyes, Huang, *et al.* point out that discrimination at the molecular level by HPLC-MS is usually successful.<sup>17</sup> Dye extracts not discriminated by UV/visible detection were also analyzed using HPLC-MS; success was achieved using 5 mm threads, but not single fibers.<sup>18</sup>

Ultra-performance liquid chromatography (UPLC) has demonstrated its utility for rapid analysis by using high pressure pumps (<15,000 psi) capable of moving samples and mobile phases through columns packed with small diameter (1.7  $\mu\text{m}$ ) stationary phase particles. UPLC can achieve very high resolution separations in short analysis times (< 5 min). As a consequence, band broadening is decreased substantially compared to HPLC and the viability of using UV/visible detection for trace analysis increases.

The objective of our present research is to establish comprehensive microextraction techniques coupled with UPLC methodology for the extraction and separation of acid, basic, and disperse dyes from nylon, acrylic, and polyester fibers. Our target fiber size is 1 mm to offset the issue of damaging evidence. We also present performance characteristics for calibration involving these analytical methods and determine limits of detection and quantitation for nine different dyes.

## EXPERIMENTAL

**Materials.** Analytical grade chlorobenzene, glacial acetic acid, pyridine, ammonium hydroxide, ammonium acetate, formic acid, and HPLC/UPLC grade acetonitrile and methanol were purchased from Fisher Scientific (Pittsburg, PA). Dyed fabric and textile dye standards were sampled from our collection of production samples, which were donated by textile and dyestuff manufacturers from the southeastern United States. The dyes used in this work are listed in Table 1 using the Color Index nomenclature (Society of Dyers and Colourists, Bradford, UK). The nine dyes selected for this study included three dyes from each of the acid, basic, and disperse classes.

**Fiber sample preparation.** Prior to extraction analysis, all samples are cut to prescribed lengths. In previous CE analyses for fiber dyes, percent relative standard deviations (RSDs) for peak areas have varied from 10-20%, of most synthetic fibers to as high as 25-35% for cotton.<sup>14-16</sup> We attributed these high RSDs to the inability to cut small fiber sizes reproducibly. Fibers that have intrinsic curled, crinkly, or helical shapes, such as cotton and acrylic fibers, must be stretched lengthwise while cutting. We have designed and machined a device to facilitate reproducible measurement and cutting of fibers down to 5 mm in length (Figure 1). The device has a metal block with a groove within which the fiber can be securely positioned; above the block is a rotating shaft on which multiple razor blades are fixed, spaced in 5 mm distance increments and aligned with cutting slots. Once the fiber is positioned, the operator selects the desired length and can safely rotate the shaft to cut the fiber.

Individual fibers 5-mm in length were cut using the fiber guillotine; 1 mm and 0.5 mm fibers were cut by hand using a table-mounted magnifying glass and scalpel. Each fiber length was cut

in triplicate. Cut fibers were then loaded into Waters Total Recovery<sup>®</sup> vials for extraction. These vials enable extractions to be performed with low solvent volumes (< 50  $\mu$ L), enabling concentration of dyes in the resulting extract. When typical low volume vial inserts were employed for extractions, solvent often condensed on the inside vial wall outside the vial insert because of poor sealing between the insert and the top of the vial.

**Calibration design.** Experimental designs for UPLC-DAD calibration were constructed for all nine dyes based on experiments at 7 levels of dye concentration (0 ppb, 100 ppb, 500 ppb, 1000 ppb, 1500 ppb, 2000 ppb, and 2500 ppb). In this high concentration calibration, a blank sample was measured 15 times as a quality control sample interspersed through the runs, and five replicate samples were analyzed for each sample containing analyte. A lower concentration design was also performed based on five replicate experiments using standard mixtures of the 9 dyes at concentrations 10 ppb, 20 ppb, 30 ppb, 40 ppb, and 50 ppb, with 18 blank injections at zero concentration. For UPLC-MS-MS, calibration designs included standards at 0 ppb, 10 ppb, 200 ppb, 400 ppb, 600 ppb, 800 ppb, and 1000 ppb, with 15 replicate experiments for the blanks and five replicates for samples containing analyte. For each dye peak, QuanLynx<sup>™</sup>, data management software included with MassLynx<sup>™</sup> (Waters Corporation, Milford, MA) was used to integrate peak areas above corrected baselines. For each dye standard at 1000 ppb concentration, the retention time window encompassing the baseline peak width was determined; this window was then employed as the dye peak integration window for all samples, including blanks.

**Instrumentation.** Dye standards and extracts were separated and detected using a Waters Acquity<sup>™</sup> UPLC H-Class equipped with a quaternary solvent pump system and a Waters PDA e $\lambda$  detector. The column was a 2.1  $\times$  50 mm I.D. 1.7  $\mu$ m particle size Waters Acquity<sup>™</sup> BEH C18 column with a 2.1  $\times$  5 mm I.D. 1.7  $\mu$ m particle size Waters Acquity UPLC<sup>®</sup> BEH C18 VanGuard precolumn. The mobile phase gradient was based on mixtures of 50 mM ammonium acetate in water and 0.15% formic acid in methanol as shown in Table 2A. The column temperature was set at 40  $^{\circ}$ C. The diode array detector scanned the wavelength range from 325 nm to 675 nm at a rate of 40 Hz and 1.2 nm resolution. The sample injection volumes were 10  $\mu$ L.

Separations with MS characterization were performed using a Waters Acquity UPLC<sup>®</sup> equipped with a binary solvent system coupled to a Waters Micromass Quattro Premier XE<sup>®</sup> tandem quadrupole mass spectrometer. For MS compatibility, the mobile phase consisted of 50 mM ammonium acetate in water and 0.15% formic acid in methanol. The mobile phase gradient for MS-MS detection shown in Table 2B differs from that for UPLC-UV/visible detection to compensate for the slower flow rate required for MS. The column was at ambient temperature during runs. Sample injection volumes were 5  $\mu$ L. The MS-MS transitions, cone voltages, and collision voltages are listed in Table 3.

**Extraction of acid dyes on nylon.** The optimum solvent conditions for extraction of acid dyes from nylon was previously investigated by Stefan, *et al.*, using a mixture of pyridine, ammonium hydroxide, and water.<sup>14</sup> Because the extraction response was robust over the center of the design, here we used equal proportions (33:33:33) of the three components for extractions. Aliquots (100  $\mu$ L) of the extractant were added to vials containing fibers, and vials were capped and extracted at 100 $^{\circ}$ C for 1 h. After extraction, the vials were uncapped and heated at 90 $^{\circ}$ C to evaporate solvent (*ca.* 30-45 min). Samples were reconstituted in a 50  $\mu$ L mixture of 50:50 methanol and

50 mM ammonium acetate buffered at pH 4.5, and vortex-mixed to ensure complete solvation of extracted dye.

**Extraction of basic dyes on acrylic.** Extraction conditions for basic dyes on nylon were also explored by Stefan, *et al.*<sup>15</sup> In the present work, 50:50 mixtures of 88% formic acid and water were employed for all extractions, in agreement with literature-cited values.<sup>6,19,20</sup> Aliquots (100  $\mu$ L) of extractant were added to the vials containing the fibers and then capped. The extraction was carried out at 100°C for 1 h, and the vials were then uncapped and evaporated at 90°C until dry (*ca.* 30-45 min). The samples were reconstituted in a 50  $\mu$ L mixture of 50:50 methanol and 50 mM ammonium acetate buffered at pH 4.5. Samples were vortex-mixed to ensure complete solvation of the extracted dye.

**Extraction of disperse dyes on polyester.** Chlorobenzene was previously reported to extract disperse dyes on polyester.<sup>21</sup> As with acid and basic dyes, aliquots of 100  $\mu$ L of extractant were added to vials containing the fibers and the extractions were carried out at 100 °C for 1 h. Vials were uncapped and heated to evaporate solvent at 90 °C until dry (*ca.* 30-45 min). The samples were then reconstituted in a 50  $\mu$ L mixture of 50:50 methanol and 50 mM ammonium acetate buffered at pH 4.5. Samples were vortex-mixed to ensure complete solvation of the extracted dye.

**MS-MS Optimization.** Electrospray ionization (ESI) and MS-MS transition parameters were tuned by infusing 1000 ppb of each dye into the source with a 0.300 mL/min mobile phase of a 50:50 mixture of 0.05 M ammonium acetate and methanol with 0.15% formic acid by volume. Desolvation temperature was set at 450 °C. Dye standards were infused at 20  $\mu$ L/min to tune the optimum cone voltage was tuned for maximum ion count, and to adjust collision voltages to maximize fragment ion counts from characteristic mass fragments. Table 3 summarizes the MS-MS parameters employed. Fiber dye extracts were reconstituted in 50  $\mu$ L volume to provide sufficient volume for such initial tuning and determination of MS conditions and transitions for target ions.

## RESULTS AND DISCUSSION

**Chromatographic analysis of dyes.** A comprehensive separation of all nine dyes was achieved using the mobile phase gradients in Table 2. In developing this gradient mixture, ammonium acetate buffered to pH 4.5 was found to broaden several dye peaks, and Basic Yellow 28 and Acid Yellow 49 dye peaks coeluted. A gradient of ammonium acetate at pH 7 produced two peaks almost baseline-resolved for these dyes. Under these conditions, the Basic Violet 16 baseline peak width decreased from 5.4 s to 4.2 s, and peak height and area increased by *ca.* 20%.

Figure 2 displays the separation, in less than five min, of all nine dyes evaluated for this work. The first (peak 1, Basic Red 46), third (peak 3, Acid Yellow 49), and last dye (peak 9, Disperse Blue 60) produced two peaks. In each case, each pair of peaks exhibited UV/visible spectra identical to those in Table 1. For the last pair of peaks, the absorbance is shifted to longer wavelength compared to many of the other dyes.

Figure 3 shows the chromatograms of dyes extracted from fibers of lengths 5 mm, 1 mm, and 0.5 mm; these extractions were performed in triplicate. All extractions were successful down to 0.5 mm except those involving Acid Yellow 49 and Disperse Blue 60, which were only successful down to 1 mm lengths. A 1 mm fiber extract of Acid Yellow 49 dye appeared to produce

sufficient signal for a 0.5 mm extract to be detectable, but analysis of a 0.5 mm fiber dyed with Acid Yellow 49 failed, either because of difficulty in handling or low dye levels. Pale yellow-colored fibers are difficult to see regardless of length. The stock fabric from which fiber dyed with Disperse Blue 60 were sampled, were lightly colored indicative of low dye loading. As seen below, Disperse Blue 60 has the highest limit of detection (LD) of all nine dyes, and although results suggest that a 0.5 mm extract is above the limit of detection, there is increased noise associated with its absorbance peak.

**Validation performance characteristics for dyes.** Tables 4 and 5 show UPLC-DAD calibration results for all nine dyes over the selected high (0-2500 ppb) and low (0-50 ppb) concentrations, respectively. Table 6 shows MS-MS calibration results over mid-range (0-600 ppb) concentrations. Figures 12-37 display calibration plots for the nine dyes investigated. All first-order linear calibration models (with intercept and slope parameters) produced coefficients of determination ( $R^2$ ) of 0.9993 or higher for the wide range calibrations. Calculated signal-to-noise ratios (SNR) were 100 or higher at 100 ppb in the wide range calibrations (based on integrated baseline root-mean-square variation from the MassLynx<sup>®</sup>). The second calibration (Table 5), performed over a range of standard concentrations that bracket the estimated dye limits of detection, produced lower  $R^2$  values of 0.9913 or higher, except for C.I. Disperse Blue 114 and C.I. Disperse Blue 60 (discussed below). The decrease in linearity over the lower range is expected due to the higher uncertainty—noise and detector linearity have a larger impact on peak shape as concentrations approach the LD—but these results are still excellent. For Disperse Yellow 114, the low-range UPLC-DAD results exhibited higher variability about the calibration line than any other dye; an  $R^2$  of 0.9687 was obtained, but the model exhibited a statistically significant lack of fit ( $p < 0.05$ ).

Table 6 displays calibration results for MS-MS based on 5 replicate standard injections at concentrations 10 ppb, 200 ppb, 400 ppb, 600 ppb, and 6 blank injections. The MS-MS models exhibit heteroscedastic behavior and greater variation at higher concentrations, and consequently these calibrations exhibited lower  $R^2$  values ranging from 0.9371 to 0.9970. Disperse Violet 77 ( $R^2=0.9700$ ) and Basic Red 46 ( $R^2=0.9371$ ) showing high residuals, possibly due to the fact that MS ionization conditions were not fully optimized.

Limits of detection are reported in Tables 4-6 are based on three different estimation approaches. Each method calculates the LD or limit of quantitation (LOQ) using

$$LD = (3.3 \times \sigma_b)/S \quad (1)$$

$$LOQ = (10 \times \sigma_b)/S \quad (2)$$

where  $\sigma_b$  is the standard deviation of the blank and  $S$  is the slope of the calibration line. The three methods used differ with how  $\sigma_b$  is estimated.  $LD_1$  estimates  $\sigma_b$  using the standard deviation of the integrated blank signals across the width of the actual peak.  $LD_2$  approximates  $\sigma_b$  using the standard deviation of the lowest non-zero concentration calibrator (at 100 ppb for the high concentration DAD calibration; at 10 ppb for the low concentration DAD and MS calibrations).  $LD_3$  estimates  $\sigma_b$  based on the standard error of the  $y$ -intercept of the calibration model; because the standard error of the  $y$ -intercept is calculated from the standard deviation of residuals, this may be inflated by the presence of lack fit of the model and by heteroscedasticity (non-constant variability at different concentration levels). There are many ways to calculate LDs; we present these three approaches to indicate a range of reasonable values for the LDs. Most UPLC-

UV/visible LDs calculated using the high concentration calibration design were 10 ppb or lower, which is the equivalent of detecting 100 pg amounts of dye.

LDs of disperse dyes using UV/visible detection are higher than the other dye types. Disperse Blue 60 had the lowest absorbance response of all dyes investigated; the low concentration (10-50 ppb) calibration was not determined because only the 50 ppb standard produced a peak that could be integrated by MassLynx<sup>®</sup>. LD<sub>1</sub> and LD<sub>3</sub> estimated the limit of detection for Disperse Blue 60 to be 13.50 ppb and 16.80 ppb, respectively. This result illustrates an important point: confirming actual detection for a sample concentration at the estimated LD is required if one plans to operate near the LD. Conducting the low concentration calibration design achieved this requirement for the present study. MS-MS calibration for Disperse Blue 60 produced LDs ranging from 2.88 to 30.50 ppb, depending on the estimation approach. The calibration in Figure 31 exhibits an R<sup>2</sup> of 0.9813; however, the curvature visible in the calibration plot is confirmed by a statistically significant lack of fit ( $p < 0.0001$ ).

Estimated LDs based on the lower concentration calibration designs for all dyes were all less than 4.38 ppb (corresponding to 43.8 pg of dye), except for the Disperse Yellow 114 dye (mentioned above). The calibration for Disperse Yellow 114 had abnormally high variance in the blanks and consequently LD<sub>1</sub> was 12.60 ppb while LD<sub>2</sub> and LD<sub>3</sub> were 1.67 ppb and 2.34 ppb. LDs calculated for ESI-MS-MS by LD<sub>1</sub> and LD<sub>2</sub> were evenly distributed between 0.38 ppb and 10.30 ppb. The high LD<sub>3</sub> values are due to the high amount of variance at 600 ppb for each dye by MS. Optimization of the MS-MS ionization conditions for higher dye concentrations might improve this outcome.

## CONCLUSIONS

Guided by previous experience with dye extractions, protocols have been devised for microextraction of acid dyes from nylon, basic dyes from acrylic, and disperse dyes from polyester fibers as small as 0.5 mm in length. Because it is not common to find more than 3-5 dyes on a single fiber, we validated these methods using three dyes from each dye class. The single UPLC method was developed for the separation of the specific acid, basic, and disperse dyes analyzed in this study. Chromatographic conditions used here are a good starting point for the analysis of other dyes from these three dye classes. For different unresolved dyes, gradient timing, composition, and rate of solvent composition change are easily adjusted to optimize separation. UPLC columns with 1.7  $\mu$ m diameter stationary phase particles achieve fast analysis times, with high pressure, and typical chromatographic analysis times in the range of 3-5 min.

Estimated limits of detection across the broad of three dye classes displayed consistency, notwithstanding a few exceptions. The calibration designs at low concentration produced lower LDs than achieved by UPLC-MS-MS. High concentration range calibrations for UV/visible and MS-MS detection showed lower detection limits than MS-MS in this study. More importantly, both methods are sensitive enough to detect and quantify well under 2 ng of dye on a 2 mm fiber. All but two dye extracts produced detectable dye amounts from 0.5 mm fibers that were only lightly dyed. We have found UPLC with UV/visible detection to yield lower detection limits than UPLC-MS-MS. Further optimization of MS ionization conditions may improve mass spectrometric performance.

Our results demonstrate that minute lengths of trace evidence fibers can be readily analyzed for dye formulation even when only very low dye amounts are present. UPLC with UV/visible detection enabled detection of dyes in extracts from single 1 mm fibers. We have developed

methods for profiling the chemical identity of constituents bound to textile fibers, including dyes, fluorescent brighteners, and finishing agents. By extracting these components from trace evidence fibers, separating them by liquid chromatography, and identifying and quantifying individual dyestuffs, match exclusions may be made based on more discriminating information than possible using visual and spectrophotometric microscopic analysis: comparisons can be based on the identity and relative amounts of dyes present in on the fibers themselves.

## ACKNOWLEDGMENTS

This research was supported by award 2010-DN-BX-K245 from the National Institute of Justice, Office of Justice Programs, U. S. Department of Justice. The opinions, findings, and conclusions or recommendations expressed in this publication are those of the author(s) and do not necessarily reflect those of the Department of Justice. Mention of commercial products does not imply endorsement on the part of the National Institute of Justice.

## REFERENCES

- (1) Robertson, J.; Grieve, M. *Forensic Examination of Fibres*; 2nd ed.; Taylor & Francis: London, 1999.
- (2) Macrae, R.; Smalldon, K. The Extraction of Dyestuffs from Single Wool Fibers. *J. Forensic Sci.* **1979**, *24*, 109–116.
- (3) Macrae, R.; Dudley, R.; Smalldon, K. The characterization of dyestuffs on wool fibers with special reference to microspectrophotometry. *J. Forensic Sci.* **1979**, *74*, 117–129.
- (4) Shaw, I. C. Micro-scale thin-layer chromatographic method for the comparison of dyes stripped from wool fibres. *The Analyst* **1980**, *105*, 729.
- (5) Home, J.; Dudley, R. Thin-layer chromatography of dyes extracted from cellulosic fibres. *Forensic Sci.Int.* **1981**, *17*, 71–78.
- (6) Beattie, I.; Roberts, H.; Dudley, R. Thin-layer chromatography of dyes extracted from polyester, nylon and polyacrylonitrile fibres. *Forensic Sci.Int.* **1981**, *17*, 57–69.
- (7) Hartshorne, A. W.; Laing, D. K. The dye classification and discrimination of coloured polypropylene fibres. *Forensic Sci.Int.* **1984**, *25*, 133–141.
- (8) Wiggins, K.; Crabtree, S.; March, B. The importance of thin layer chromatography in the analysis of reactive dyes released from wool fibers. *J. Forensic Sci.* **1996**, *41*, 1042–1045.
- (9) Laing, D.; Boughey, L.; Hartshorne, A. The standardisation of thin layer chromatographic systems for comparison of fibre dyes. *J. Forensic Sci. Soc.* **1990**, *30*, 299–307.
- (10) Laing, D.; Hartshorne, A.; Bennet, D. Thin layer chromatography of azoic dyes extracted from cotton fibres. *J. Forensic Sci. Soc.* **1990**, *30*, 309–315.
- (11) Rendle, D. F.; Wiggins, K. G. Forensic analysis of textile fibre dyes. *Review of Progress in Coloration and Related Topics* **1995**, *25*, 29–34.
- (12) Rendle, D. F.; Crabtree, S. R.; Wiggins, K. G.; Salter, M. T. Cellulase digestion of cotton dyed with reactive dyes and analysis of the products by thin layer chromatography. *Journal of the Society of Dyers and Colourists* **1994**, *110*, 338–341.
- (13) Crabtree, S. R.; Rendle, D. F.; Wiggins, K. G.; Salter, M. T. The release of reactive dyes from wool fibres by alkaline hydrolysis and their analysis by thin layer chromatography. *Journal of the Society of Dyers and Colourists* **1995**, *111*, 100–102.
- (14) Stefan, A. R.; Dockery, C. R.; Nieuwland, A. A.; Roberson, S. N.; Baguley, B. M.; Hendrix, J. E.; Morgan, S. L. Forensic analysis of anthraquinone, azo, and metal complex acid

dyes from nylon fibers by micro-extraction and capillary electrophoresis. *Anal. Bioanal. Chem* **2009**, *394*, 2077–85.

(15) Stefan, A. R.; Dockery, C. R.; Baguley, B. M.; Vann, B. C.; Nieuwland, A. a; Hendrix, J. E.; Morgan, S. L. Microextraction, capillary electrophoresis, and mass spectrometry for forensic analysis of azo and methine basic dyes from acrylic fibers. *Anal. Bioanal. Chem* **2009**, *394*, 2087–94.

(16) Dockery, C. R.; Stefan, a R.; Nieuwland, a a; Roberson, S. N.; Baguley, B. M.; Hendrix, J. E.; Morgan, S. L. Automated extraction of direct, reactive, and vat dyes from cellulosic fibers for forensic analysis by capillary electrophoresis. *Anal. Bioanal. Chem* **2009**, *394*, 2095–103.

(17) Huang, M.; Russo, R.; Fookes, B. G.; Sigman, M. E. Analysis of Fiber Dyes By Liquid Chromatography Mass Spectrometry (LC-MS) with Electrospray Ionization: Discriminating Between Dyes with Indistinguishable UV-Visible Absorption Spectra. *J. Forensic Sci* **2005**, *50*, 1–9.

(18) Huang, M.; Yinon, J.; Sigman, M. E. Forensic identification of dyes extracted from textile fibers by liquid chromatography mass spectrometry (LC-MS). *J. Forensic Sci* **2004**, *49*, 238–49.

(19) Beattie, I. B.; Dudley, R. J.; Smalldon, K. W. The Extraction and Classification of Dyes on Single Nylon, Polyacrylonitrile and Polyester Fibres. *Journal of the Society of Dyers and Colourists* **1979**, *95*, 295–302.

(20) Petrick, L. M.; Wilson, T. A; Ronald Fawcett, W. High-performance liquid chromatography-ultraviolet-visible spectroscopy-electrospray ionization mass spectrometry method for acrylic and polyester forensic fiber dye analysis. *J. Forensic Sci* **2006**, *51*, 771–9.

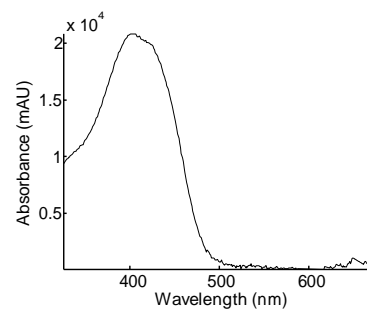
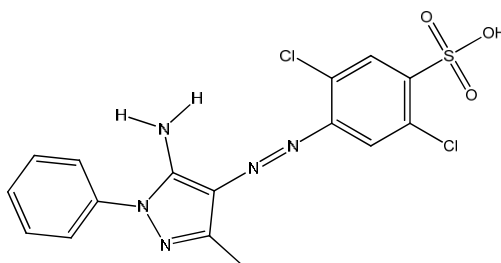
(21) West, J. C. Extraction and analysis of disperse dyes on polyester textiles. *J. Chromatogr. A* **1981**, *208*, 47–54.

Table 1. List of textile dyes, molecular structures, and UV/visible absorbance spectra.

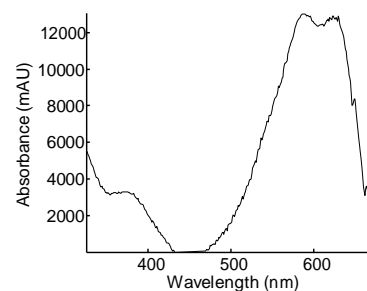
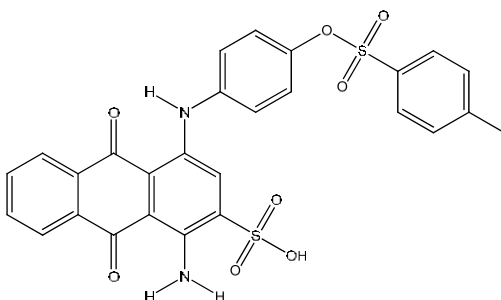
C.I. Name, Formula, Mol. Wt. (g/mol)	Structure	Absorbance Spectrum
Basic Red 46 $C_{18}H_{21}BrN_6$ 401.30		
Basic Violet 16 $C_{23}H_{29}N_2^+$ 333.49		
Basic Yellow 28 $C_{20}H_{24}N_3O^+$ 322.42		
Acid Red 337 $C_{17}H_{12}F_3N_3O_4S$ 411.36		

Table 1. Continued.

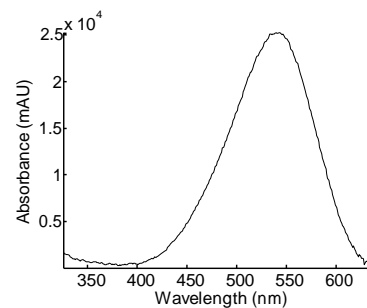
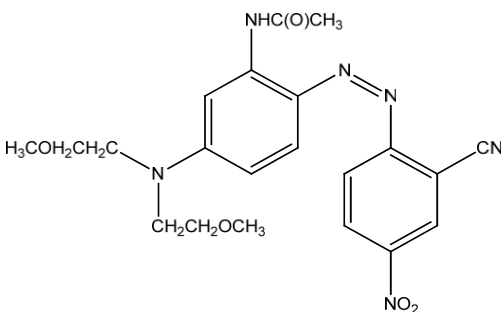
Acid Yellow 49  
 $C_{16}H_{13}Cl_2N_5O_3S$   
 426.28



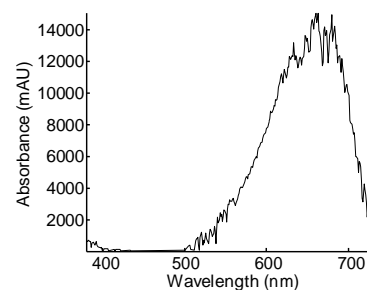
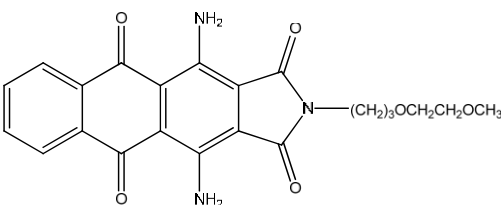
Acid Blue 281  
 $C_{27}H_{20}N_2O_8S_2$   
 564.59



Disperse Violet  
 77  
 $C_{21}H_{24}N_6O_5$   
 440.45



Disperse Blue  
 60  
 $C_{22}H_{21}N_3O_6$   
 423.42



Disperse  
 Yellow 114  
 $C_{20}H_{16}N_4O_5S$   
 424.43

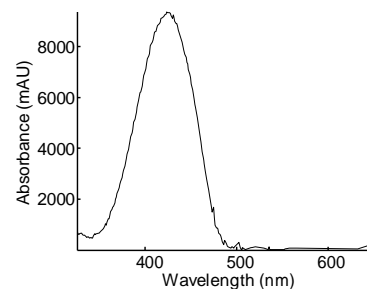
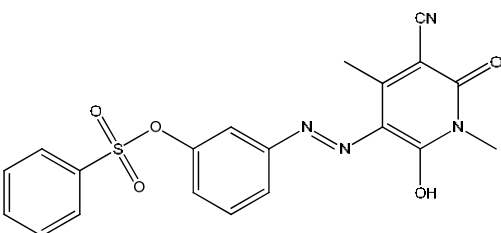


Table 2. Mobile phase gradient profiles.

## A. UPLC mobile phase gradient for UV/visible detection

Time (min)	Flow rate (mL/min)	Methanol with 0.15 % formic acid (%)	50 mM Ammonium acetate (%)
0.0	0.6	10	90
0.5	0.6	10	90
4.0	0.6	90	10
4.5	0.6	90	10
4.6	0.6	10	90
6.5	0.6	10	90

## B. UPLC mobile phase gradient for MS-MS detection

Time (min)	Flow rate (mL/min)	Methanol with 0.15% FA (%)	50 mM Ammonium acetate (%)
0.0	0.3	20	80
0.5	0.3	20	80
4.0	0.3	90	10
4.5	0.3	90	10
4.6	0.3	20	80
6.5	0.3	20	80

Table 3. MS-MS transitions and voltages.

Dye	Transition (m/z)	Cone Voltage (V)	Collision Voltage (V)
Basic Red 46	321-196	30	16
Basic Violet 16	333-319	39	29
Basic Yellow 28	322-136	33	30
Acid Red 337	412-161	45	33
Acid Yellow 49	426-144	40	35
Acid Blue 281	565-409	40	30
Disperse Violet 77	441-221	36	21
Disperse Blue 60	424-348	32	18
Disperse Yellow 114	425-178	47	30

Table 4. High range (0-2500 ppb) UPLC-UV/visible calibration results.

Dye	R <sup>2</sup>	LOD <sub>1</sub> (ppb)	LOD <sub>2</sub> (ppb)	LOD <sub>3</sub> (ppb)	LOQ <sub>1</sub> (ppb)	LOQ <sub>2</sub> (ppb)	LOQ <sub>3</sub> (ppb)
C.I. Basic Red 46	0.9996	4.77	5.41	11.80	14.45	16.39	35.76
C.I. Basic Violet 16	0.9999	3.62	1.69	6.32	10.97	5.12	19.15
C.I. Basic Yellow 28	0.9995	6.97	1.07	14.10	21.12	3.24	42.73
C.I. Acid Red 337	0.9998	9.50	2.17	8.90	28.79	6.58	26.97
C.I. Acid Yellow 49	0.9997	3.22	1.96	10.40	9.76	5.94	31.52
C.I. Acid Blue 281	0.9999	4.87	1.56	6.79	14.76	4.73	20.58
C.I. Disperse Violet 77	0.9998	10.10	0.37	9.42	30.61	1.12	28.55
C.I. Disperse Blue 60	0.9993	37.00	13.50	16.80	112.12	40.91	50.91
C.I. Disperse Yellow 114	0.9999	11.30	4.68	7.60	34.24	14.18	23.03

Table 5. Low range (0-50 ppb) UPLC-UV/visible calibration results.

Dye	R <sup>2</sup>	LOD <sub>1</sub> (ppb)	LOD <sub>2</sub> (ppb)	LOD <sub>3</sub> (ppb)	LOQ <sub>1</sub> (ppb)	LOQ <sub>2</sub> (ppb)	LOQ <sub>3</sub> (ppb)
C.I. Basic Red 46	0.9914	2.37	3.12	1.21	7.18	9.45	3.67
C.I. Basic Violet 16	0.9952	1.84	2.09	0.91	5.58	6.33	2.76
C.I. Basic Yellow 28	0.9965	2.69	0.93	0.77	8.15	2.82	2.33
C.I. Acid Red 337	0.9957	3.07	1.89	0.86	9.30	5.73	2.61
C.I. Acid Yellow 49	0.9940	4.26	2.59	1.01	12.91	7.85	3.06
C.I. Acid Blue 281	0.9913	4.38	0.41	1.22	13.27	1.24	3.70
C.I. Disperse Violet 77	0.9942	2.23	1.28	0.99	6.76	3.88	3.00
C.I. Disperse Blue 60	—	—	—	—	—	—	—
C.I. Disperse Yellow 114	0.9687	12.60	1.67	2.34	38.18	5.06	7.09

Table 6. MS-MS (0-600 ppb) UPLC-MS-MS calibration results.

Dye	R <sup>2</sup> <sub>MS</sub>	LOD <sub>1</sub> (ppb)	LOD <sub>2</sub> (ppb)	LOD <sub>3</sub> (ppb)	LOQ <sub>1</sub> (ppb)	LOQ <sub>2</sub> (ppb)	LOQ <sub>3</sub> (ppb)
C.I. Basic Red 46	0.9371	1.70	6.44	57.30	5.2	19.5	173.6
C.I. Basic Violet 16	0.9970	0.38	2.55	12.00	1.2	7.7	36.4
C.I. Basic Yellow 28	0.9840	2.34	3.87	28.10	7.1	11.7	85.2
C.I. Acid Red 337	0.9953	10.30	8.08	15.20	31.2	24.5	46.1
C.I. Acid Yellow 49	0.9858	6.41	4.76	26.50	19.4	14.4	80.3
C.I. Acid Blue 281	0.9879	7.09	4.67	27.40	21.5	14.2	83.0
C.I. Disperse Violet 77	0.9700	0.62	1.46	38.80	1.9	4.4	117.6
C.I. Disperse Blue 60	0.9813	4.67	2.88	30.50	14.2	8.7	92.4
C.I. Disperse Yellow 114	0.9833	2.89	7.62	28.80	8.8	23.1	87.3

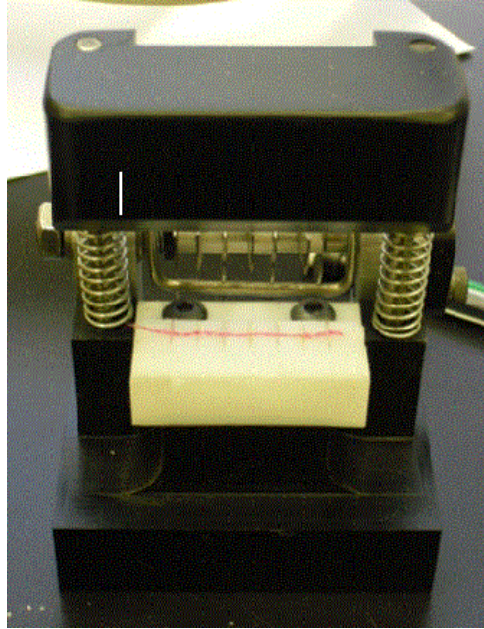


Figure 1. Guillotine device for cutting fibers to 5 mm lengths.

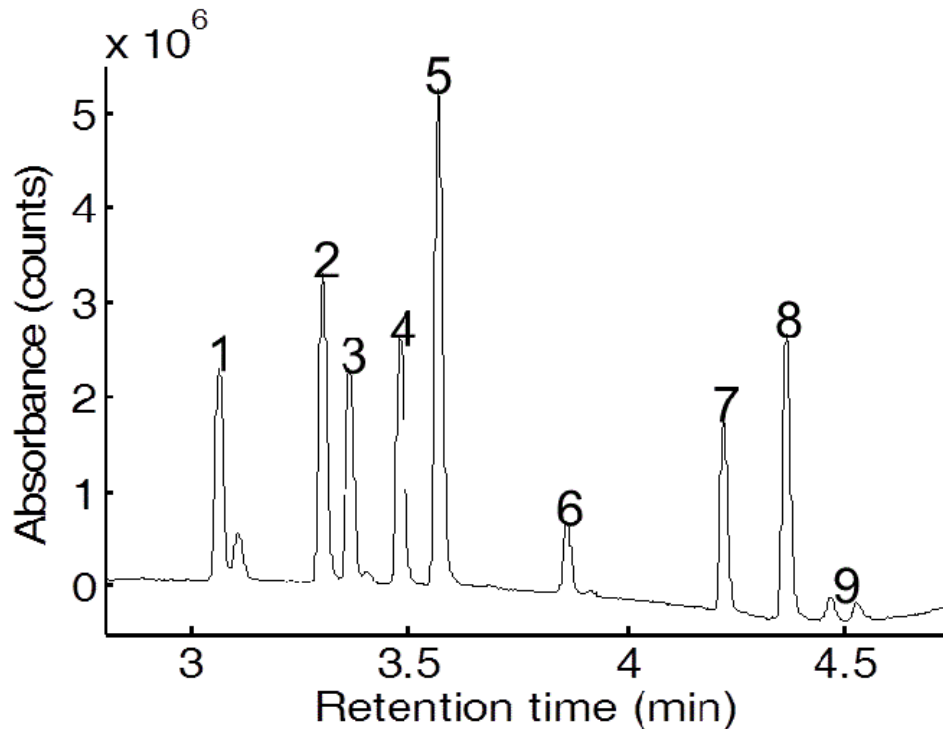


Figure 2. Separation of acid, basic, and disperse dyes at 1 ppm concentration. Peak identification: (1) Basic Red 46 (two peaks); (2) Basic Yellow 28; (3) Acid Yellow 49 (two peaks); (4) Acid Red 337; (5) Basic Violet 16; (6) Disperse Yellow 114; (7) Acid Blue 281; (8) Disperse Violet 77; and, (9) Disperse Blue 60 (two peaks).

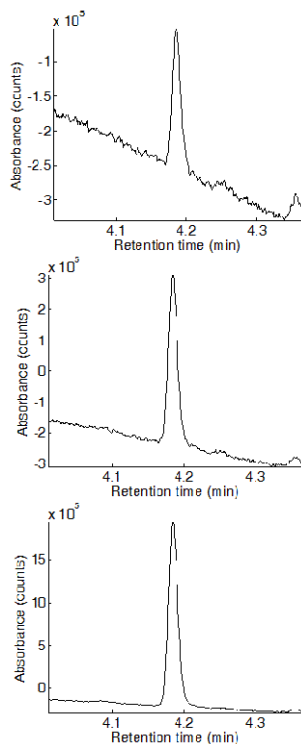


Figure 3. UPLC-DAD chromatograms for Acid Blue 281 extracted from a 0.5 mm fiber (top), 1 mm fiber (middle), and 5 mm fiber (bottom).

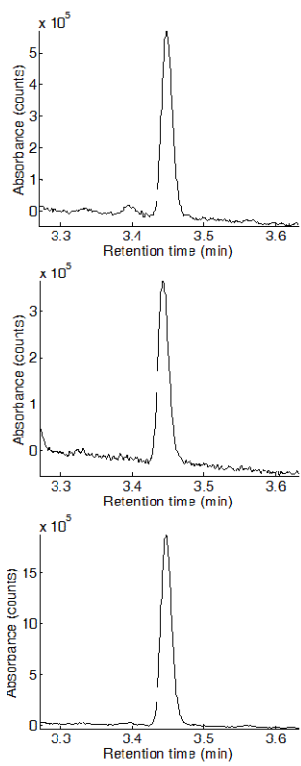


Figure 4. UPLC-DAD chromatograms for Acid Red 337 extracted from a 0.5 mm fiber (top), 1 mm fiber (middle), and 5 mm fiber (bottom).

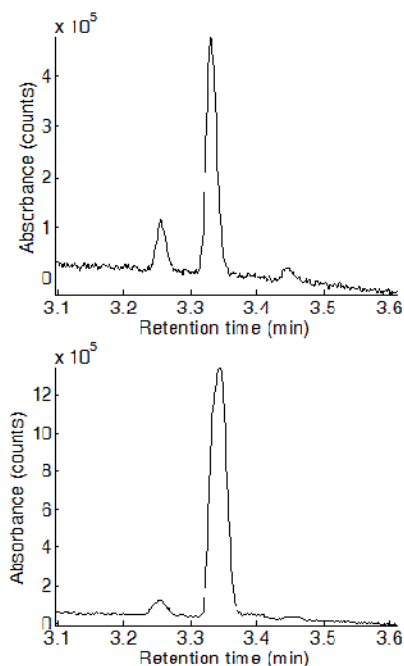


Figure 5. UPLC-DAD chromatograms for Acid Yellow 49 extracted from a 1 mm fiber (top) and a 5 mm fiber (bottom).

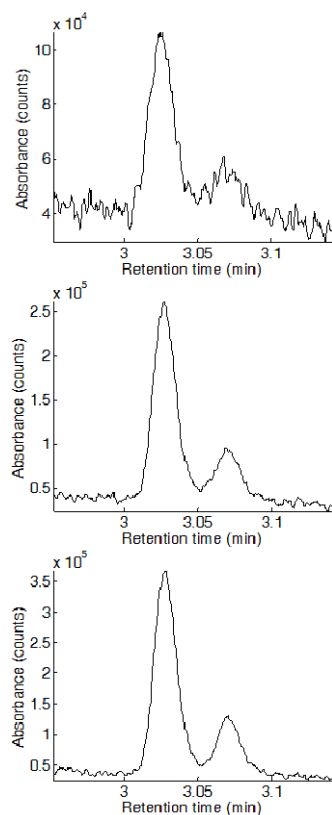


Figure 6. UPLC-DAD chromatograms for Basic Red 46 extracted from a 0.5 mm fiber (top), 1 mm fiber (middle), and 5 mm fiber (bottom).

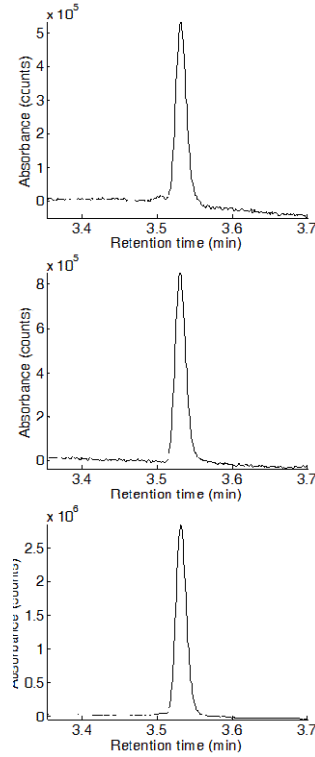


Figure 7. UPLC-DAD chromatograms for Basic Violet 16 extracted from a 0.5 mm fiber (top), 1 mm fiber (middle), and 5 mm fiber (bottom).

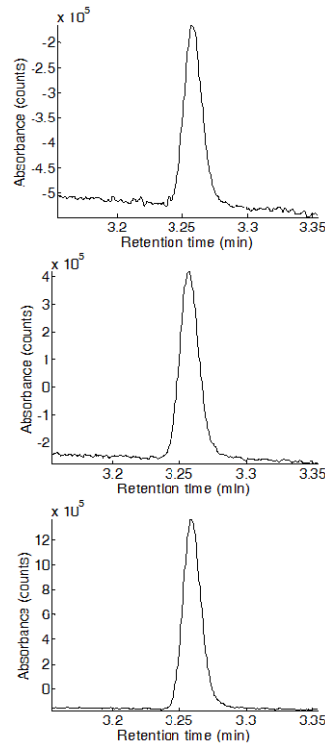


Figure 8. UPLC-DAD chromatograms for Basic Yellow 28 extracted from a 0.5 mm fiber (top), 1 mm fiber (middle), and 5 mm fiber (bottom).

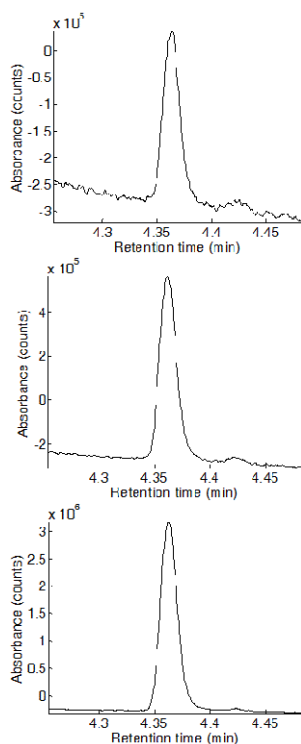


Figure 9. UPLC-DAD chromatograms for Disperse Violet 77 extracted from a 0.5 mm fiber (top), 1 mm fiber (middle), and 5 mm fiber (bottom).

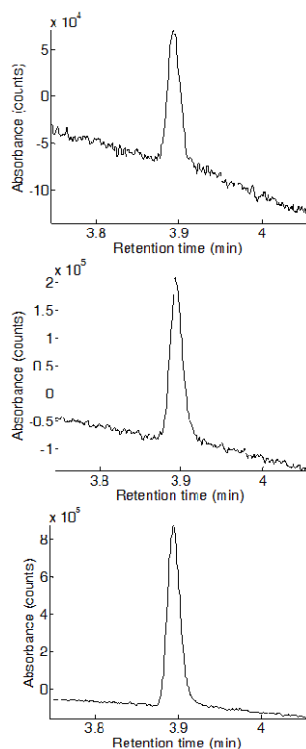


Figure 10. UPLC-DAD chromatograms for Disperse Yellow 114 extracted from a 0.5 mm fiber (top), 1 mm fiber (middle), and 5 mm fiber (bottom).

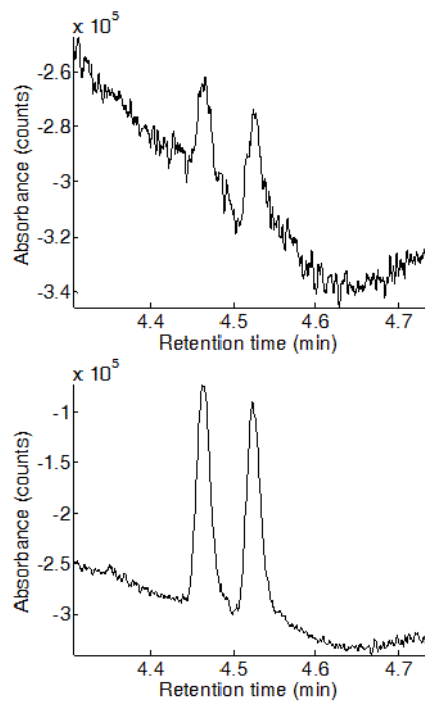


Figure 11. UPLC-DAD chromatograms for Disperse Blue 60 extracted from a 0.5 mm fiber (top), 1 mm fiber (middle), and 5 mm fiber (bottom).

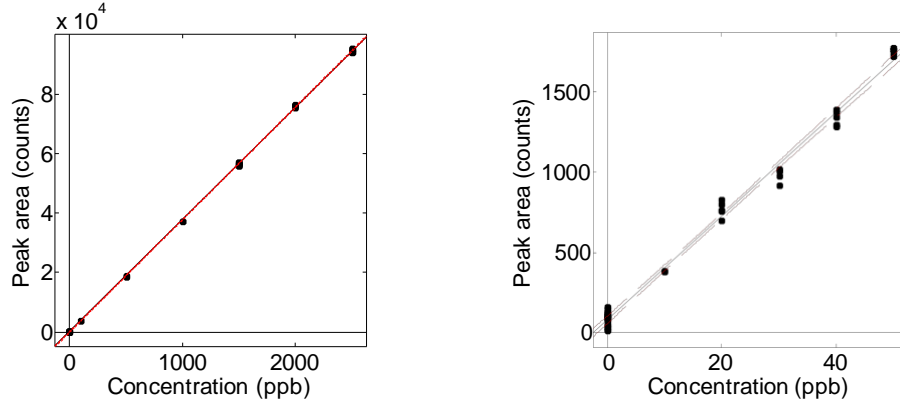


Figure 12. (Right) High and (left) low concentration UPLC-UV/visible calibrations for Acid Blue 281.

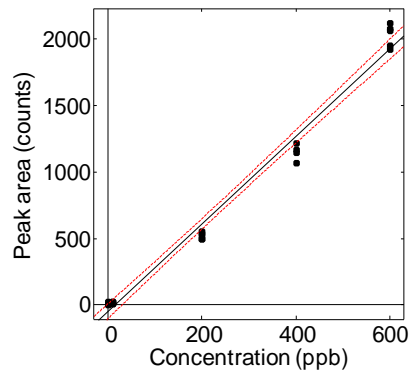


Figure 13. UPLC-MS-MS Calibration plot for Acid Blue 281.

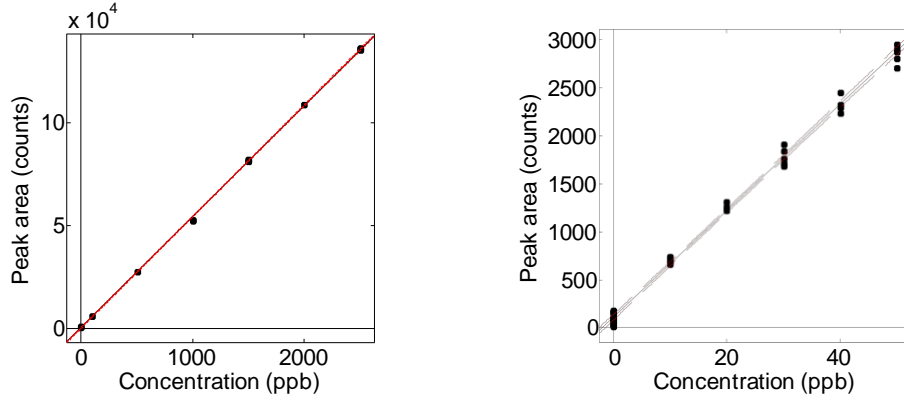


Figure 14. (Right) High and (left) low concentration UPLC-UV/visible calibrations for Acid Red 337.

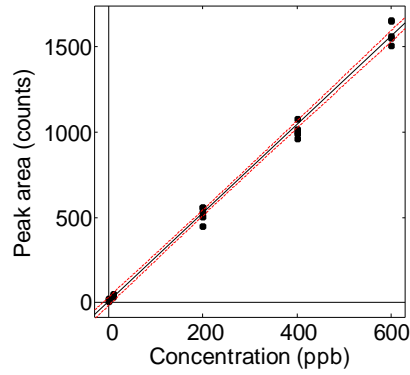


Figure 15. UPLC-MS-MS Calibration plot for Acid Red 337.

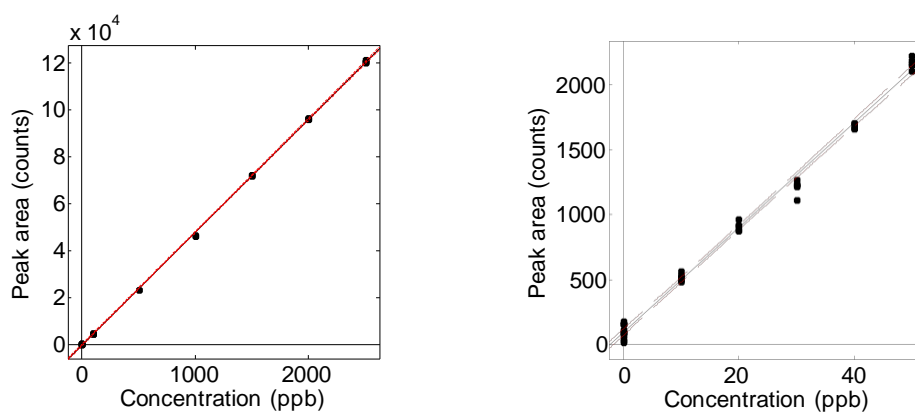


Figure 16. (Right) High and (left) low concentration UPLC-UV/visible calibrations for Acid Yellow 49.

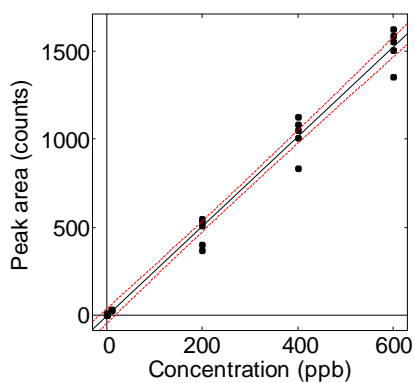


Figure 17. UPLC-MS-MS Calibration plot for Acid Yellow 49.

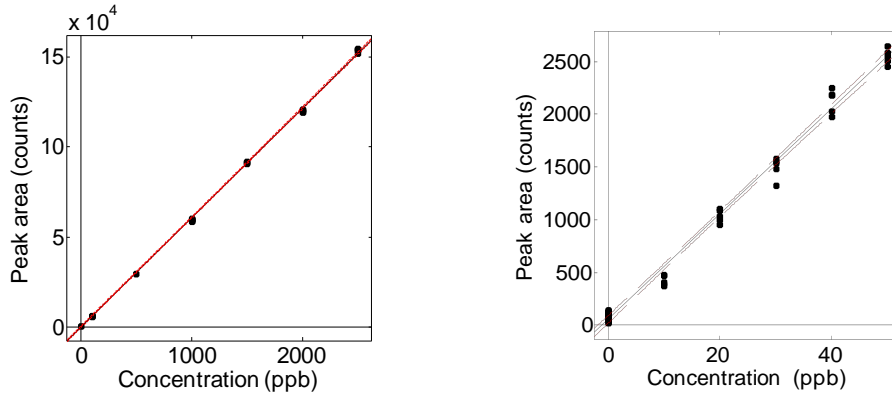


Figure 18. (Right) High and (left) low concentration UPLC-UV/visible calibrations for Basic Red 46.

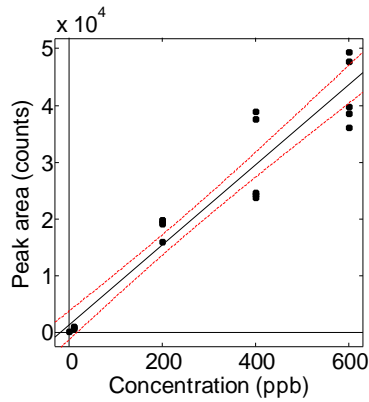


Figure 19. UPLC-MS-MS Calibration plot for Basic Red 46.

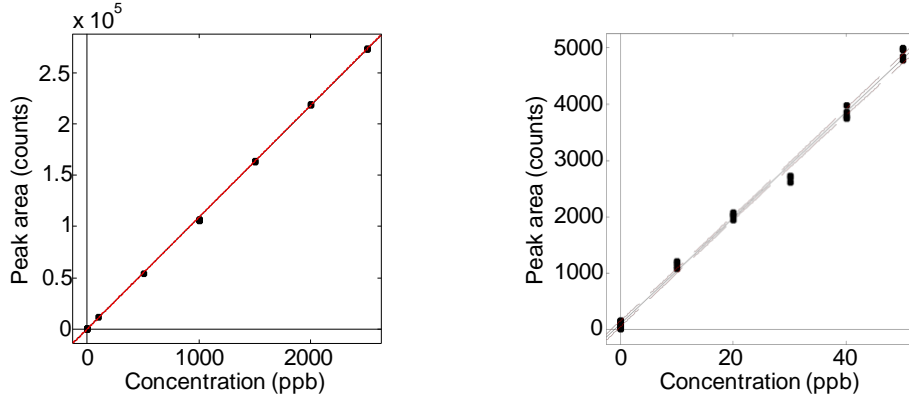


Figure 20. (Right) High and (left) low concentration UPLC-UV/visible calibrations for Basic Violet 16.

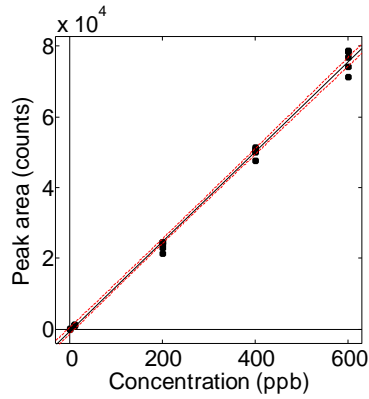


Figure 21. UPLC-MS-MS calibration plot for Basic Violet 16.

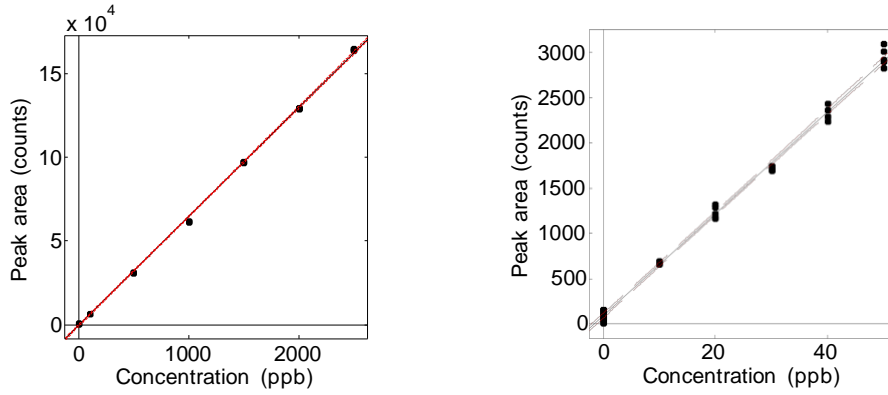


Figure 22. (Right) High and (left) low concentration UPLC-UV/visible calibrations for Basic Yellow 28.

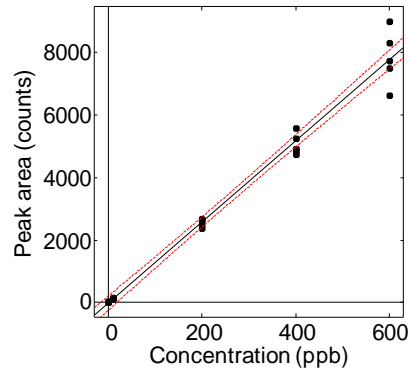


Figure 23. UPLC-MS-MS Calibration plot for Basic Yellow 28.

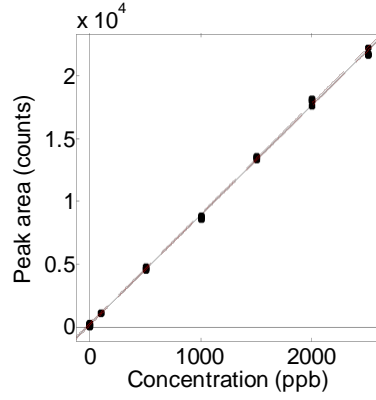


Figure 24. High concentration UPLC-UV/visible calibration for Disperse Blue 60.

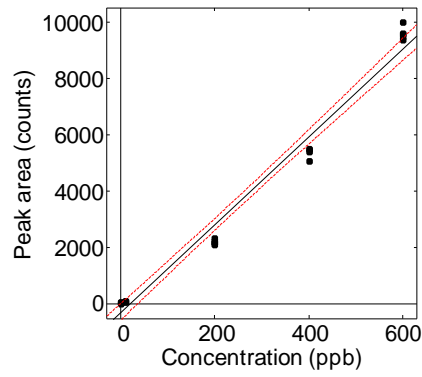


Figure 25. UPLC-MS-MS Calibration plot for Disperse Blue 60.

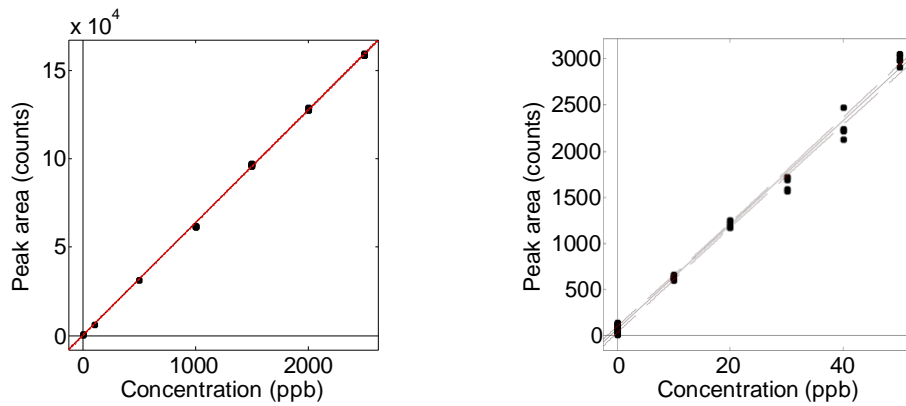


Figure 26. (Right) High and (left) low concentration UPLC-UV/visible calibrations for Disperse Violet 77.

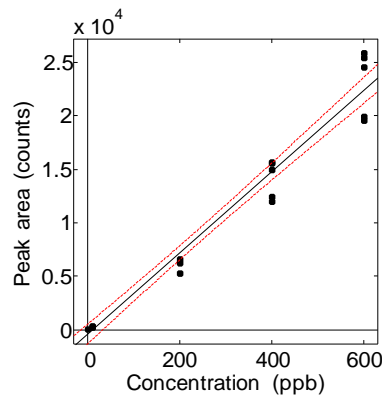


Figure 27. UPLC-MS-MS Calibration plot for Disperse Violet 77.

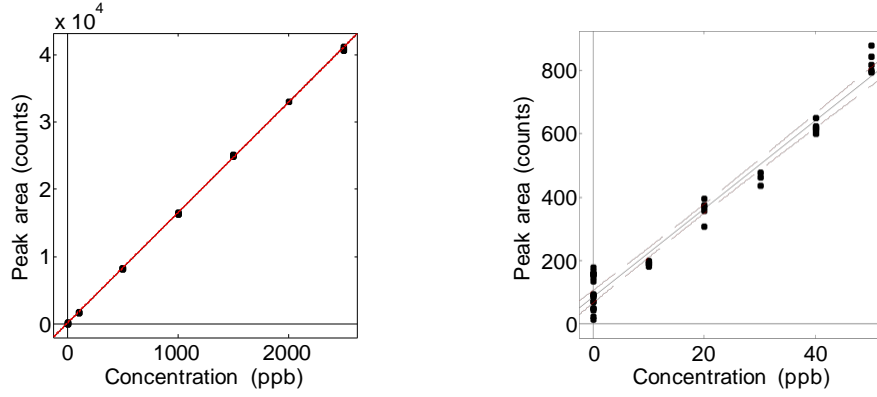


Figure 28. (Right) High and (left) low concentration UPLC-UV/visible calibrations for Disperse Yellow 114.

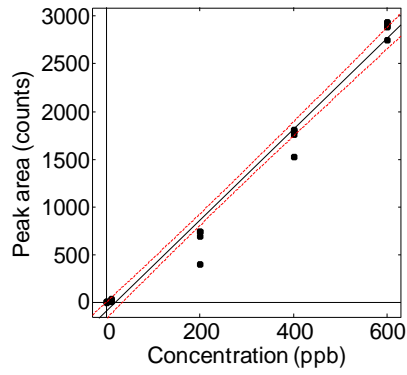


Figure 29. UPLC-MS-MS calibration plot for Disperse Yellow 114.

## **B. Extraction of direct dyes and indigo vat dye from trace cotton fibers for forensic characterization by ultra-performance liquid chromatography.**

Scott J. Hoy, Molly R. Burnip, Kaylee R. McDonald, and Stephen L. Morgan, Department of Chemistry and Biochemistry, University of South Carolina, Columbia, SC 29208

### **ABSTRACT**

Microextraction, followed by ultra-performance liquid chromatography, can distinguish similar fibers containing different, but similar, dyes with the combination of retention time matching, UV/visible spectral comparison, and structural analysis by mass spectrometry. The analysis of cotton fibers is challenging because they can be dyed with three different classes of dye, each requiring a different method for extraction and analysis. This work focuses on the chemistries of direct dyes and indigo and their optimum extraction conditions and chromatographic methods. We have successfully extracted direct dyes from cotton fibers as small as 1 mm in length and have quantitated dye amounts by UPLC with UV/visible detection. Analytical figures of merit and validation statistics, including extraction reproducibility, linearity, limits of detection and quantitation, and precision, are reported.

### **INTRODUCTION**

Forensic fiber analysis involves the comparison of "known" and "questioned" fibers using various microscopic techniques in an attempt to establish associations between crime scenes, suspects, and victims. Cotton is an abundant fiber material and cotton fibers are easily identified using polarized light microscopy by their refractive index and visually based on their unique morphology.<sup>1</sup> Additional discriminating information can be obtained from fibers using techniques such as infrared spectroscopy and UV-visible microspectrophotometry.<sup>2</sup> These techniques are non-destructive to the fiber sample, and thus preferred; however, limited information on the identity and amount of chemical constituents on the fibers is provided.

Though many different types of fibrous textiles are commonly manufactured, 80% of all fibers found as criminal evidence are made of cotton, nylon, polyester, or acrylic.<sup>1-4</sup> Cotton is of high interest due to its popularity in clothing. Cotton is a natural fiber made of cellulose, a polysaccharide containing hydroxyl groups and acetal linkages. The absence of ionic sites on the polymer backbone necessitates the use of direct dyes that are attached through hydrogen bonding, and reactive dyes that are covalently bound to the hydroxyl groups of the polymer. An additional dyeing technique involves water-insoluble vat dyes which migrate into the cellulose in their reduced form and are then oxidized and "locked" into the cellulose polymer. Direct, reactive, and vat dyes account for approximately 82% of all dyes used in the dyeing of cotton.<sup>5</sup>

Direct dyes are soluble in water due to the abundance of sulfonic acid, amine, and hydroxyl groups in their structures. The anionic dyes coat the fiber during the dyeing process and are held in place through hydrogen bonding. The removal of these dyes requires the disruption of the hydrogen bonds using alkaline solvents. A 4:3 (v/v) mixture of pyridine and water has been widely reported to extract direct dyes from cotton efficiently.<sup>6,7</sup>

Vat dyes are water-insoluble pigments used to dye cotton and account for approximately 15-25% of all cotton dyes consumed in the last 20 years.<sup>8,9</sup> This usage is due largely to indigo, an historically important and the oldest discovered vat dye, which is used today as the primary color of blue jeans. Due to their water-insoluble nature, vat dyes must first be chemically reduced to

their water-soluble *leuco* form before application to cotton. Figure 1 shows this reduction process for indigo. This process is commonly referred to as “vatting” in the textile industry as it is usually performed in a large vat. Vatting is typically conducted using sodium dithionite at very high pH conditions. Once the *leuco* form of the dye has been formed, the dye can migrate into the hydrophilic cellulose backbone of cotton. After the dye permeates into the cotton, it is reoxidized back to its original water-insoluble form, mechanically trapping the dye within the cellulose lattice. This leads to exceptionally high fastness to cotton, comparable to reactive dyes.

Indigo and its derivatives are unique vat dyes in that they require a weaker reducing agent than anthraquinone vat dyes to convert into their *leuco* forms. Additionally, indigo can be extracted from plants and textiles without being reduced. Several methods have been reported for indigo extraction including acidified methanol<sup>10</sup>, chloroform and pyridine in water<sup>6</sup>, and dimethyl sulfoxide (DMSO).<sup>11</sup> For UPLC analysis techniques, these extraction methods are desirable over reduction because they eliminate the possibility of over reduction and degradation of the dye, as well as injection of strong reducing agents that can damage the stationary phase.

This study focuses on the extraction of direct dyes and indigo, and the analysis of the resulting extracts by ultra-performance liquid chromatography (UPLC). Because the extraction process is destructive to the fiber and because forensic fiber examiners wish to preserve as much of the actual fiber evidence as possible, only a small segment of an original evidence fiber can be subjected to analysis. In many cases, fibers of 2 mm size or less may be all that is found at a crime scene. Fibers of lengths of 1-10 mm can contain between 2-200 ng of dye.<sup>4</sup> Various cotton dyes and dyestuffs have a large polarity range and varying solubility conditions which necessitates a widely compatible analysis technique. UPLC instruments employ a higher pressure pump system compared to HPLC, which enables the use of smaller particle stationary phases of exquisite efficiency. UPLC columns are packed tighter and are shorter than typical HPLC columns, which allows for significantly faster chromatographic analyses, sharper peaks, and higher signal-to-noise measurements. As in other forms of liquid chromatography, both the column and mobile phase systems can be tuned for the separation of samples of varying chemical makeup.

## EXPERIMENTAL

**Materials and Instrumentation.** All dyed fabrics and matching dye standards (Direct Orange 39, Direct Blue 71, Direct Blue 80, and indigo with structures shown in Table 1) were current production samples donated by dyestuff manufacturers in the southeastern United States. Dye names follow the Color Index nomenclature. All fibers were dyed at levels consistent with commercial use (2–4% by weight). All dye standards were solid in phase and stored in a dark room to avoid photodegradation. Photographs of cotton fibers were made with a Nikon (Melville, NY) model SMZ1500 microscope with a DS-Fi1 camera at 11.25× magnification.

Analytical grade water, acetone, pyridine, ammonium acetate, dimethyl sulfoxide (DMSO), chloroform, formic acid, glacial acetic acid, and HPLC/UPLC grade acetonitrile and methanol were purchased from Fisher Scientific (Pittsburg, PA).

Dye standards and extracts were separated and detected using a Waters Acquity™ UPLC H-Class equipped with a quaternary solvent pump system and a Waters PDA eλ detector. The column was a 2.1 × 50 mm I.D. 1.7 μm particle size Waters Acquity™ BEH C18 column with a 2.1 × 5 mm I.D. 1.7 μm particle size Waters Acquity UPLC® BEH C18 VanGuard precolumn. Mobile phase gradients are shown in Table 3 and Table 4. The column temperature was set at 40

°C. The diode array detector scanned at a rate of 40 Hz and 1.2 nm resolution. The sample injection volumes were 10  $\mu$ L.

**Direct Dye Extraction Optimization.** Direct Blue 71 (structure in Table 1) was selected as a representative direct dye for cotton fibers. Table 2 displays the solvent conditions at which the extraction efficiency was evaluated for fibers dyed with this single dye. This three-component mixture experimental design<sup>12,13</sup> was generated using Design Expert<sup>®</sup> 7 (StatEase, Inc., Minneapolis, MN, USA). For each of the ten design points, four replicate 1 cm threads dyed with Direct Blue 71 were individually subjected to microextraction.

Extractions at each design point were performed on four replicate fibers of the same length, for a total of 40 extractions. Extractions were conducted in Waters Total Recovery Vials because the narrow diameter of the vial allows the entire fiber sample to be submerged in less solvent than that of a typical conical vial, concentrating the extract. The threads were extracted by adding 1 mL of solvent, capped, and heated in an oven at 100°C for 60 min. Following extraction, the vials were uncapped and the solvents were evaporated at 95°C and then reconstituted in 1 mL of water for UPLC analysis. A Waters (Milford, MA) Acquity H-Class Quaternary Solvent UPLC coupled to a Waters PDA e $\lambda$  diode array detector for UV-visible analysis and equipped with a Waters Acquity BEH C<sub>18</sub> column (1.7  $\mu$ m particle size, 2.1 mm ID x 50 mm length) was used for all analysis. The mobile phase gradient conditions are given in Table 3. The diode array detector measured absorbance from 400-700 nm at 40 Hz and 1.2 nm resolution. The integrated area of dye peaks were used as the response, and ternary response surface models were generated using Design Expert<sup>®</sup> 7.

**Indigo Dye Extraction Optimization.** A second ternary component mixture containing chloroform, pyridine, and DMSO was studied for the extraction of indigo. As with the direct dye optimization study, five replicate fibers were extracted at each design point and then quantified by UPLC. The solvents used were DMSO, chloroform, and pyridine. Extractions were carried out at 100°C for 60 min in 1 mL of solvent. The solvent was then boiled off and samples were reconstituted in 1 mL of 50:50 methanol and water. UPLC gradient conditions for indigo analysis are listed in Table 4.

**Limits of Detection and Extract Quantitation.** Standard mixtures of direct dyes were made 1-10 ppm concentrations. The direct dye mixtures contained Direct Blue 80, Direct Blue 71, and Direct Orange 39 in 90:10 (v/v) 0.2 M ammonium acetate and acetonitrile. The dye mixtures were analyzed (five replicates) using UPLC. A calibration plot was generated for each dye and limits of detection were determined.

**Direct Dye Extraction.** For the extraction of direct dyes, fibers 1 cm in length, dyed with Direct Orange 39, Direct Blue 71, or Direct Blue 80, were cut using a fiber guillotine and loaded into total recovery vials. 100  $\mu$ L of optimal extraction solvent mixture (50% distilled water, 25% pyridine, 25% acetone) was dispensed into the vial. The vials were sealed with screw tops to minimize solvent evaporation and were placed in a laboratory oven at 100°C for 60 min. The vials were uncapped and allowed to completely evaporate in the oven at 95°C. Dye residues were reconstituted with 50  $\mu$ L 90% 0.2 M ammonium acetate and 10% acetonitrile and vortex-mixed to ensure solvation. The dyes were then analyzed by UPLC-DAD using the same chromatographic conditions as the extraction study.

**Indigo Extraction.** It was determined from the indigo extraction optimization that the optimum extraction solvent was 100% DMSO. Extractions were carried out by adding 100  $\mu$ L of DMSO

to the fibers in the vials which were then capped and heated to 100°C for 60 min. After extraction, the extractant was allowed to cool to room temperature and then injected.

Dye samples were analyzed using a diode array detector measuring absorbance from 400-700 nm. The area of the peak on the chromatogram was acquired for each dye using the corresponding maximum wavelength (for Direct Orange 39, Direct Blue 80, and Direct Blue 71 at 420, 571, and 586 nm, respectively), and compared to standard mixtures of dyes to quantify the amount of dye on each fiber.

## RESULTS AND DISCUSSION

**Extraction optimization for direct dyes.** Figure 2 displays the fitted three-dimensional surface and contour plot for the absorbance of direct dye extracts as a function of solvent conditions. Optimum absorbance is predicted at 51.5% A (water), 20.6% B (pyridine), and 27.9% C (acetone). Because the region around this optimum is relatively flat, this outcome is relatively robust: slight variations in solvent conditions do not diminish significantly the amount of dye extracted. For ease of use, 50% water, 25% pyridine, and 25% acetone was employed for direct dye extractions.

Table 5 shows variability of UPLC peak retention and area for extracts of Direct Blue 80 for ten replicate dyed cotton fibers taken from the same 1 cm thread. Variability in amounts of dye extracted from single fibers originates from several sources. The Q test rejected the data from Fiber 4 as an outlier at the 99% level of confidence. The percent relative standard deviation (%RSD) for the fiber extractions, if the datum from Fiber 4 is retained, was 47.4%.; after deleting the outlier, the RSD drops to 35.4%. These results are typical for cotton. Unlike synthetic fibers (*e.g.*, nylon), natural cotton fibers exhibit biological variety and differ in morphology among fibers and even along the length of the same fiber. Physical parameters that may differ include diameter, cross section shape, degree of fiber convolutions, and surface area. Many of these characteristics are affected by the processes to which cotton is subjected prior to dyeing, such as desizing, bleaching, or mercerization. Although mercerization (treatment with sodium hydroxide) commonly makes cotton cross section more rounded and decreases convolutions, process variations may impart variations in fiber shape.<sup>14</sup>

Figure 3 shows an optical microscopy photograph of several cotton fibers. Because cotton fiber morphology exhibits variability, dye amounts on an individual fiber can vary significantly from the other 80-100 fibers taken from the same segment of thread. Dye uptake could also be affected if fibers on the inside of the thread "shield" by those on the outside during the dyeing process,.

**Extraction optimization for indigo.** Figure 4 shows the fitted response surface for the indigo extraction optimization study. The calculated model-F value indicated that a linear model best fit the data. According to the model, the optimum extraction solvent mixture is pure DMSO. This result is favorable because mixtures of DMSO, chloroform, and pyridine when heated evolved pungent fumes that smelled characteristic of hydrogen sulfide. DMSO is also compatible with C18 stationary phase, thus the reconstitution step after dye extraction can be skipped and the extract injected after cooling to room temperature, minimizing potential sample loss during evaporation.

**UPLC of dye standards.** Separation of the direct dye standards shows that some of the dyes have multiple components. In Figure 5, Direct Orange 39 is clearly comprised of two dye

components. Many smaller peaks are also obvious in the expanded view of Figure 6. These peaks can be attributed to various "dyestuffs" that are added during the dyeing process such as compounds that aid in the dye-uptake by the fibers, finishing agents, and fluorescent brighteners. Indigo did not contain any miscellaneous peaks and its chromatogram is shown in Figure 7. UV/visible spectra for the main dye peaks are shown in Table 3.1.

**Calibration performance characteristics.** Limits of detection (LOD) and limit of quantitation (LOQ) were calculated using the equations,

$$\text{LOD} = (3.3 \times \sigma_b)/S \quad (1)$$

$$\text{LOQ} = (10 \times \sigma_b)/S \quad (2)$$

where  $\sigma_b$  is the standard deviation of the blank and  $S$  is the slope of the calibration model. LOD and LOQ values are reported in Table 6 using three different methods that differ in how  $\sigma_b$  is estimated.  $\text{LOD}_1$  and  $\text{LOQ}_1$  estimate  $\sigma_b$  using the standard deviation of the integrated noise signal across the width of the actual peak.  $\text{LOD}_2$  and  $\text{LOQ}_2$  estimate  $\sigma_b$  by calculating the standard deviation of the lowest concentration calibrator and require this concentration to be near the actual LOD to be considered accurate.  $\text{LOD}_3$  and  $\text{LOQ}_3$  estimate  $\sigma_b$  using the standard deviation of the y-intercept of the calibration line. Variance in the high concentration calibrators will increase the variance of the y-intercept leading  $\text{LOD}_3$  to provide a high estimate for limits of detection and quantitation.

Calibration models exhibited coefficients of determination of 0.9997 for Direct Orange 39 and Direct Blue 71, 0.9946 for Direct Blue 80, and 0.9986 for Indigo. The calibration plot for Direct Blue 80 is shown in Figure 8. Detection limits were below 1 ppb for three of the dyes according to  $\text{LOD}_1$  due to low and reproducible noise.  $\text{LOD}_2$  showed values in the 25-60 ppb range for the direct dyes and 6.07 ppb for Indigo.  $\text{LOD}_2$  for Indigo is lower due to the addition of a 500 ppb calibrator not present for the direct dyes. Direct Blue 80 has the lowest  $\text{LOD}_2$  value despite having higher  $\text{LOD}_1$  and  $\text{LOD}_3$  values because it has the lowest detector response of all the dyes, resulting in a lower standard deviation for the lowest calibrator. The  $\text{LOD}_3$  values are the highest overall due to the number of high concentration calibrators. Variance in the high concentration region of a calibration model can lead to high variance of the y-intercept. Together,  $\text{LOD}_1$ ,  $\text{LOD}_2$ , and  $\text{LOD}_3$  present a possible range for the true limit of detection to reside. With exception to  $\text{LOD}_3$ , all calculated detection limits indicate that detection of 2 ng of dye from a 1 mm fiber is possible.

**Trace fiber extractions.** Direct dyes were extracted and detected from fibers of lengths down to 1 mm. Because of their non-uniform morphology, cotton fibers do not lay flat. Cutting cotton fibers reproducibly to small lengths is difficult. We found that cutting an entire thread to the desired length and then unweaving the fibers from that thread produced many fibers of lengths very close to the desired length. These fibers can then be examined under a magnifying glass using a ruler and similar length fibers can be selected. As fiber length decreases down to 1 mm, handling of the fibers becomes difficult. It is very important to ensure that the fiber is deposited on the bottom of the inside of the vial, and that extractant covers the entire fiber. Additionally, during the extractant evaporation stage, care must be taken to not let the extractant boil. Otherwise extracted dye will be deposited all over the inside of the vial and lower the amount that is successfully reconstituted.

A batch of three 1 mm fibers that were cut from a thread dyed with Direct Blue 71 were analyzed. Of the three samples, only one was extracted successfully. This was due entirely to the difficulty of handling 1 mm fibers. The chromatogram for the 1 mm fiber extract is shown in Figure 9. The dye peak is located at 1.85 min. The RMS signal-to-noise for the dye peak of interest is 118.05. The negative response and sloping baseline is due to the mobile phase gradient response on the UV/visible detector.

Another extraction study was conducted on 5 mm fibers to compare their extraction success to the 1 mm extraction study. Five samples were taken from the same 5 mm thread and similar length fibers were chosen for extraction. Of the five samples, four were extracted successfully and the data is presented in Table 7. The %RSD for the four successful 5 mm extractions was 38.73% and is comparable to the 35.42% RSD for the 1 cm reproducibility study.

Indigo was successfully extracted from a 1 mm fiber and detected by UPLC-DAD. A set of five 1 mm indigo-dyed cotton fibers were extracted using DMSO. Because DMSO has such a high boiling point and is compatible with the C18 stationary phase, the boil-off and reconstitute step of the extraction process was skipped, and the extract was injected directly into the UPLC after cooling to room temperature. The extract chromatogram had a RMS signal-to-noise of 62.80 and is shown in Figure 10.

## CONCLUSIONS

Solvent conditions were optimized for the extraction of direct and indigo dyes from cotton. UPLC separation methods were also devised that, together with the optimized extraction conditions, was successful in detecting extracts from single 1 mm length fibers with RMS signal- to-noise ratios of 118.05 and 62.80 for Direct Blue 71 and Indigo respectively. Calibration models yielded limits of detection and quantification as low as 2.1 pg and 6.2 pg for Direct Blue 721 and Indigo, respectively, supporting the analysis of sub-millimeter length fibers. Handling fibers of millimeter and sub-millimeter lengths continues to be a challenge and new fiber handling techniques need to be developed. Future work will involve mass spectrometry characterization of the various dye stuffs present in the dye standards as well as characterizing finishing agents from fiber extracts.

## ACKNOWLEDGMENTS

This research was supported by award 2010-DN-BX-K245 from the National Institute of Justice, Office of Justice Programs, U. S. Department of Justice. The opinions, findings, and conclusions or recommendations expressed in this publication are those of the author(s) and do not necessarily reflect those of the Department of Justice. Mention of commercial products does not imply endorsement on the part of the National Institute of Justice.

## REFERENCES

- (1) Robertson, J.; Grieve, M. *Forensic Examination of Fibres*; 2nd ed.; Taylor & Francis: London, 1999.
- (2) Rendle, D. F.; Wiggins, K. G. Forensic analysis of textile fibre dyes. *Review of Progress in Coloration and Related Topics* **1995**, *25*, 29–34.
- (3) Gaudette, B. D. The forensic aspects of textile fiber examination. Chapter 5 in: *Forensic Science Handbook*, vol. 2, R. Saferstein, Ed.; Prentice Hall: Englewood Cliffs, NJ, 1988.
- (4) Macrae, R.; Smalldon, K. The Extraction of Dyestuffs from Single Wool Fibers. *J. Forensic Sci.* **1979**, *24*, 109–116.

- (5) Shore, J.; Colourists, S. of D. and *Colorants and Auxiliaries: Colorants*; Society of Dyers and Colourists, 2002.
- (6) Laing, D.; Dudley, R.; Hartshorn, A.; Home, J.; Rickard, R.; Bennet, D. The extraction and classification of dyes from cotton and viscose fibres. *Forensic Sci.Int.* **1991**, *50*, 23–35.
- (7) Cheng, J.; Wanogho, S. O.; Watson, N. D.; Caddy, B. The extraction and classification of dyes from cotton fibres using different solvent systems. *J. Forensic Sci. Soc.* **1991**, *31*, 31–40.
- (8) Meksi, N.; Ben Ticha, M.; Kechida, M.; Mhenni, M. F. Using of ecofriendly  $\alpha$ -hydroxycarbonyls as reducing agents to replace sodium dithionite in indigo dyeing processes. *Journal of Cleaner Production* **2012**, *24*, 149–158.
- (9) Hunger, K. *Industrial dyes: Chemistry, Properties, Applications*; Wiley-VCH, 2003.
- (10) Surowiec, I.; Quye, A.; Trojanowicz, M. Liquid chromatography determination of natural dyes in extracts from historical Scottish textiles excavated from peat bogs. *J. Chromatogr. A* **2006**, *1112*, 209–17.
- (11) Michel, R. H.; Lazar, J.; McGovern, P. E. The chemical composition of the indigoid dyes derived from the hypobranchial glandular secretions of Murex molluscs. *Journal of the Society of Dyers and Colourists* **1992**, *108*, 145–150.
- (12) Deming, S. N.; Morgan, S. L. *Experimental Design: A Chemometric Approach*, 2nd ed., Elsevier Science Publishers, Amsterdam, 1993.
- (13) Smith, W. F. *Experimental Design for Formulation*, Society for Industrial and Applied Mathematics, Philadelphia, PA, 2005.
- (14) Cotton Incorporated Staff, C. I. *Cotton Dyeing and Finishing: A Technical Guide*; Cotton, Incorporated, Cary, NC, 1997.

Table 1. Structures and spectra of direct dyes and indigo.

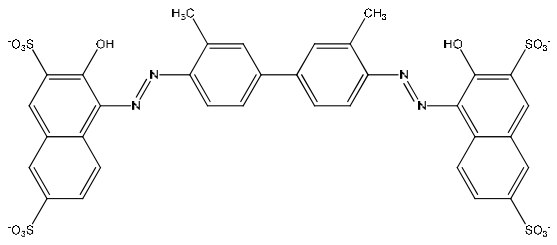
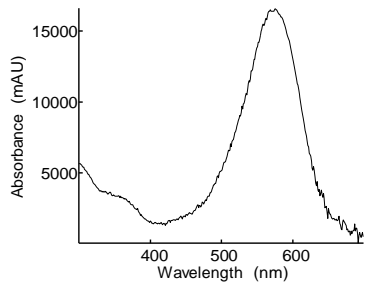
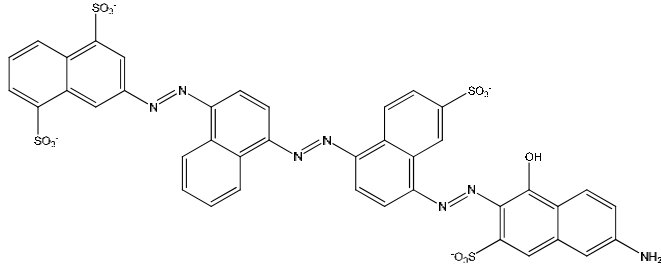
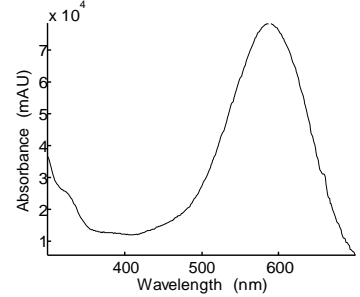
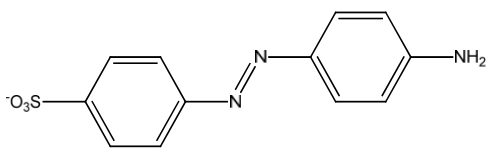
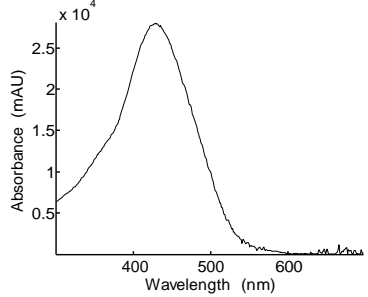
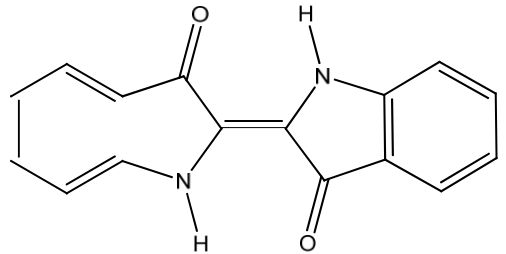
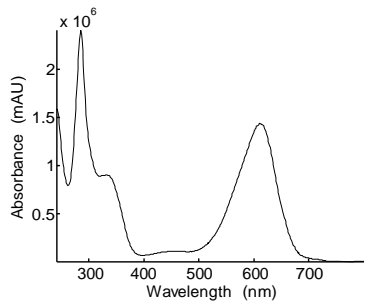
Structure	Absorbance Spectra
 <p>Direct Blue 80</p>	
 <p>Direct Blue 71</p>	
 <p>Direct Orange 39</p>	
 <p>Indigo</p>	

Table 2. Solvent compositions for each design point for the extraction optimization for direct-dyed cotton fibers.

Design Point	A: Water (%)	B: Pyridine (%)	C: Acetone (%)
1	100	0	0
2	0	100	0
3	0	0	100
4	50	50	0
5	50	0	50
6	0	50	50
7	33.33	33.33	33.33
8	66.66	16.66	16.66
9	16.66	66.66	16.66
10	16.66	16.66	66.66

Table 3. Mobile phase conditions for the analysis of direct dyes by UPLC.

Time (min)	Flow Rate (mL/min)	% Methanol	% 0.2 M Ammonium Acetate	% Acetonitrile
Initial	0.45	5	90	5
5	0.45	5	5	90
6	0.45	5	90	5
8	0.45	5	90	5

Table 4. Mobile phase conditions for the analysis of indigo by UPLC.

Time (min)	Flow Rate (mL/min)	% Water (0.15% Formic Acid)	% Methanol
0	0.5	70	30
0.25	0.5	70	30
2	0.5	0	100
3	0.5	0	100
3.1	0.5	70	30
5.5	0.5	70	30

Table 5. Peak retention time and area reproducibility for 1 cm fibers dyed with Direct Blue 80.

Fiber	Retention time (min)	Area (counts)
1	1.34	28667.68
2	1.35	14122.29
3	1.34	25609.83
4	1.33	68574.72
5	1.34	34615.79
6	1.34	21941.95
7	1.34	37175.18
8	1.33	49014.68
9	1.34	33480.44
10	1.34	20549.12

Table 6. Limits of detection and quantitation of the direct and indigo dyes. Calculations based on the standard deviation of the blanks (LOD/LOQ<sub>1</sub>), the standard deviation of the lowest concentration calibrator (LOD/LOQ<sub>2</sub>), and the standard deviation of the y-intercept of the calibration plot (LOD/LOQ<sub>3</sub>).

Dye	R <sup>2</sup>	LOD <sub>1</sub> (ppb)	LOD <sub>2</sub> (ppb)	LOD <sub>3</sub> (ppb)	LOQ <sub>1</sub> (ppb)	LOQ <sub>2</sub> (ppb)	LOQ <sub>3</sub> (ppb)
Direct Blue 80	0.9946	1.39	26.3	166	4.21	79.7	503.03
Direct Orange 39	0.9997	0.83	59.3	39.6	2.5	179.7	120
Direct Blue 71	0.9997	0.21	44.2	39.5	0.63	133.94	119.7
Indigo	0.9986	0.74	6.07	79.9	2.23	18.39	242.12

Table 7. Peak areas for four 5 mm fiber extracts for Direct Blue 71.

Fiber	Peak Area
1	19319.44
2	25204.23
3	28823.84
4	10275.35
%RSD	38.73

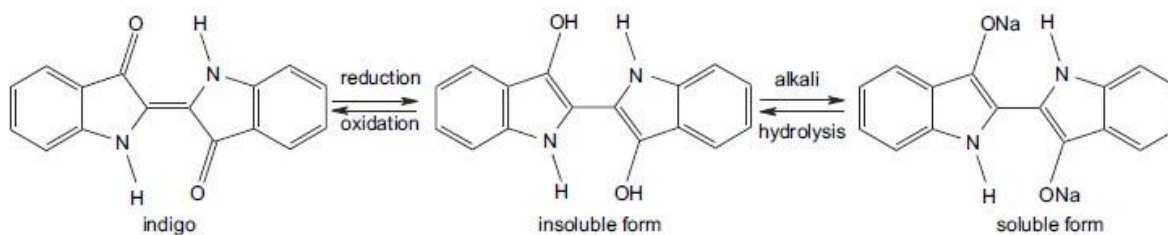


Figure 1. Reduction of indigo to its water-soluble leuco form.

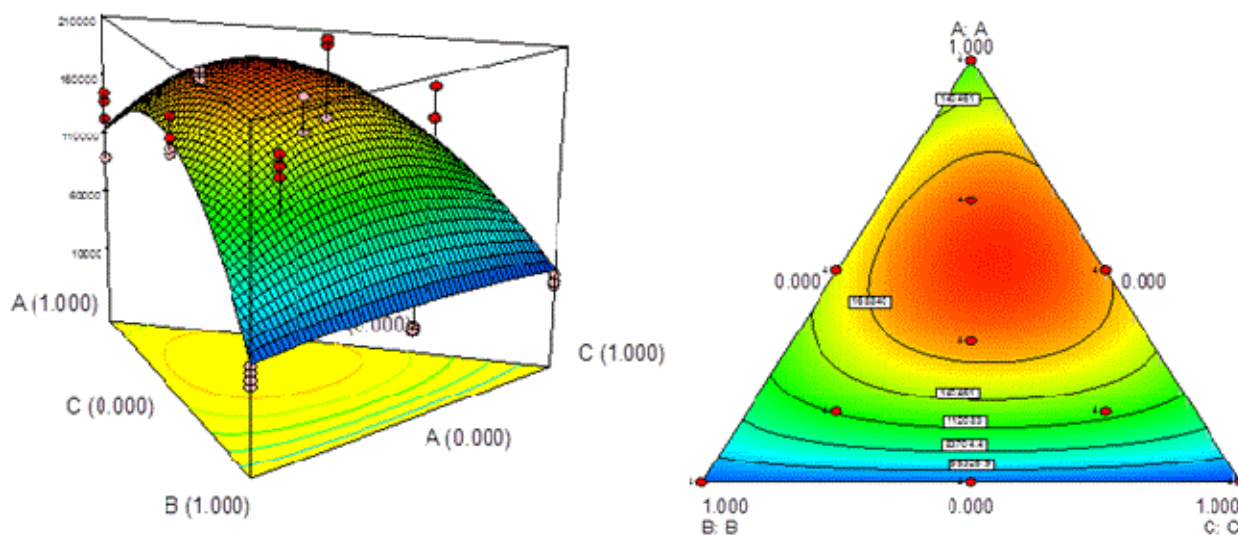


Figure 2. Perspective view (left) and contour plot (right) of fitted absorbance response surface for direct dye extraction as a function of solvent conditions. Design points from Table 3.2 are indicated by solid dots. A, Water; B, Pyridine; C, Acetone.

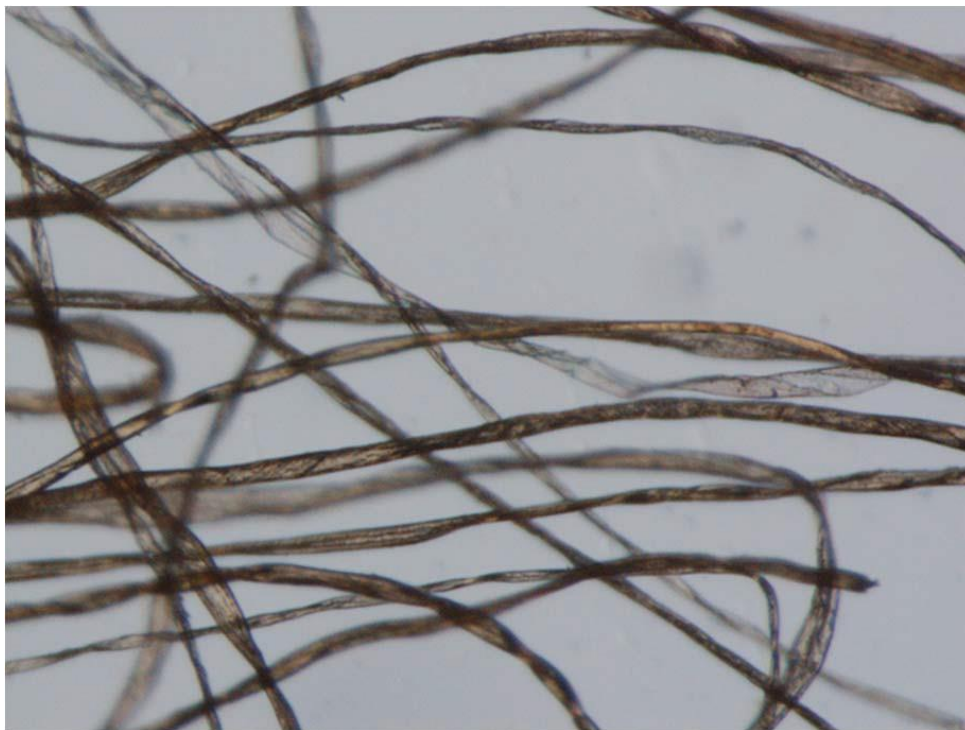


Figure 3. Optical microscope image (magnification 12.5 $\times$ ) of cotton fibers dyed with Direct Orange 39.

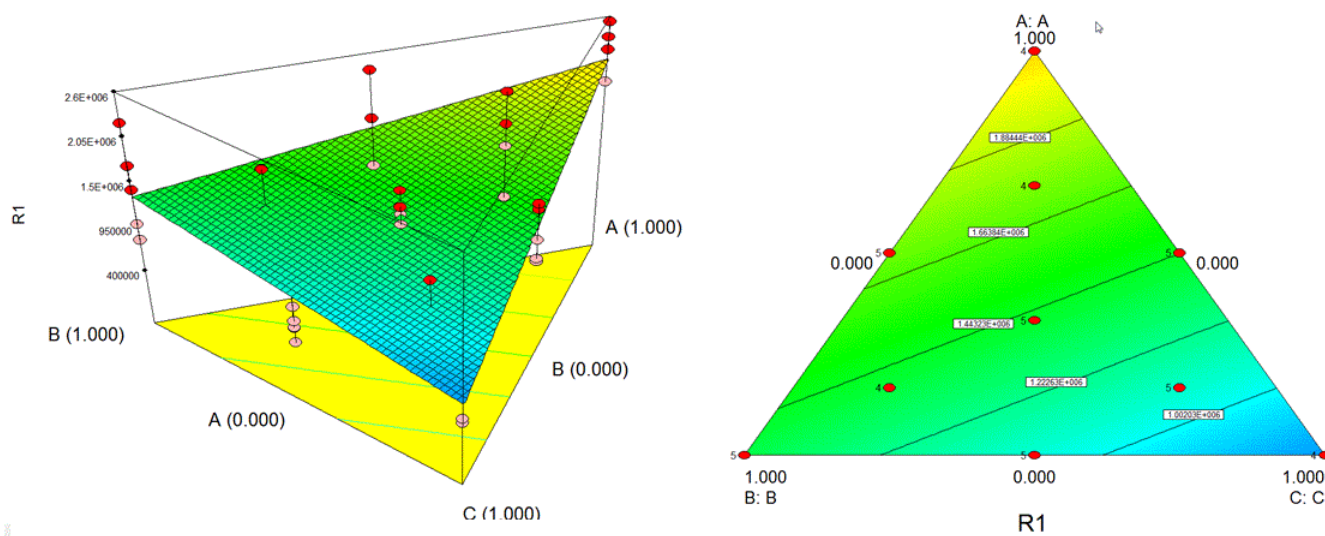


Figure 4. Fitted linear absorbance response surface for indigo dye extraction from cotton as a function of solvent conditions. Design points follow those from Table 4.2 and are indicated by solid dots. Solvent components: (A) DMSO; (B) chloroform; and, (C) pyridine.

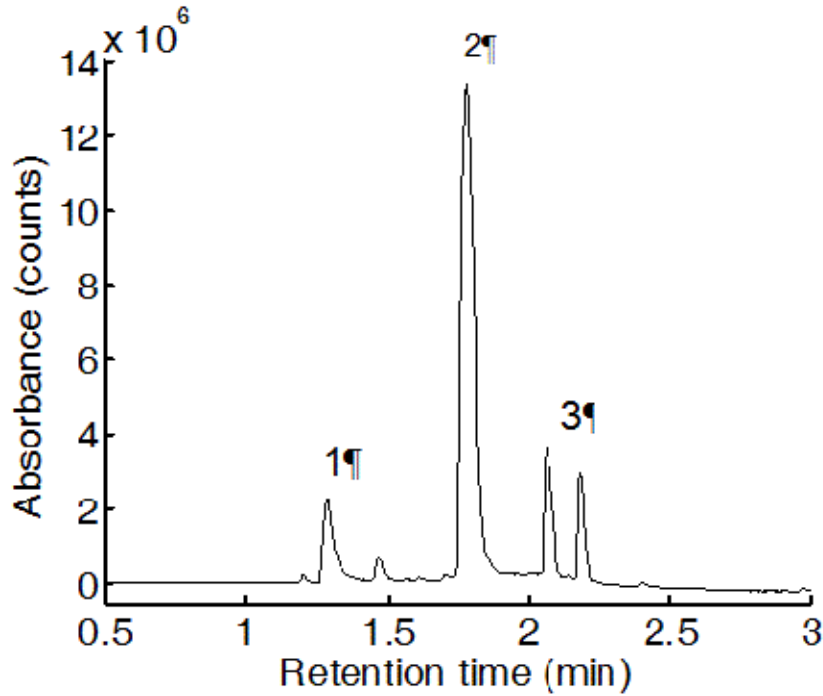


Figure 5. Chromatogram showing separation of all three direct dyes. Peak identification: (1) Direct Blue 80; (2) Direct Blue 71; and. (3) Direct Orange 39.

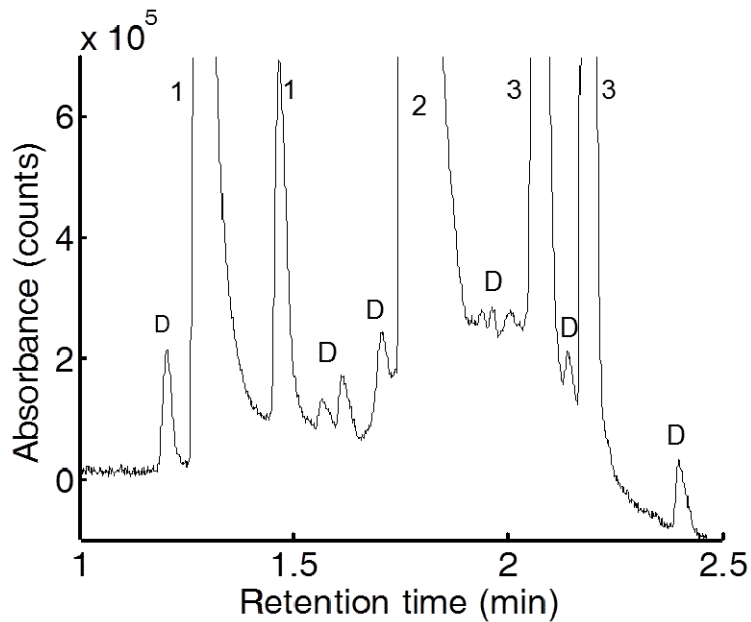


Figure 6. Expanded view of multiple direct dye components in the chromatographic region of 1 to 2.5 min from Figure 5. Peak identification: (1) Direct Blue 80; (2) Direct Blue 71; (3) Direct Orange 39; (D) miscellaneous dye stuffs.

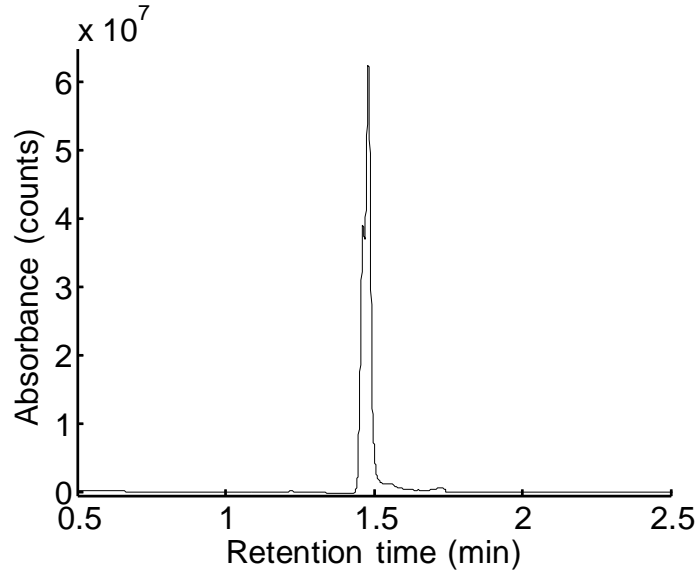


Figure 7. UPLC-DAD chromatogram of indigo dye sample.

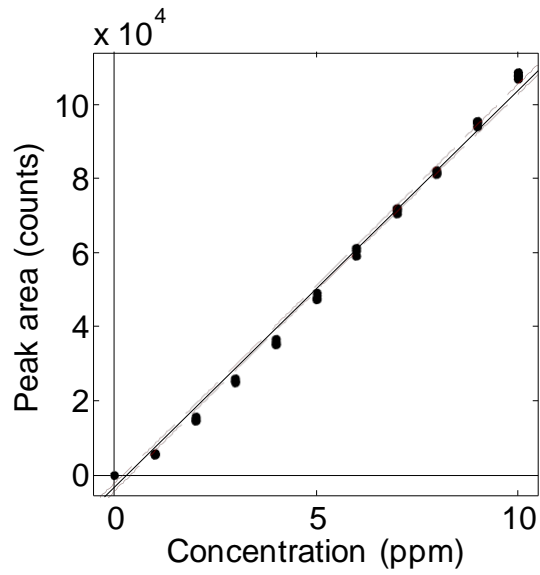


Figure 8. Calibration relationship for Direct Blue 80.

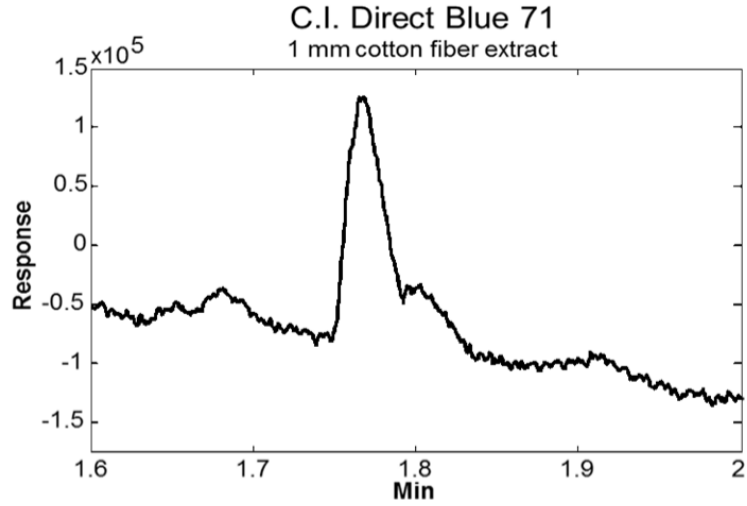


Figure 9. Chromatogram showing extraction of Direct Blue 71 from a 1 mm single fiber.

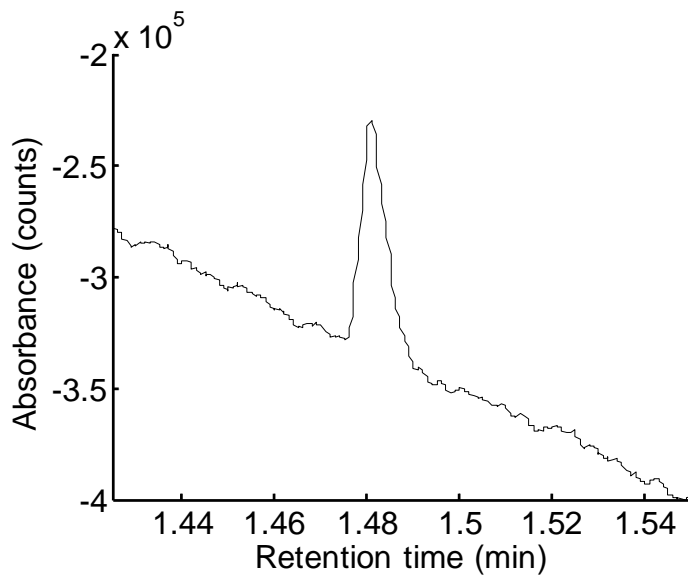


Figure 10. Chromatogram showing extraction of indigo from a single 1 mm cotton fiber.

### **C. Extraction and characterization of reactive dyes and their hydrolysis products from trace cotton fibers by ultra-performance liquid chromatography**

Scott J. Hoy, Molly R. Burnip, and Stephen L. Morgan, Department of Chemistry and Biochemistry, University of South Carolina, Columbia, SC 29208

#### **ABSTRACT**

Microextraction and ultra-performance liquid chromatography methods have been developed for reactive dyes on cotton. Reactive dyes are chemically bound to the cellulose structure of the fiber and present an analytical challenge to the forensic fiber examiner because release of these dyes requires breaking of the covalent bond using hot sodium hydroxide. The resulting hydrolysis reactions can also cleave amide bonds and possibly other chemical bonds in the dye molecule. The various structural changes that can take place leads, in many cases, to production of multiple reaction products from a single dye molecule. We demonstrate successful extraction of reactive dyes from single 1 mm cotton fibers with detection limits as low as 3.3 pg. Systematic experiments at varying reaction conditions, with product analysis by mass spectrometry, were also performed to characterize the degradation of reactive dyes under hydrolysis, and to facilitate interpretation of reactive dye extractions.

#### **INTRODUCTION**

Population studies have shown cotton to be the most common textile fiber found on indoor and outdoor surfaces.<sup>1-3</sup> Cotton fibers are unique in the textile industry because they can be dyed with three different classes of dyes: direct, vat, and reactive. Reactive dyes differ from most other dye classes in that they are covalently bound to the fiber. This makes reactive dyes the most substantive of dyes used on cotton because the covalent bonding of the dye to the fiber provides excellent fastness to laundering. As a result, reactive dyes are the most popular dye class used to color cotton textiles. Figure 1 summarizes worldwide consumption of cotton dyes in 2003, showing that reactive dyes constitute 50% of all dyes on cotton textiles.<sup>4</sup>

The reactive dyeing process typically involves the reaction of a haloheterocycle such as a chlorotriazine on the dye with a hydroxyl group on the fiber.<sup>5,6</sup> Reactive dyes can also attach to cotton via vinylsulphone groups that form activated alkenes when treated with sodium hydroxide, as shown in Figure 2. The extraction of reactive dyes from cotton requires the hydrolysis of the covalent bond using sodium hydroxide at elevated temperatures via the mechanism shown in Figure 3.<sup>6</sup>

This study focuses on the extraction of reactive dyes from cotton followed by separation and detection using ultra-performance liquid chromatography (UPLC). This chemical extraction process is destructive to the fiber and the dyes because sodium hydroxide and heat are used to break the covalent fiber-dye bond. Our research hypothesis is that, despite chemical degradation of the original dye to various products, separation of the resulting product mixture and (ultimately, identification of components by mass spectrometry) can provide forensic profiling to discriminate reactive dyes from one another. Improved understanding of reactive dye degradation can also assist interpretation of extracted components and potentially enable identification of the parent reactive dye. Trace evidence fibers can often be as short as 10 mm and contain between 2-200 ng of dye.<sup>7</sup> Our goal in the present work was the optimization of microextraction and UPLC conditions for analysis of reactive dyes from single 1 mm cotton fibers.

## EXPERIMENTAL

Analytical grade water, sodium hydroxide, ammonium acetate, ammonium hydroxide, and HPLC/UPLC grade acetonitrile were purchased from Fisher Scientific (Pittsburg, PA).

Dyed fabrics and matching dyes standards were current production samples donated by dyestuff manufacturers in the southeastern United States. Dye names reported here follow the Color Index nomenclature (Society of Dyers and Colourists, Bradford, UK). All fibers were dyed at levels consistent with commercial use (2-4% by weight). All dye standards were solid in phase and stored in a dark room to avoid photodegradation.

Literature has suggested that 1.5% NaOH and heat should be used to facilitate the extraction of reactive dyes from cotton.<sup>6-12</sup> Previous reactive dye extraction work in our laboratory has also employed these conditions.<sup>6</sup> Hydrolysis presents a number of potential issues. The dye to be extracted may change its chemical form under hydrolysis conditions. Strongly alkaline solutions are also not compatible with many stationary phases for liquid chromatography. In the present work, reactive dye standards were treated with 1.5% sodium hydroxide and heated at 100 °C for 60 min. The resulting solution was then treated with equimolar hydrochloric acid to neutralize any excess sodium hydroxide remaining prior to liquid chromatography.

Fibers of lengths 10 mm, 5 mm, and 1 mm dyed with Reactive Yellow 160, Reactive Blue 220, or Reactive Orange 72 (structures shown in Table 1) were cut with a fiber guillotine and placed into 200 µL conical Total Recovery Vials (Waters Associates, Milford, MA). A 50 µL aliquot of 0.1875 M sodium hydroxide was dispensed into the vial and sealed to prevent evaporation. Extraction was carried out in the laboratory oven at 100°C for 60 min. The dyes were reconstituted by addition in sequence of 25 µL of 0.375 M hydrochloric acid (equimolar with the sodium hydroxide), Aliquots containing 25 µL of 10 mM ammonium acetate adjusted to pH 9.3. Dyes were separated using a Waters Acquity UPLC system coupled to a diode array detector (DAD). The system was equipped with a room temperature sample manager and a Waters Acquity BEH C18 column (1.7 µm particle size, 2.1 mm ID × 50 mm length) heated to 40 °C. The mobile phase solvent gradient conditions employed for all runs is listed in Table 2. The sample injection volumes were 10 µL.

Dyes samples were detected using a UV/visible diode array detector scanning absorbance from 300-700 nm. The peak area on the chromatogram was acquired for each dye using the corresponding maximum wavelength (for Reactive Yellow 160, Reactive Blue 220, and Reactive Orange 72 at 405 nm, 610 nm, and 478 nm, respectively), and was used for comparison to standard dye mixtures to determine the amount of dye on each fiber.

Limits of detection and quantitation were determined from calibration models based on the UPLC-DAD analysis of reactive dye standards at varying concentrations. Calibration solutions were made for each dye in water at concentrations 100 ppb, 200 ppb, 400 ppb, 600 ppb, 800 ppb, and 1000 ppb. Five replicates samples were prepared at each concentration level and analyzed by UPLC with UV/visible detection.

## RESULTS AND DISCUSSION

A chromatogram showing the separation of the mixture of three reactive dyes is shown in Figure 4. Figure 5 shows a magnified view of the retention time window for 0.75 to 2.75 min within

which multiple additional components are present. As indicated, most of these peaks have UV/visible absorbance spectra that match those of the one of three primary reactive dyes. We initially assumed that these peaks are secondary degradation products derived from the corresponding primary dyes, or represent other contaminants introduced during the dye manufacturing process. UV/visible absorbance spectra of the main dye peaks are shown in Table 1. During method development, the first eluting peak, Reactive Blue 220, displayed poor chromatographic peak shape and lower peak height than the other dyes. The addition to the mobile phase of 10 mM ammonium acetate adjusted to pH 9.3 resulted in sharpening this peak.

**UPLC-DAD analysis of extracted reactive dyes.** UPLC-DAD analysis of reactive dyes treated with 1.5% NaOH confirmed that additional reactions occur during the extraction process. Figure 6 shows the chromatograms for Reactive Orange 72 standard and “extracted” (treated with NaOH). The standard chromatogram shows a single peak corresponding to the dye with an absorbance maximum of 478 nm. The extracted chromatogram shows two peaks, both of which increased in retention, and the main peak having an absorbance maximum of 473 nm. Because the second peak showed a similar absorbance maximum, we hypothesized that both peaks were “dye” and that one of the peaks was due to the incomplete base-hydrolysis of the dye standard.

To test this hypothesis, a nominal starting ratio of NaOH to dye was first established. Assuming that a single 1 cm cotton fiber contained 20 ng of dye, using 50  $\mu\text{L}$  of 1.5% NaOH to extract the dye from the fiber gives a ratio of  $9.375 \times 10^{-7}$  moles of NaOH to 1 ng of dye. For the purposes of later comparisons, other ratios were expressed as a percentage of this value. Several 1 ppm standards of Reactive Orange 72 were then treated with amounts of NaOH varying 10%-150% of that amount, neutralized with equimolar HCl, and analyzed by UPLC-DAD. Figure 7 displays the dependence of the resulting peak areas on NaOH amount. Approximately 50% of the nominal amount of NaOH is required to completely hydrolyze the dye molecule. Due to the variability of the amount of dye on cotton fibers, 75% of the nominal amount was selected as a compromise between ensuring complete extraction and hydrolysis of the dye and maintaining a low amount of NaOH in solution. Thus, a 1 cm length of a single cotton fiber requires 50  $\mu\text{L}$  of 0.28125 M NaOH for the extraction of a reactive dye. The amount of NaOH can then be adjusted depending on the length of the cotton fiber of interest.

**HPLC-MS of reactive dyes.** HPLC-MS confirms that reactive dyes undergo additional reactions during NaOH extraction from cotton. Both C. I. Reactive Orange 72 and Reactive Yellow 160 were analyzed using negative-ion electrospray ionization (ESI-) mass spectrometry. C. I. Reactive Blue 220 did not appear in HPLC-MS due to the requirements of using an acidic buffer for the MS analysis (basic buffer is required to maintain a proper chromatographic peak shape for Reactive Blue 220).

Analysis of the C. I. Reactive Yellow 160 standard by HPLC-MS shows at least four derivatives of the dye molecule (Figure 8). The molecular mass of Reactive Yellow 160 is 653 g/mol and elutes at a retention time of 16.61 min with a characteristic ion of  $m/z$  652 due to deprotonation of the dye in solution. Derivatives of this molecule appearing at  $m/z$  572 and 554 are probably due to the loss of a sulfonic acid and a sulfate functional group, respectively. The longer retention time for these products can be attributed to the decrease in their mobile phase solubility on losing these functional groups, and their increased affinity for the non-polar  $\text{C}_{18}$  stationary phase. Additional fragments of mass  $m/z$  572 and 554 appear in the mass spectra of Reactive Yellow 160 peak at 16.61 min. The structure of the component of  $m/z$  614 is unknown, however

it has an almost identical absorbance spectra to that of the dye molecule and its other derivatives (Figure 9), suggesting that it also is a derivative of the dye.

Further experiments were conducted to evaluate the effect of sodium hydroxide treatment on reactive dyes. Treatment of Reactive Yellow 160 dye standard with NaOH to simulate the extraction conditions yielded two products observable by HPLC-MS (ESI-), as shown in Figure 10. The combination of NaOH and heat (100°C) hydrolyzes the amide bond and removes the sulfate group, as seen in the second product at 18.66 min. This compound fragments further with the cleavage of the azo group. Because this compound is a beta-keto acid, it undergoes decarboxylation under basic conditions and heat, with loss of carbon dioxide, resulting in the product eluting at 15.07 min.

Analysis of the Reactive Orange 72 dye standard by HPLC-MS also shows multiple derivatives of the dye. The total ion chromatogram shows only a single chromatographic peak with a mass spectrum containing a spectral peak at 474 m/z, as seen in Figure 11. This result is unexpected because the reported mass for Reactive Orange 72 is 572 g/mol. Isolation of 572 m/z from the chromatogram yields a broad chromatographic peak, and the combined spectra for this peak shows what appears at first glance to be a fragmentation pattern for the dye molecule. However, ESI should not yield much, if any, fragmentation as it is a “soft” ionization technique. Extraction of the prominent masses 572 m/z, 492 m/z, 474 m/z, and 417 m/z from the TIC yields four separated chromatographic peaks, shown in Figure 12, suggesting that our Reactive Orange 72 dye standard is actually a mixture of multiple compounds. The combination of this result for Reactive Orange 72 with the multiple derivatives of Reactive Yellow 160 suggests mixtures of multiple compounds may be common for all reactive dyes.

Reactive Orange 72 was also treated with NaOH to simulate an extraction. The resulting chromatogram, shown in Figure 13, as expected only contained one peak of interest. Unlike Reactive Yellow 160, Reactive Orange 72 has an “external” amide bond which upon hydrolysis leaves the bulk of the dye molecule unchanged.

#### *Limits of Detection*

Limits of detection (LOD) and limit of quantitation (LOQ) were calculated using

$$\text{LOD} = (3.3 \times \sigma_b)/S \quad (1)$$

$$\text{LOQ} = (10 \times \sigma_b)/S \quad (2)$$

where  $\sigma_b$  is the standard deviation of the blank and S is the slope of the calibration model. LOD and LOQ values are reported in Table 6 using three different methods that differ in how  $\sigma_b$  is estimated.  $\text{LOD}_1$  and  $\text{LOQ}_1$  estimate  $\sigma_b$  using the standard deviation of the integrated noise signal across the width of the actual peak.  $\text{LOD}_2$  and  $\text{LOQ}_2$  estimate  $\sigma_b$  by calculating the standard deviation of the lowest concentration calibrator and requires this concentration to be near the actual LOD to be considered accurate.  $\text{LOD}_3$  and  $\text{LOQ}_3$  estimate  $\sigma_b$  using the standard deviation of the y-intercept of the calibration line. Variance in the high concentration calibrators will increase the variance of the y-intercept leading  $\text{LOD}_3$  to provide a high estimate for limits of detection and quantitation.

The calibration models produced high coefficients of determination of 0.9987 for Reactive Yellow 160, 0.9989 for Reactive Blue 220, and 0.9993 for Reactive Orange 72. All three LOD estimates yield LOD detection limits in the 3 pg to 83 pg range (based 10  $\mu\text{L}$  injections) which is

low enough to detect extracts from 1 mm fibers. LOQ values range from 10 pg and 252 pg and suggests the possibility of conducting quantitative comparisons between 1 mm fiber extracts.

*Trace fiber extractions.* All three reactive dyes were extracted and detected from fibers of lengths down to 1 mm. Because of their non-uniform morphology, cotton fibers do not lay flat. Cutting and handling cotton fibers reproducibly as their length decreases to 1 mm requires patience and practice. The reactive extractions showed the same amount of variance in the amount extracted from equal length fibers from the same thread. This variance is explained by the biological nature of cotton which produces fibers of different diameters and shapes capable of containing different amounts of dye. Analysis of this variability was conducted in Chapter 3. Figure 17 shows successful extraction and detection of a 10 mm, 5 mm, and 1 mm cotton fiber dyed with Reactive Yellow 160. Close inspection of the 1 mm extraction chromatogram suggests that 1 mm fibers dyed with Reactive Yellow 160 are near the detectable fiber length limit of this method. The calibration model for Reactive Yellow 160 returns concentrations of 135 ppb, 35 ppb, and 12 ppb for the 10 mm, 5 mm, and 1 mm extractions respectively. Comparing these values to those in Table 3 confirms that the 1 mm extract of Reactive Yellow 160 is detectable.

## CONCLUSIONS

Methods for the extraction of reactive dyes from cotton using sodium hydroxide have been reported. Extraction using hot sodium hydroxide results in hydrolysis of the dye-cellulose bond as well as hydrolysis of the amide bonds in the dye molecule. We have established a scientific basis for interpretation of multiple derivative products produced by the hydrolysis-driven extraction of reactive dyes from cotton—one that may add information to the task of reactive dye identification.

Extraction methods developed for basic dyes on acrylic, acid dyes on nylon, and disperse dyes on polyester fibers involve extraction with solvents that do not affect the chemical composition of the polymer, and thus do not impose limitations on use of the fiber for further examinations. With acrylic, nylon, or polyester fibers, IR can be conducted on previously extracted samples if needed. Extraction of reactive dyes from cotton requires base hydrolysis with sodium hydroxide to disrupt their covalent bonding. In this work, use of 0.1875 M sodium hydroxide did not result in chemical products from cellulose itself. We have demonstrated that base hydrolysis reaction can also produce derivatives of the original reactive dye which show up in the resulting chromatograms. It remains to be tested as to whether the cotton fiber remaining after extraction produces identical IR spectra compared to the sample prior to extraction. UPLC-DAD produced detection limits in the range of 0.33-1.42 ppb and quantitation limits as low as 1.00-4.30 ppb. Detection and quantification of extracts from single of 1-10 mm cotton fibers dyed with several reactive dyes were confirmed.

## ACKNOWLEDGMENTS

This research was supported by award 2010-DN-BX-K245 from the National Institute of Justice, Office of Justice Programs, U. S. Department of Justice. The opinions, findings, and conclusions or recommendations expressed in this publication are those of the author(s) and do not necessarily reflect those of the Department of Justice. Mention of commercial products does not imply endorsement on the part of the National Institute of Justice.

## REFERENCES

- (1) S. Cantrell, C. Roux, P. Maynard, J. Robertson, A textile fibre survey as an aid to the interpretation of fibre evidence in the Sydney region, *Forensic Sci. Int.* **123** (2001) 48-53.
- (2) R. Watt, C. Roux, J. Robertson, The population of coloured textile fibres in domestic washing machines, *Sci. Justice* **45** (2005) 75-83.
- (3) M.C. Grieve, T.W. Biermann, The population of coloured textile fibres on outdoor surfaces, *Sci. Justice* **37** (1997) 231-239.
- (4) Bozic, M.; Kokol, V. Ecological alternatives to the reduction and oxidation processes in dyeing with vat and sulphur dyes. *Dyes and Pigments*, **2008**, *76*, 299-309.
- (5) Christie, R. *Colour Chemistry*. RSC Paperbacks: Cambridge, England, 2001.
- (6) Dockery, C. R.; Stefan, A R.; Nieuwland, a a; Roberson, S. N.; Baguley, B. M.; Hendrix, J. E.; Morgan, S. L. Automated extraction of direct, reactive, and vat dyes from cellulosic fibers for forensic analysis by capillary electrophoresis. *Anal. Bioanal. Chem* **2009**, *394*, 2095–103.
- (7) Christie, R. *Colour Chemistry*. RSC Paperbacks: Cambridge, England, 2001.
- (8) Shore, J. *Colorants and Auxiliaries*, vol. 1, 2nd edition. Society of Dyers and Colourists, West Yorkshire: England, 2002; pp. 18–23.
- (9) Gaudette, B. D. The forensic aspects of textile fiber examination. Chapter 5 in: *Forensic Science Handbook*, vol. 2, R. Saferstein, Ed.; Prentice Hall: Englewood Cliffs, NJ, 1988.
- (10) Home, J.; Dudley, R. Thin-layer chromatography of dyes extracted from cellulosic fibres. *Forensic Sci.Int.* **1981**, *17*, 71–78.
- (11) Sirén, H.; Sulkava, R. Determination of black dyes from cotton and wool fibers by capillary zone electrophoresis with UV detection: application of marker technique. *J. Chromatogr. A* **1995**, *717*, 149-155.
- (12) Xu, X.; Leijenhorst, H.; Van den Hoven, P.; De Koeijer, J.A.; Logtenberg, H. Analysis of single textile fibres by sample-induced isotachopheresis-micellar electrokinetic capillary chromatography. *Sci. Justice* **2001**, *41*, 93-105.

Table 1. Structures and absorbance spectra for reactive dyes.

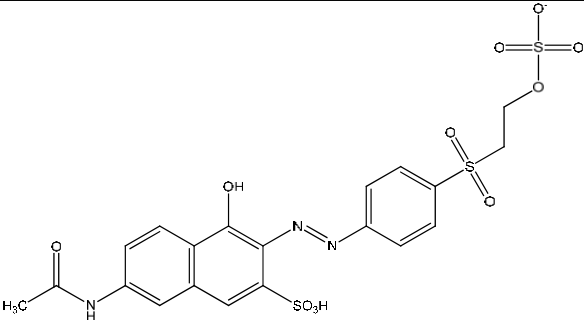
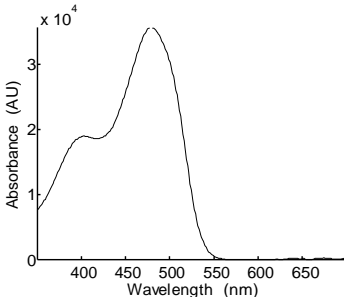
Structure	Absorbance Spectrum
 <p style="text-align: center;">Reactive Orange 72</p>	



Table 2. Mobile phase conditions for the analysis of reactive dyes by UPLC.

Time (min)	Flow rate (mL/min)	% 1) mM Ammonium acetate (pH 9.3)	% Acetonitrile
Initial	0.400	95	5
2	0.400	50	50
3	0.400	95	5
5	0.400	95	5

Table 3. Limits of detection and quantitation of the reactive dyes. Calculated based on the standard deviation of the blanks (LOD/LOQ<sub>1</sub>), the standard deviation of the lowest concentration calibrator (LOD/LOQ<sub>2</sub>), and the standard deviation of the y-intercept of the calibration plot (LOD/LOQ<sub>3</sub>).

Dye	R <sup>2</sup>	LOD <sub>1</sub> (ppb)	LOD <sub>2</sub> (ppb)	LOD <sub>3</sub> (ppb)	LOQ <sub>1</sub> (ppb)	LOQ <sub>2</sub> (ppb)	LOQ <sub>3</sub> (ppb)
Reactive Yellow 160	0.9987	0.33	2.68	8.31	1.00	8.12	25.18
Reactive Blue 220	0.9989	1.42	6.81	8.09	4.30	20.64	24.52
Reactive Orange 72	0.9993	1.05	1.50	6.31	3.18	4.55	19.12

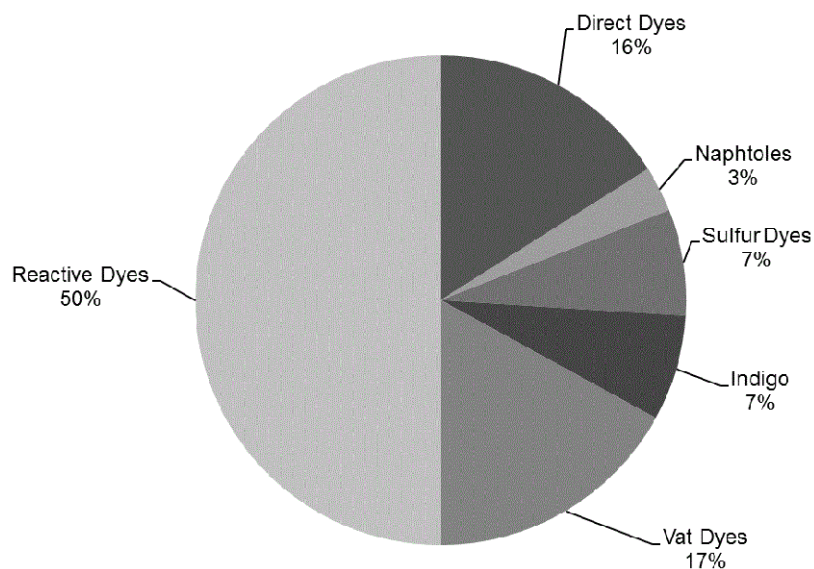


Figure 1. Worldwide consumption of cotton dyes.<sup>1</sup>

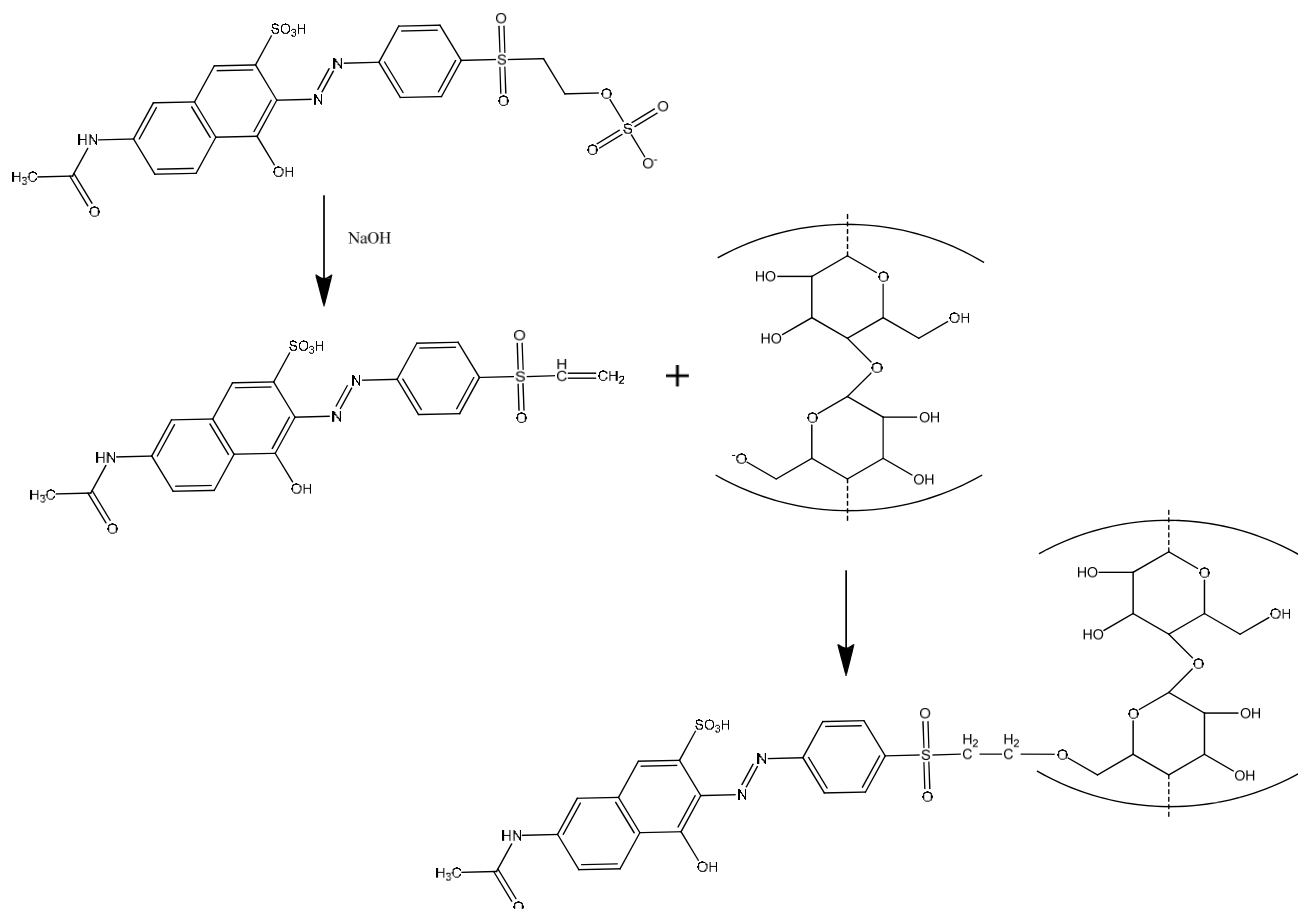


Figure 2. Mechanism for the dyeing of cellulose by Reactive Orange 72.<sup>5</sup>

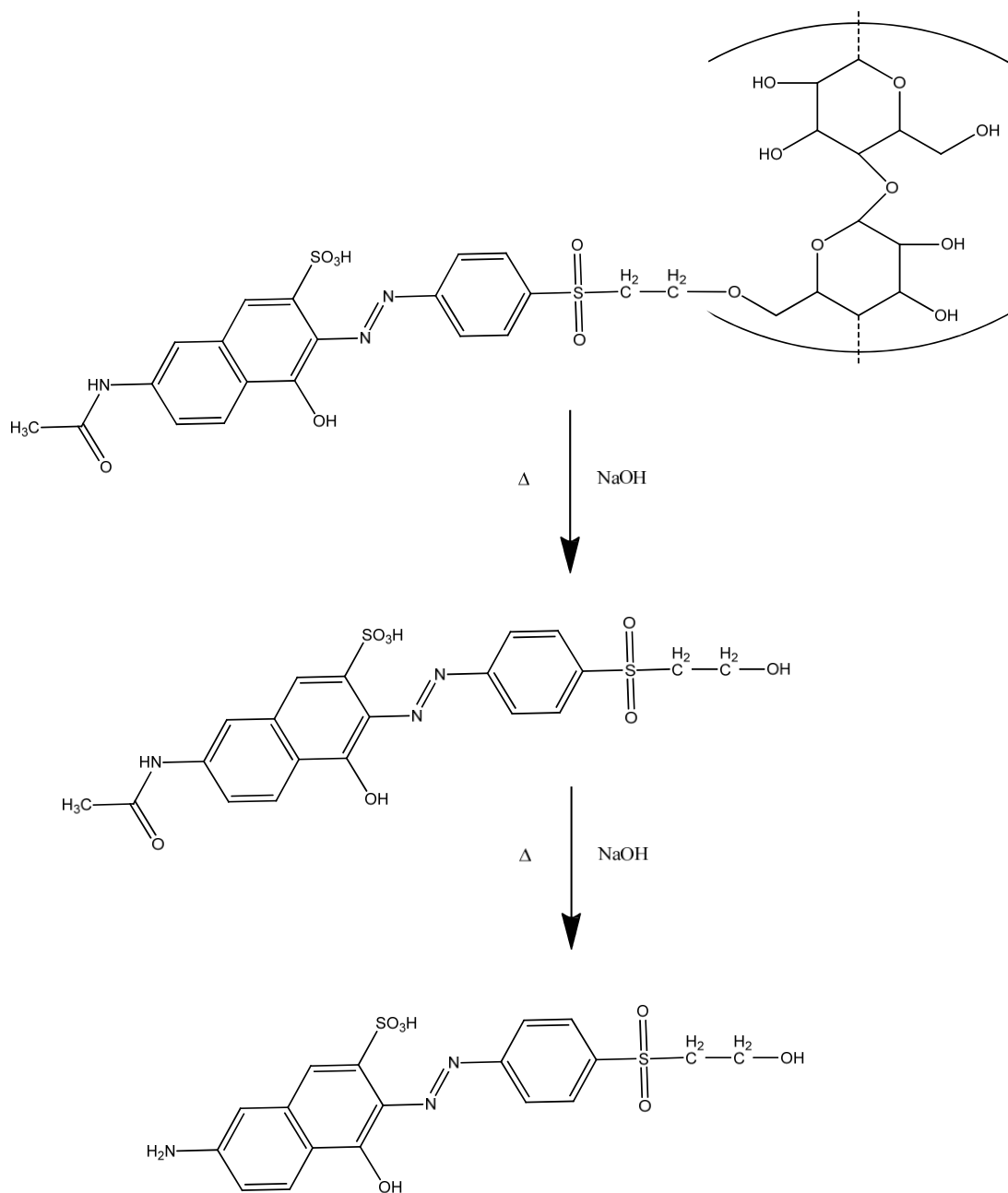


Figure 3. Mechanism showing the extraction of Reactive Orange 72 from cellulose, involving dye hydrolysis due to excess  $\text{NaOH}$ .

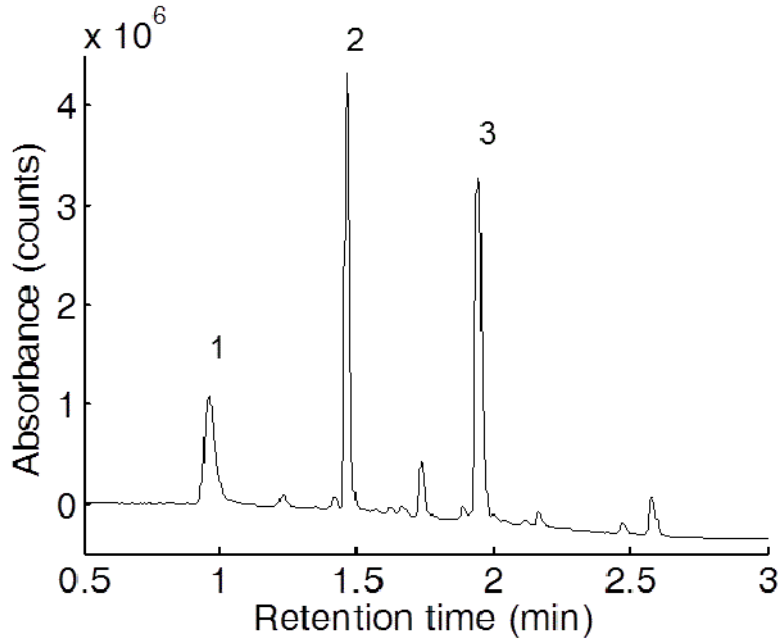


Figure 4. Chromatogram of all three reactive dyes. Peak identification: (1) Reactive Blue 220; (2) Reactive Orange 72; (3) Reactive Yellow 160.

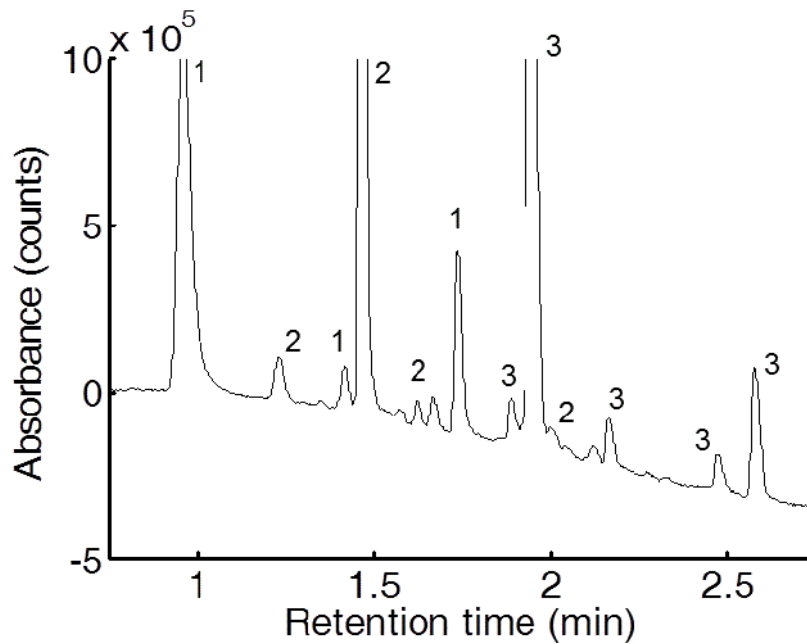


Figure 5. Expanded view of multiple reactive dye components in the chromatographic region of 0.8 to 2.6 min from Figure 4. Peak component identification: (1) Reactive Blue 220 components; (2) Reactive Orange 72; (3) Reactive Yellow 160.

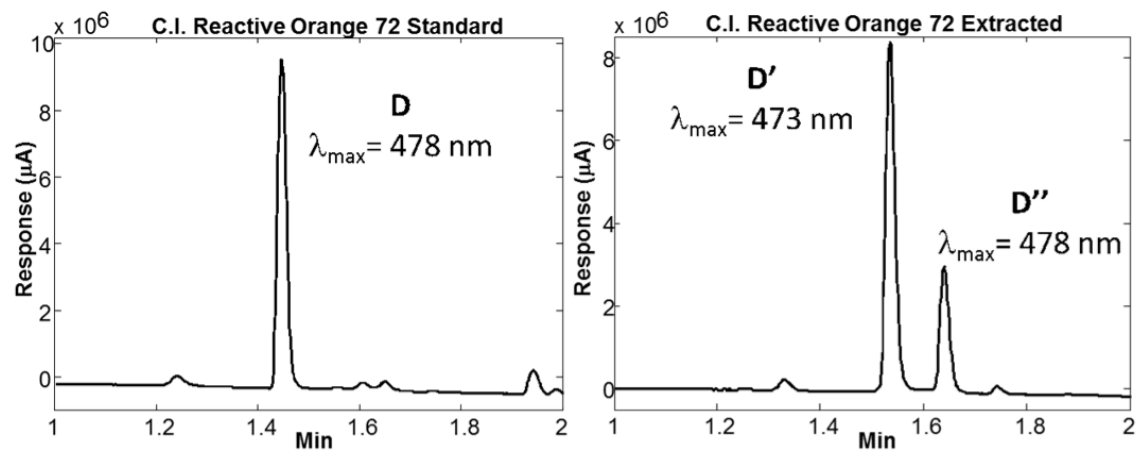


Figure 6. (Left) UPLC chromatograms for Reactive Orange 72 standard and (right) extracted (standard treated with NaOH and heat).

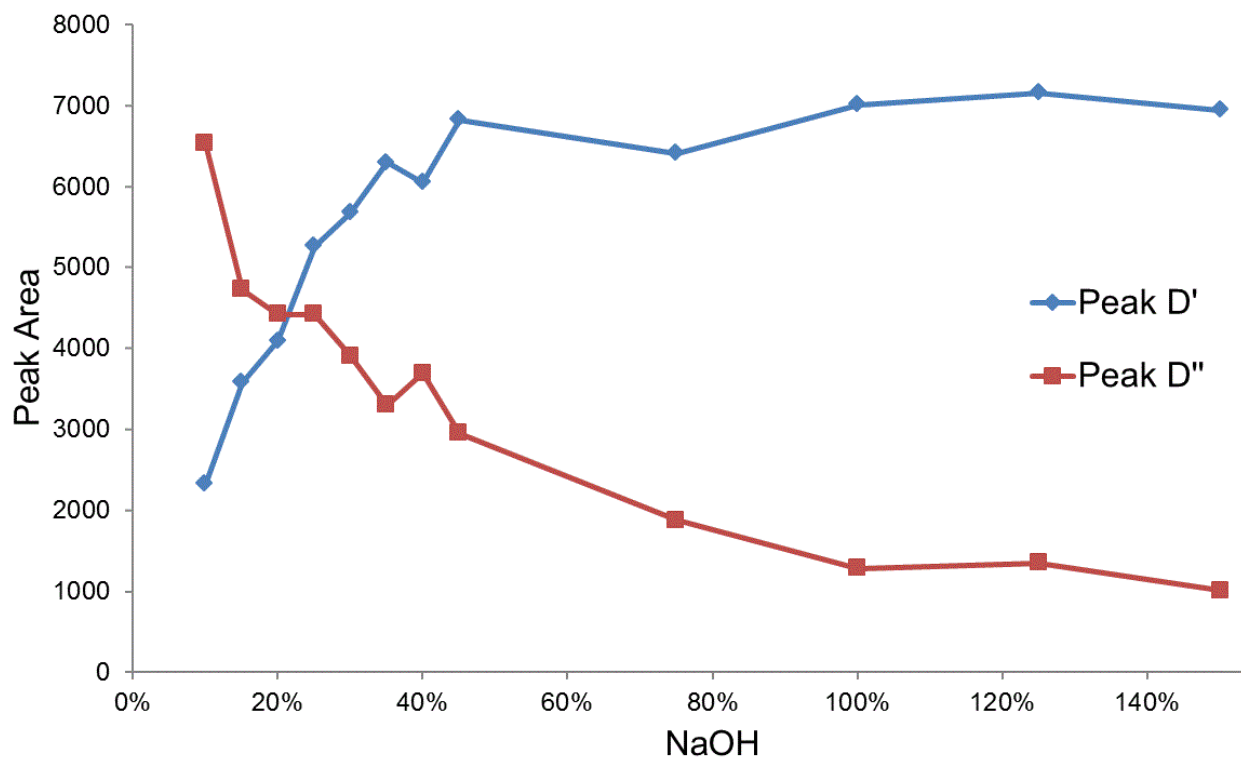


Figure 7. Areas of peaks D' and D'' observed after treatment of Reactive Orange 72 with varying amounts of NaOH. 100% represents  $9.375 \times 10^{-7}$  moles of NaOH to 1 ng of dye.

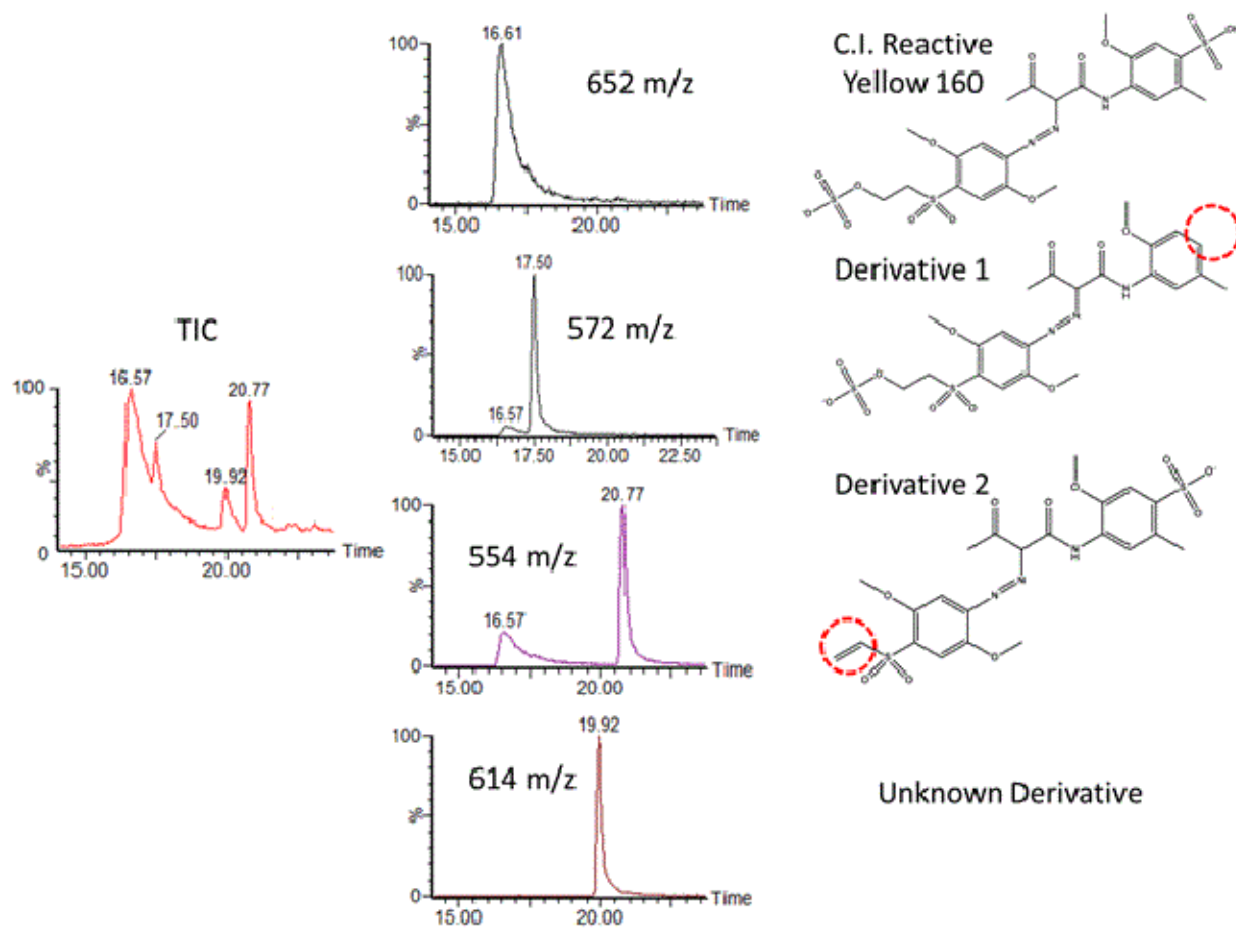


Figure 8. Total ion chromatogram of Reactive Yellow 160 standard and isolated molecular ions of four dye derivatives.

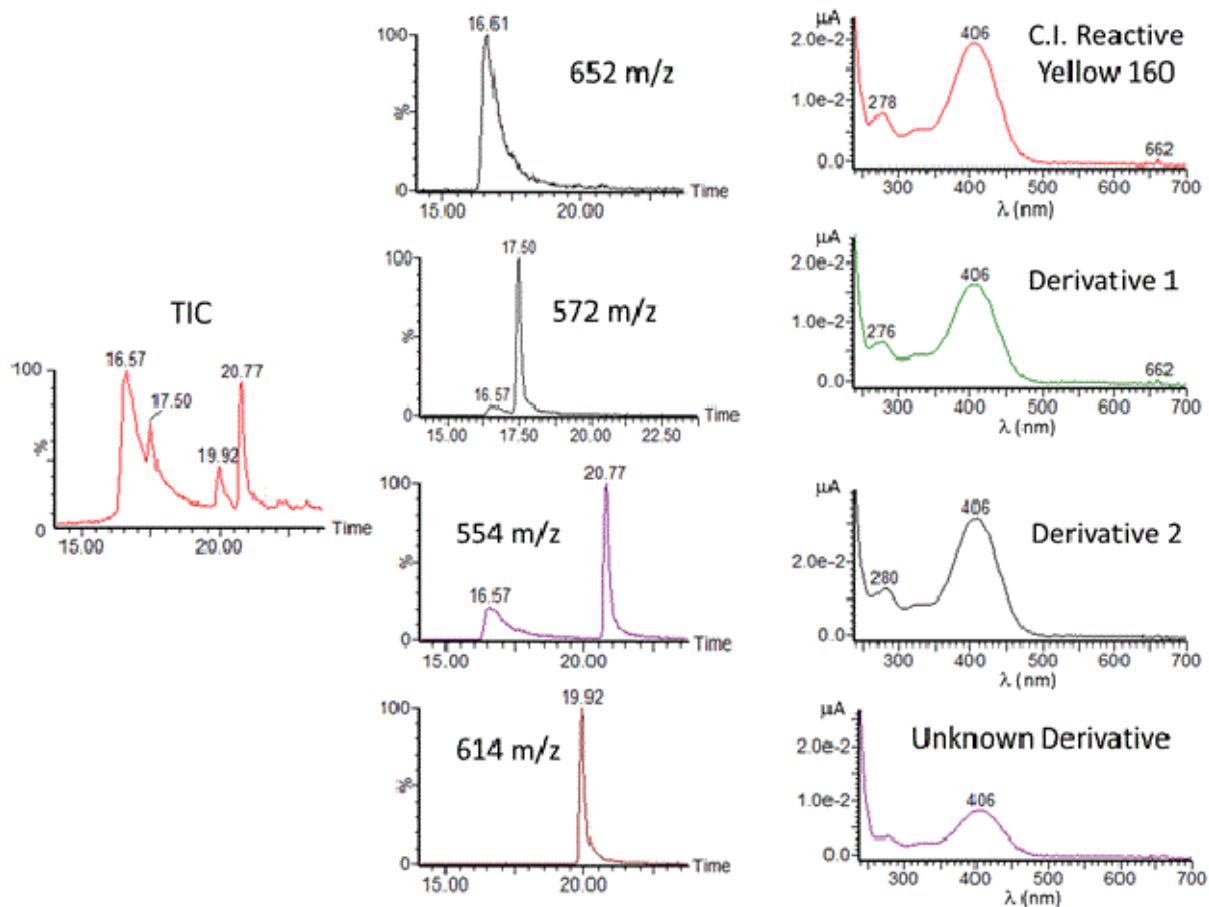


Figure 9. Total ion chromatogram of the Reactive Yellow 160 standard, isolated molecular ions of the potential dye derivatives, and their corresponding UV/visible absorbance spectra.

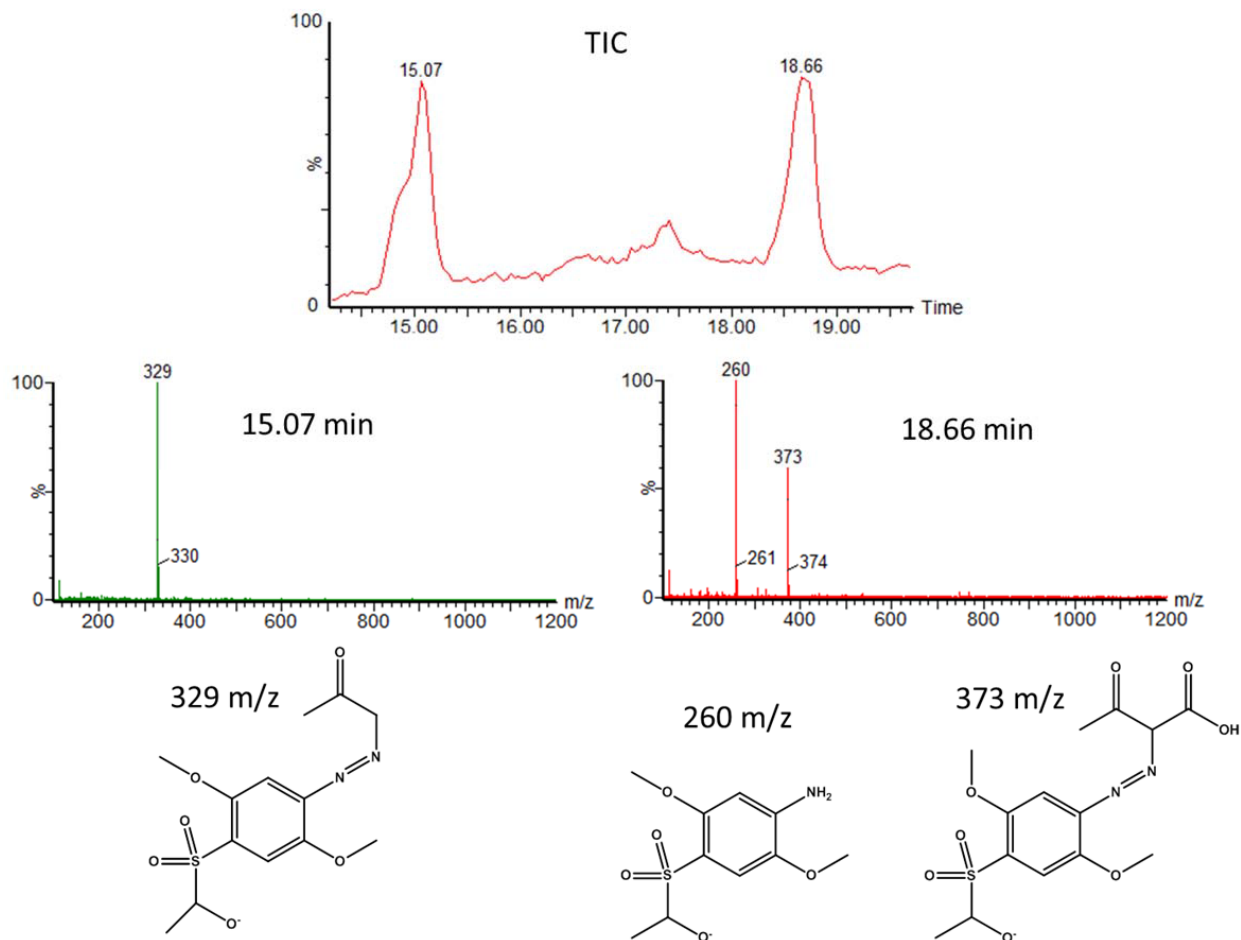


Figure 10. TIC of Reactive Yellow 160 after being treated with NaOH and heat (100°C). Two products were visible by HPLC-MS.

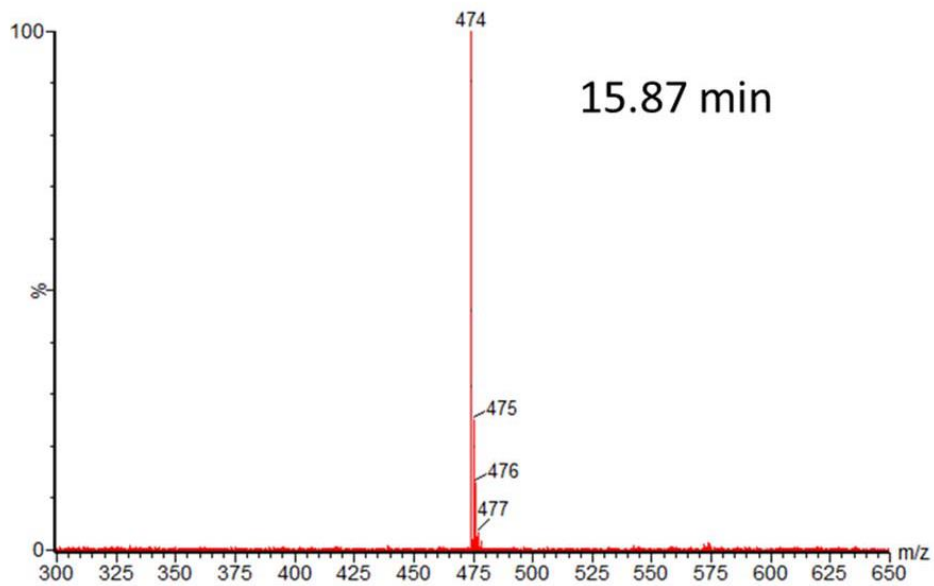
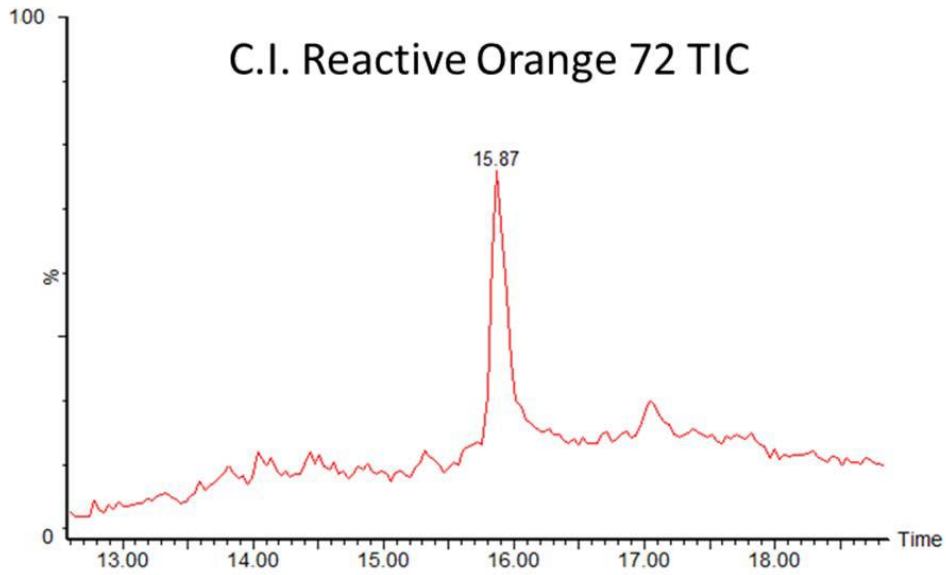


Figure 11. TIC of Reactive Orange 72 showing the only visible chromatographic peak and its mass spectra.

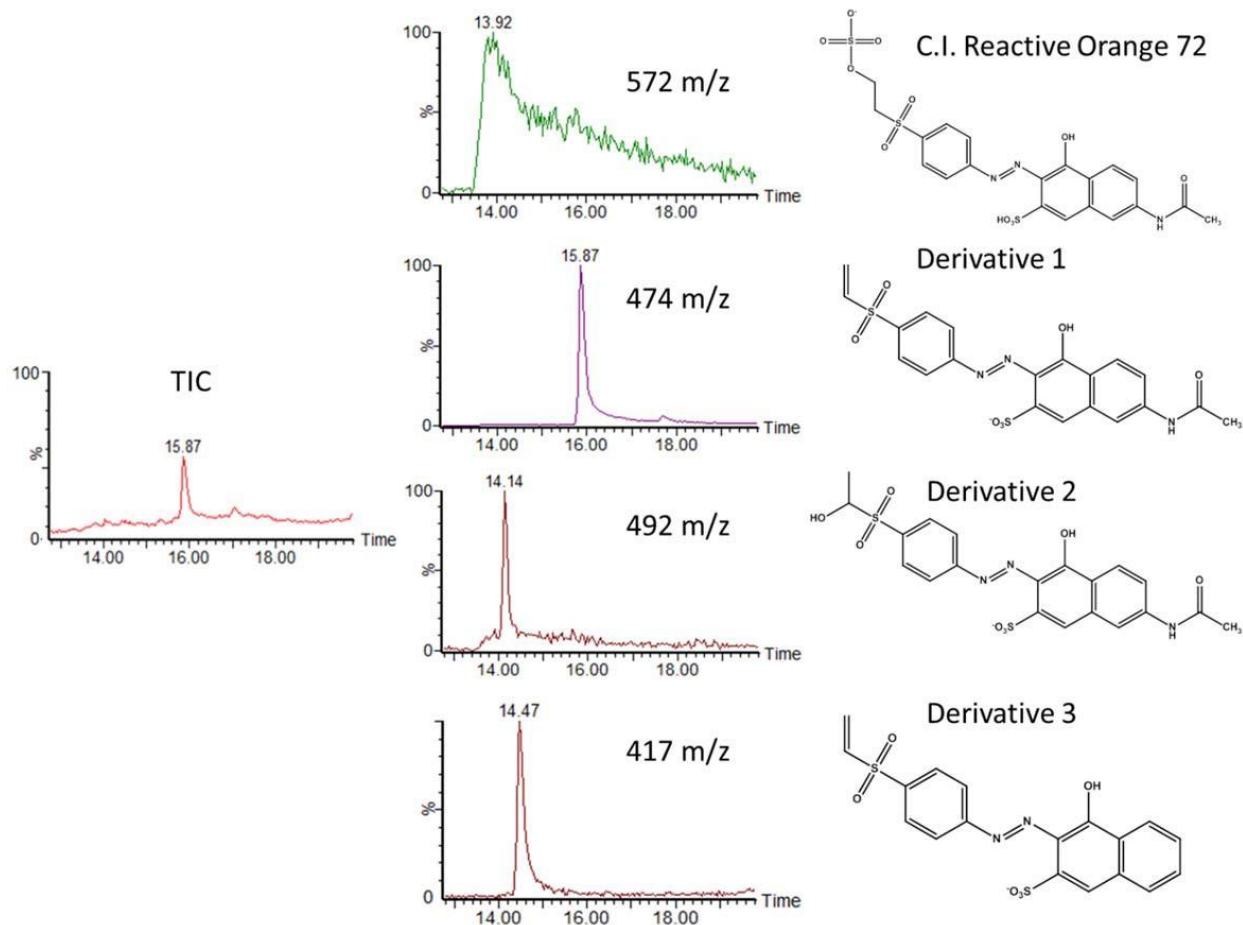


Figure 12. Extracted ion chromatograms for m/z 572, 474, 492, and 417 from the analysis of Reactive Orange 72. Individual chromatographic peaks for each mass suggest multiple compounds present in the standard.

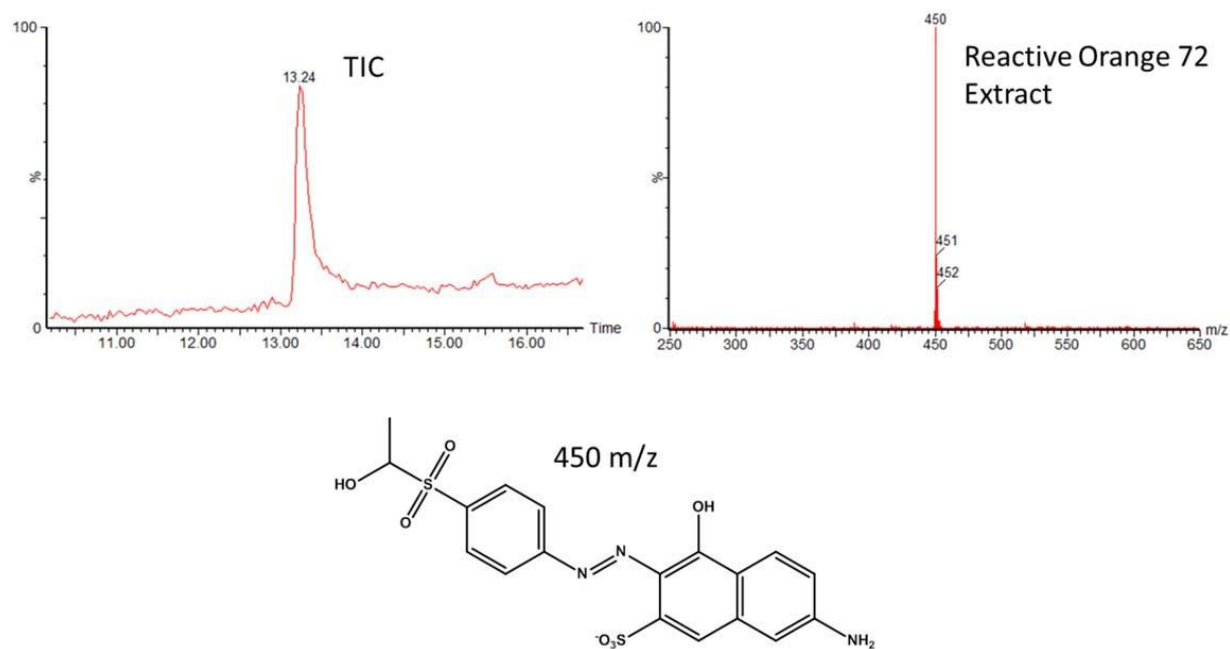


Figure 13. TIC and mass spectra of Reactive Orange 72 after treatment with NaOH and heat (100°C).

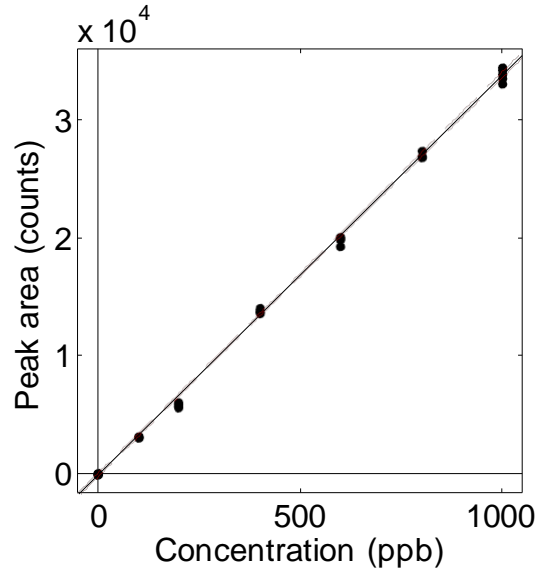


Figure 14. Calibration relationship for Reactive Blue 220.

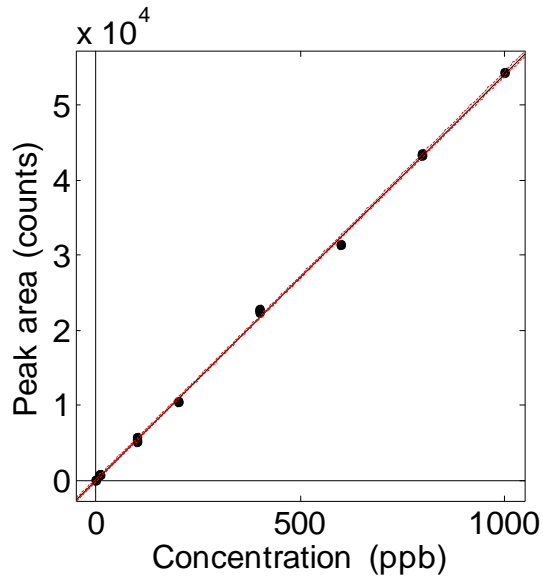


Figure 15. Calibration relationship for Reactive Orange 72.

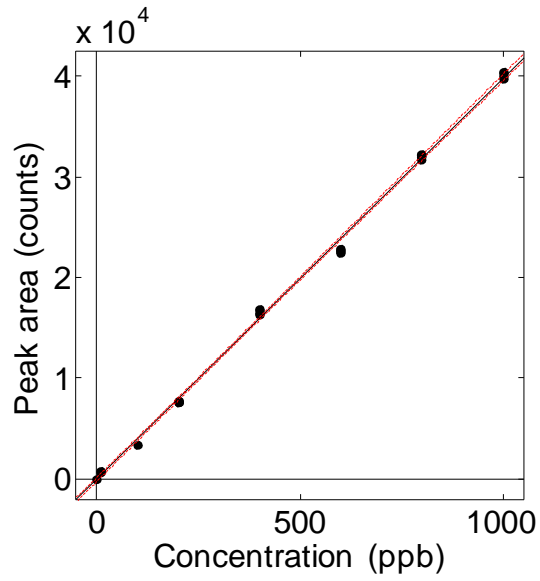


Figure 16. Calibration relationship for Reactive Yellow 160.

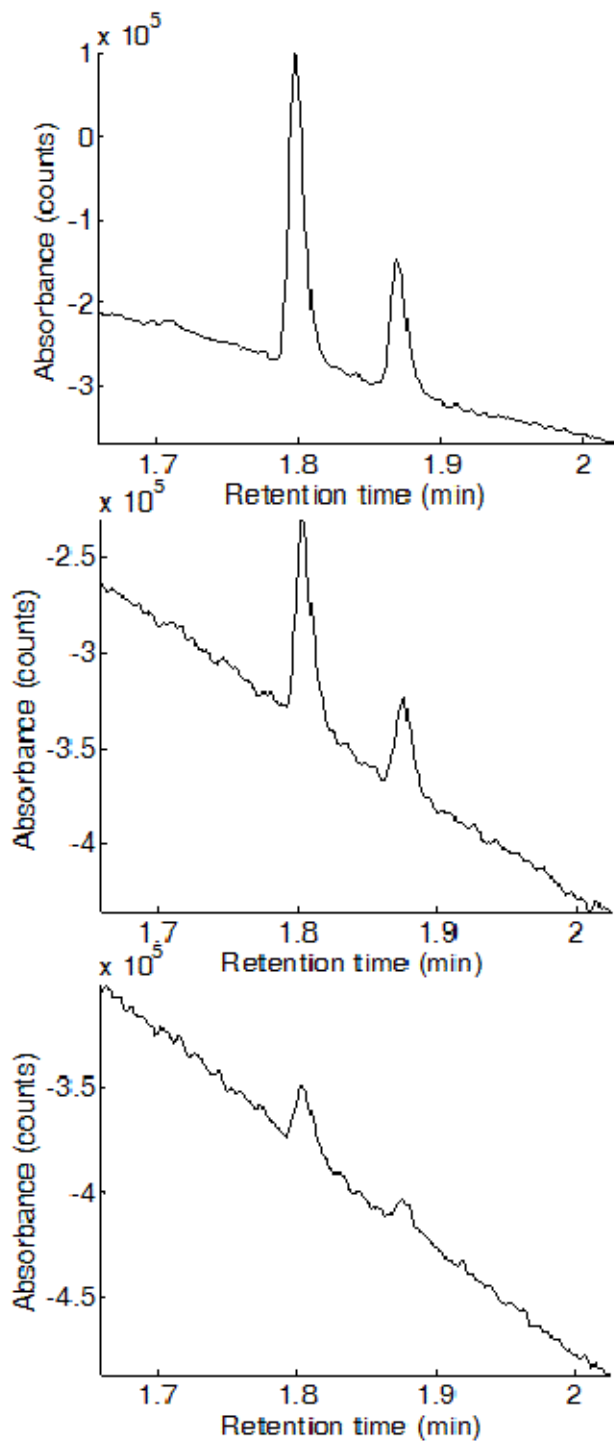


Figure 17. UPLC-DAD chromatograms of extracted Reactive Yellow 160 from a 10 mm fiber (top), a 5 mm fiber (middle) and a 1 mm fiber (bottom).

## **D. Forensic Analysis of Fluorescent Brighteners, Dyes and Textile Fiber Degradation by Capillary Electrophoresis, Liquid Chromatography/Mass Spectrometry, and Ultra Performance Liquid Chromatography**

Molly R. Burnip, Oscar G. Cabrices, Anthony R. Trimboli, Micheline Goulart, James E. Hendrix, and Stephen L. Morgan, Department of Chemistry and Biochemistry, University of South Carolina, Columbia, SC 29208

### **ABSTRACT**

Analytical methods based on microextraction and separations by capillary electrophoresis with UV/visible detection or liquid chromatography with mass spectrometric detection have been applied to the analysis of fluorescent brighteners and other finishing agents extracted from textile fibers. We demonstrate trace analysis of dyestuff residues from single 1- 10 mm thread or fibers of acrylic, cotton, nylon, and polyester to characterize changes that occur in textile fibers as a result of exposure to environmental conditions. Three different analytical techniques have been used to illustrate the applicability of modern trace instrumental techniques: capillary electrophoresis with UV/visible detection, liquid chromatography/mass spectrometry, and UPLC-UV/visible detection by liquid chromatography with mass spectrometry. Analyses of fluorescent brighteners extracted from white fibers offer new opportunities for investigators to discriminate essentially colorless fibers. The ability to detect dyestuffs on environmentally weathered fibers also offers potential value for forensic investigators attempting to interpret the forensic relevance of environmental effects on fiber evidence.

### **INTRODUCTION**

Textile fibers have become an increasingly informative forensic science due to their abundance at crime scenes. Fibers may represent evidence of contact between suspect and victim, or victim and inanimate objects such as cars, windows, and screen doors. Discovery of a particular fiber, its color, and identification polymer type does not provide unambiguous information. Fibers are class evidence that may share common characteristics with similar mass produced fibers whose prevalence may be unknown. In particular, white fibers are often considered to lack discriminating features that might offer probative value to a forensic investigation. However, in addition to dyeing with dyestuffs that absorb in the visible light range (400-700 nm), many fibers may also be dyed with fluorescent brighteners (FBs) that absorb ultraviolet light (around 360 nm) and re-emit light within visible spectrum (around 440 nm). These fluorescent dyes mask yellowness and can make textiles appear a brighter white color. Most of the interest in the analytical literature has been with FBs from detergents (2-7), rather than those that have such finishing properties.

Fibers are rarely found in pristine condition. Environmental conditions to which a textile fabric is subjected to over the course of its lifetime can produce changes in their dye components. These perturbations can be caused by photodegradation of the dyes and brightening agents, breakdown of the fiber polymers, or by the presence of contaminants picked up from the environment. Complications may arise in the forensic trace evidence comparison when fiber and dye components change and degrade because of conditions to which they are exposed. Two fibers from the same source may not match one another visually if one fiber has undergone changes due to environmental exposure. Even fibers that resemble one another visually might not match well with one another using microspectrophotometry because of changes caused by the exposure. The analysis of fibers following extraction of a dye and other finishing agents increases the

potential for discriminating analyses by enabling comparisons between the amounts of dyes, finishing agents, or other contaminants detected on fibers.

Thin layer chromatography (TLC), capillary electrophoresis (CE) and liquid chromatography (LC) have all been used for separation of extracted dyes (9-25). Because recovered trace evidence fibers typically range from 2-10 mm in length and contain 2-200 ng of dye, forensic analytical methods for analysis of dye extracts require high sensitivity (8). Both CE and LC with UV/visible or mass spectrometric detection offer sensitivity, selectivity, short analysis time, low organic solvent consumption, low sample requirements, and relatively low running costs. CE is well suited for dye analysis because many dyes are ionized, depending on their  $pK_a$  and solution pH. However, the ability to optimize mobile and stationary phases in liquid chromatography enables the analyst to tune separations of organic dyestuffs to adjust for the ionic or ionizable character of solutes. The research objective of this work was to evaluate applicability of CE with UV/visible detection, and of LC with MS or UV/visible detection for analysis of dyestuffs extracted from challenging forensic samples: white fibers, and fibers that have lost visible color as a result of environmental weathering.

## EXPERIMENTAL

**Materials.** Pyridine, ammonium hydroxide, ammonium acetate, sodium hydroxide, formic acid and methanol were obtained from Fisher Scientific (Pittsburg, PA) as analytical grade reagents. All dyed fabrics and matching dyes standards were current production samples donated by dyestuff manufacturers in the southeastern United States. The six different fluorescent brighteners from different subclasses on three substrates (acrylic, cotton, and nylon) are listed in Table 1. For confidentiality reasons, chemical name and supplier of each dye is not provided. Figure 1 shows representative chemical structures of each class of fluorescent brighteners used in this study.

**Cotton fiber dyeing.** Because fabrics specifically dyed with proprietary fluorescent brighteners used in the project were not provided, fabric samples were dyed in our laboratory. Rectangular swatches of white cotton fiber samples were dyed at 60 °C for 30 min with a paste of finely powdered fluorescent whitening agents with a concentration 0.5% by the weight of substrate. The swatches were submerged in a 0.1 M sodium hydroxide solution inside of an oven; the temperature increased from 30 °C to 60 °C at 2°C / min; and then for 15 min at 60 °C. The treated swatches were removed from the treatment bath, rinsed and dried in conventional manner (28).

**Acrylic fiber weathering.** Rectangular swatches of acrylic fiber samples were prepared and sent to exposure testing sites in Phoenix, AZ and Miami, FL. Samples were exposed for up to one year in these conditions, with samples retired at 3 month intervals up to 12 months. Natural, or real-time, outdoor weathering was performed in two different climates: Miami, Florida and Phnix, Arizona. Both climates average approximately 22-23 °C throughout the year, but Miami experiences five times more rainfall than the desert. The exposure protocol followed method ASTM G 147-02(26) and 7-05 (27), with the most exposed samples (12 months) subjected to a total of 341 MJ/m<sup>2</sup> (Arizona) and 309 MJ/m<sup>2</sup> (Florida) of UV light (295-385 nm). Accelerated weathering was also performed, both as a backup to the natural weathering and as a form of replication. Utilizing an apparatus composed of Fresnel mirrors, samples were exposed to environmental conditions at 8-fold intensity. A cooling system was employed to maintain practical temperatures to minimize thermal degradation. Two different sets of conditions were

used: hot and arid, and hot and humid, where water was introduced to simulate atmospheric moisture. These accelerated samples were exposed to 70 MJ/m<sup>2</sup> per “3 month equivalent” cycle, totaling 280 MJ/m<sup>2</sup> (12 month equivalent), under ASTM test methods 147-02 and 90-98. Figure 2 shows the appearance of nylon fabrics after 3 months of natural weathering in Florida and Arizona. Samples left outside in either Miami or Phoenix after one year of exposure show substantial color loss to the extent that the original color is not easily perceived.

**Dye extraction.** A fiber guillotine was built in house with 6 blades spaced 5 mm apart. A string of a single fiber was placed on top of a hinged surface under the cutting blades and was cut in various length segments. For CE and LC/MS analyses, cotton fibers were treated with 60:40 pyridine:water (total volume of 100  $\mu$ L) at 100 °C for 60 min, and acrylic fibers were treated with 50:50 formic acid: water (total volume 100  $\mu$ L) at 100 °C for 60 min. Extracts were evaporated to dryness under a stream of nitrogen at 70 °C. All extracts were dried at 70 °C to remove extraction solvents and reconstituted in 100  $\mu$ L of water for CE analysis and 100  $\mu$ L of methanol for LC/MS analysis. For UPLC analysis,

**Capillary electrophoresis.** Capillary electrophoresis was performed using a Beckman Coulter P/ACE-MDQ CE system (Brea, CA) equipped with a diode array detector (DAD) monitoring absorbance from 190 to 600 nm. CE was performed using a fused silica capillary with an internal diameter of 50-75  $\mu$ m and length of 50 cm (40 cm effective length) from Polymicro Technologies (Phoenix, AZ, USA). Liquid chromatography/mass spectrometry was performed using a Waters Acquity H-Class UPLC system (Milford, MA) coupled to a Waters Quattro Premier mass spectrometer. The analytical column was a Pinnacle DB Biphenyl 50 $\times$ 2.1 mm I.D., and 1.9  $\mu$ m particle size (Restek Corporation., Bellefonte, PA).

Capillary ends were burned before use to prevent degradation of polyimide coating. The capillary was conditioned by rinsing with 0.5 M ammonium hydroxide for 12 min, water for 10 min, and electrophoresis buffer for 12 min between injections. The electrolyte consisted of 15 mM ammonium acetate in acetonitrile:water (40:60, v/v), at pH 9.3. Standard solutions of fluorescent brighteners were prepared in deionized water at concentrations of 1.0 mg/mL. Injections were done in hydrodynamic mode at 0.2 psi for 2 s. Separations were performed at 25 °C with an applied voltage of 30 kV. The electrolyte was replaced after every five runs to minimize solvent evaporation effects that might cause irreproducible electro-osmotic flow and migration times.

**LC/MS.** All analyses were performed using a Waters Acquity H-Class UPLC™ system with a Micromass Quattro Premier MS system. The separation employed a Pinnacle DB Biphenyl 50  $\times$  2.1 mm I.D., 1.9  $\mu$ m particle size (Restek Corporation, Bellefonte, PA). The mobile phase for LC/MS analyses used methanol (containing 0.05% formic acid) and water (containing 0.05% formic acid) in a gradient for which methanol was held at 50% for 2 min then increased to 95% in 6 min and held for 2 min. At the end of each run, methanol was decreased to 50% in 1 min, and held for 3 min to wash the column. Column flow rate was 0.5 mL/min and the run time was 14 min. Mass spectrometry was performed by scanning at 100-1000 Da in positive electrospray mode. The needle voltage was 3 kV, source temperature was 550°C, the nebulizer gas (nitrogen) set at 30 psi, and turbo heater gas (nitrogen) was at 50 psi.

**UPLC/UV-visible analysis.** Dye standards and extracts were separated and detected using a Waters Acquity™ UPLC H-Class equipped with a quaternary solvent pump system and a Waters PDA e $\lambda$  detector. The column was a 2.1  $\times$  50 mm I.D. 1.7  $\mu$ m particle size Waters Acquity™

BEH C18 column with a  $2.1 \times 5$  mm I.D.  $1.7 \mu\text{m}$  particle size Waters Acquity UPLC<sup>®</sup> BEH C18 VanGuard precolumn. The mobile phase gradient was based on mixtures of 50 mM ammonium acetate in water and 0.15% formic acid in methanol as shown in Table 2A. The column temperature was set at  $40^\circ\text{C}$ . The diode array detector scanned the wavelength range from 325 nm to 675 nm at a rate of 40 Hz and 1.2 nm resolution. The sample injection volumes were 10  $\mu\text{L}$ .

## RESULTS AND DISCUSSION

**CE analysis of fluorescent brighteners.** An electropherogram showing the separation of all 6 FBs chosen in this study using CE/DAD is shown in Figure 3. The excellent separation reveals the universality of the method applied to three different fluorescent brightener classes used on textile fibers. Clearly even without complete identification of the dyestuffs, forensic sample comparisons could be accomplished on the basis of migration times and UV/visible absorbance spectra. Although separating acid dyes (used on nylon) along with direct dyes (used on cotton) and basic dyes (used on acrylic) is a forensically meaningless exercise, the applicability of a comprehensive separation protocol useful for these different fluorescent brighteners simplifies routine use and method validation.

Figure 4 shows the CE analysis of the extract from a 10-mm thread of cotton fiber dyed with a distyrylbiphenyl fluorescent brightener. The dye peak is the major peak in the electropherogram; the minor peak corresponds to unevaporated pyridine remaining from the microextraction process. Migration times of distyrylbiphenyl are reproducible to within a few seconds, enabling matching of peaks and their associated spectra to standard reference samples. Also shown is the electropherogram of an extract from a 1-mm thread of the same cotton fiber. Although this sample produced unreliable spectra, the migration time of distyrylbiphenyl matched that of the standard with a signal to noise ratio high enough to confirm analyte presence.

**LC/MS analyses of weathered acrylic fibers.** Acrylic fibers were dyed with C.I. Basic Violet 16 and treated with two water repellent finishing agents by the manufacturer (Figure 5). Basic dyes are water soluble, and adhere to acrylic fibers via salt linkages, hydrogen bonding and van der Waals forces. Both finishing agents applied are commercial water-resist agents. Figure 6 shows an LC/MS chromatogram of a 10-mm unweathered finished acrylic fiber extract. The dye extract was identified by the intense  $[\text{M}+\text{H}]^+$  ion ( $m/z$  333) in the mass spectrum, and matching retention time to that of the standard solution. The finishing agents were also characterized by the adjacent peaks relative to that of the dye extract and by mass spectral interpretation. Finishing agent 1 had less retention on the column and an intense fragment at  $m/z$  201. Finishing agent 2 was retained longer due to its more nonpolar polymeric chain, and exhibited three identifiable fragments at  $m/z$  804,  $m/z$  623 and  $m/z$  391.

After both accelerated and natural environmental exposure, acrylic samples were faded due to dye degradation. Figures 7 and 8 display LC/MS total ion chromatograms and total chromatogram ion mass spectra of extracts from 10-mm fibers after outdoor (hot and humid) weathering procedures conducted in Miami. The dye and finishing agent peaks disappear from the total ion chromatogram after 6 months of exposure. However, peak at ion  $m/z$  333 for Basic Violet 16 and the peak at ion  $m/z$  397 for finishing agent 2 is still visible out to 12 months under these conditions. Finishing agent 1 (with a characteristic peak at  $m/z$  201) is not seen in the weathered fiber extracts, presumably finishing agent 2 is more hydrophobic.

Figures 9 and 10 show chromatograms and mass spectra of samples also exposed in Miami to hot and humid conditions, but under accelerated weathering conditions. These samples served as a controlled replicate experiment and with near identical results, validate the natural weathering outcomes.

Although the same peaks are seen in both cases, the accelerated weathering conditions removed more of the finishing agent. The Arizona hot and dry conditions produced greater dye degradation effects than the hot and humid conditions in Miami. Although peaks for the finishing agents are not seen in the total ion chromatograms, total ion mass spectra of the fibers at different weathering stages reveal traces of the  $m/z$  391 ion from finishing agent 2. That the hot and arid conditions in Miami led to a higher loss of the finishing agent 2 at  $m/z$  391 peak, compared to the hot and humid conditions, was expected because of the relative hydrophobicities of the two finishing agents.

Figures 11 and 12 show a chromatogram and mass spectrum from a single 10-mm fibers extracted after natural weathering in Phoenix, AZ; Figures 13 and 14 show corresponding results after natural weathering in Miami, FL. All chromatograms show degradation of dye signal as weathering time increased. The hot and humid weather of Florida caused increased loss of the acrylic dye compared to exposure in Arizona. Mass spectra in Figures 12 and 14 also showed the  $m/z$  391 ion trace for finishing agent 2. Moreover, the mass spectra also reveal an abundance of ions in the low  $m/z$  range (100-300 Da) that might be attributable to possible natural components deposited on the fibers as a result of natural exposure. If these components were found to be characteristic of the geographical location this information could be useful for discrimination of questioned and unknown fibers.

**UPLC/UV-visible analysis of weathered acrylic, nylon, and polyester samples.** Detection limits in the 2-40 ppb range by both UV/visible and tandem mass spectrometry are sufficient for confident detection and identification of dyes residues remaining on acrylic, nylon, and polyester fabrics after outdoor exposure. Figures 15 and 16 show UPLC/UV/visible chromatograms of an extract from a 10-mm thread composed of ~40 individual acrylic fibers after exposure to hot and humid outdoor weather conditions in Miami, FL, and arid and dry outdoor weather conditions in Phoenix, AZ, respectively. Dye peaks are easily seen in the chromatograms. Although the finishing agents are not identified at present, some smaller peaks in the chromatograms may, on further inspection, turn out to be identifiable as fluorescent brighteners. Figures 17 and 18, and 19 and 20, display results for nylon and polyester under the same conditions. It is clear from the high signal-to-noise ratios and reproducibility of retention times that dye extraction and UPLC analysis and identification of dyes from weathered samples is practical and has potential to provide probative information for trace fiber examinations involved fabrics that have been environmentally exposed.

## CONCLUSIONS

The high efficiency and sensitivity of capillary electrophoresis and liquid chromatography with diode array detection or mass spectrometry has been demonstrated for the analysis of fluorescent brighteners and environmentally weathered fibers. We have demonstrated that CE and UPLC, with UV/visible detection, provide separation and identification of dyestuffs extracted from mm-sized threads and single fibers of textile fabrics. These analyses were conducted at sampling levels characteristic of two different forensic scenarios: a situation in which complete threads of textile material are available, possibly from a victim's clothing; and, a more sample-limited

situation of having only a single 10 mm trace fiber. The success with which these samples have been analyzed supports the premise that these techniques may offer substantial probative value in regard to characterization of fibers found at crime scenes. We have also shown analyses of fibers similar to those found in degraded condition after heavy environmental exposures. LC/MS analyses have shown that dye extracts and manufacturer finishing agents may be detected on 10-mm single fibers after as much as a year of accelerated and natural weathering. UPLC analyses on acrylic Further studies on understanding processes that results in the photodegradation of dyes exposed to weathering conditions could be helpful in understanding the forensic significance of fibers found at outdoor crime scenes.

## ACKNOWLEDGMENTS

This project was supported by Award No. 2010-DN-BX-K245 awarded by the National Institute of Justice, Office of Justice Programs, U.S. Department of Justice. The support of the Federal Bureau of Investigation through contract J-FBI-04-181 is acknowledged. The opinions, findings, and conclusions or recommendations expressed in this publication are those of the author(s) and do not necessarily reflect those of the Department of Justice, or the Federal Bureau of Investigation.

## REFERENCES

1. Robertson J.; Grieve, M., Eds., *Forensic Examination of Fibres*, 2nd edition. London: Taylor and Francis, London, 1999.
2. Lloyd, J.B. *J. Forensic Sci. Soc.* **1978**, *17*, 145-152.
3. McPherson, B.P.; Omelczenko, N. *J. Amer. Oil Chem. Soc.* **1980**, *57*, 388-391.
4. Micali, G.; Curro, P.; Calabro, G. *Analyst* **1984**, *109*, 155-158.
5. Jasperse, J.L.; Steiger, P.H. *J. Am. Oil Chem. Soc.* **1992**, *69*, 621-625.
6. Ogura, I.; DuVal, D.L.; Miyajima, K. *J. Am. Oil Chem. Soc.* **1995**, *72*, 827-833.
7. Stoll, J.-M.A.; Giger, W. *Anal. Chem.* **1997**, *69*, 2594-2599.
8. Macrae, R.; Smalldon, K.W. *J. Forensic Sci.* **1979**, *24*, 109-116.
9. Macrae, R.; Dudley, R. J.; Smalldon, K. W. *J. Forensic Sci.* **1979**, *24*, 117-129.
10. Resua, R. *J. Forensic Sci.* **1980**, *25*, 168-173.
11. Shaw, I. C. *Analyst* **1980**, *105*, 729-730.
12. Home, J. M.; Dudley, R. J. *Forensic Sci.Int.* **1981**, *17*, 71-78.
13. Beattie, B.; Roberts, H.; Dudley, R. J. *J. Forensic Sci. Soc.* **1981**, *21*, 233-237.
14. Hartshorne, A. W.; Laing, D. K. *Forensic Sci.Int.* **1984**, *25*, 133-141.
15. Wiggins, K. G.; Crabtree, S. R.; March, B. M. *J. Forensic Sci.* **1996**, *41*, 1042-1045.
16. Laing, D. K.; Boughey, L.; Hartshorne, A. W. *J. Forensic Sci. Soc.* **1990**, *30*, 299-307.
17. Laing, D. K.; Hartshorne, A. W.; Bennett, D. C. *J. Forensic Sci. Soc.* **1990**, *30*, 309-315.
18. Rendle, D. F.; Wiggins, K. G. *Review of Progress in Coloration and Related Topics* **1995**, *25*, 29-34.
19. Rendle, D. F.; Crabtree, S. R.; Wiggins, K. G.; Salter, M. T. *J. Soc. Dyers Colour* **1994**, *110*, 338-341.
20. Crabtree, S. R.; Rendle, D. F.; Wiggins, K. G.; Salter, M. T. *J. Soc. Dyers Colour* **1995**, *111*, 100-102.
21. Wheals, B.B.; White, P.C.; Paterson, M.D. *J. Chromatogr.* **1985**, *350*, 205-215.
22. Laing, D. K.; Gill, R.; Blacklaws, C.; Bickley, H.M. *J. Chromatogr.* **1988**, *442*, 187-208.
23. Stefan, A. R.; Dockery C. R.; Nieuwland, A. A.; Roberson, S. N.; Baguley, B. M.; Hendrix, J. E.; Morgan, S. L. *Anal. Bioanal. Chem.* **2009**, *394*, 2077-2085.

24. Dockery C. R.; Stefan, A. R.; Nieuwland, A. A.; Roberson, S. N.; Baguley, B.M.; Hendrix, J. E.; Morgan, S. L. *Anal. Bioanal. Chem.* **2009**, *394*, 2095-2103.
25. Stefan, A. R.; Dockery, C. R.; Baguley, B.M.; Vann, B. C.; Nieuwland, A. A.; Hendrix, J. E.; Morgan, S. L. *Anal. Bioanal. Chem.* **2009**, *394*, 2087-2094.
26. ASTM G 147-02, "Standard Practice for Conditioning and Handling of Nonmetallic Materials for Natural and Artificial Weathering Tests," ASTM International.
27. ASTM G7-05 "Standard Practice for Atmospheric Environmental Exposure Testing of Nonmetallic Materials," ASTM International.
28. Trotman, E.R. *Dyeing and Chemical Technology of Textile Fibres*; Griffin, London, **1964**.

Chemical class	Dye class	Fiber Type
pyrazoline	Cationic	Acrylic
heterocycle	Cationic	Acrylic
distyrylbiphenyl	Direct	Cotton
stilbene	Direct	Cotton
coumarin	Acid	Nylon
thiopheneoxazole	Acid	Nylon

**Table 1.** Fluorescent brighteners.

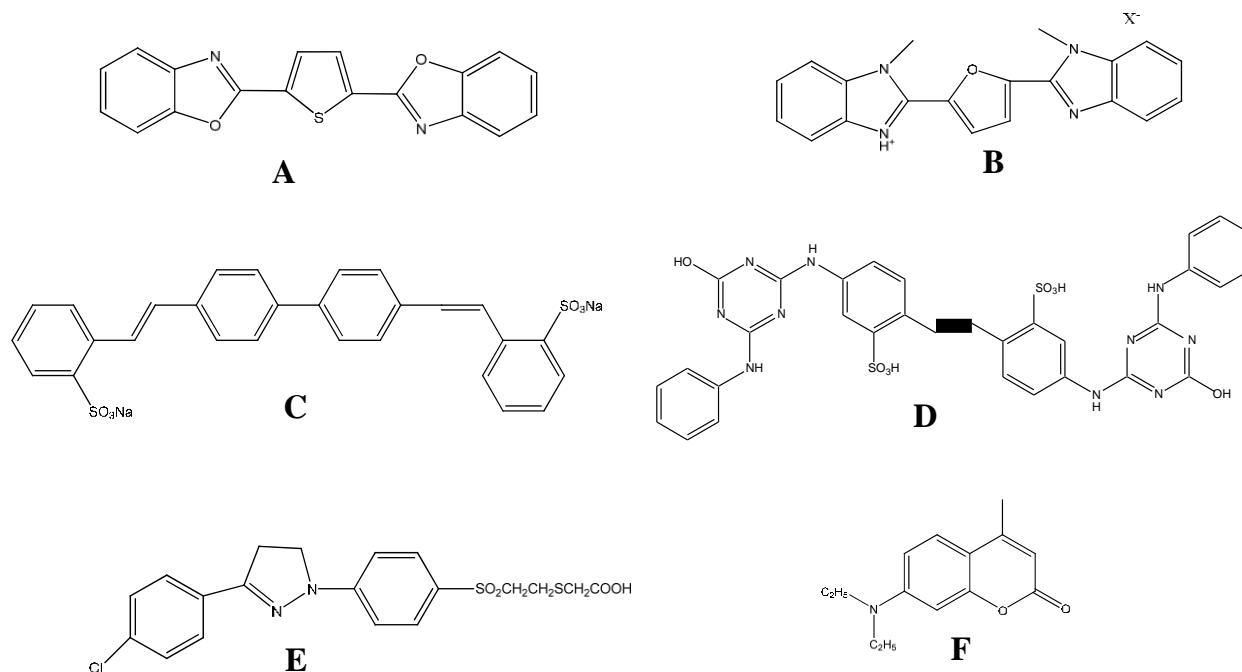


Figure 1. Representative chemical structures of fluorescent brighteners: (A) thiopheneoxazole, (B) heterocycle, (C) distyrylbiphenyl, (D) stilbene, (E) pyrazoline, and (F) coumarin.

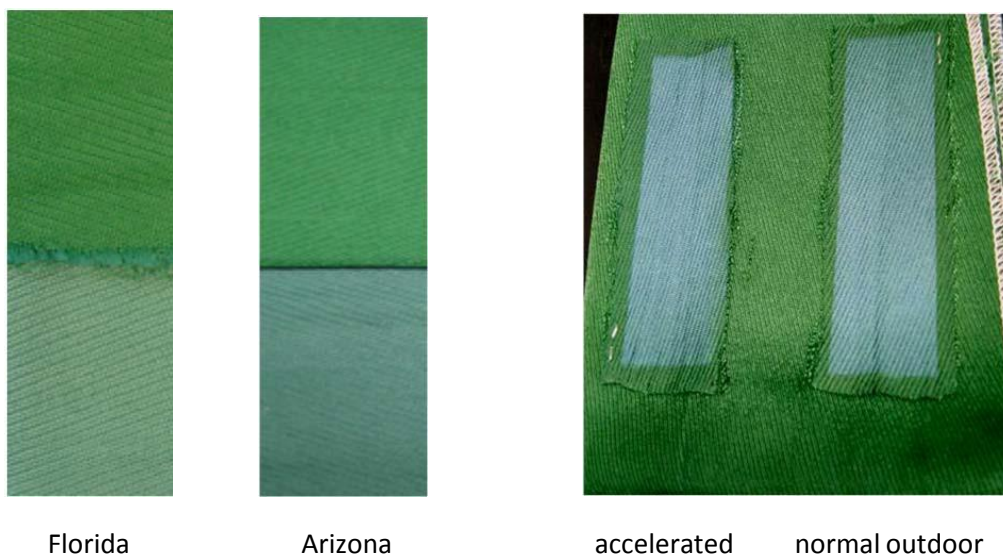


Figure 2. (Left) Nylon fabric specimens that have been exposed for 3-months to natural weathering in Florida (hot-humid climate) and Arizona (hot-dry climate); top is unexposed fabric, bottom is weathered fabric. (Right) Fabric specimens that have been exposed to 6 months of accelerated weathering in the hot and wet climate of Miami. Each sample is shown on a background of unexposed fabric.

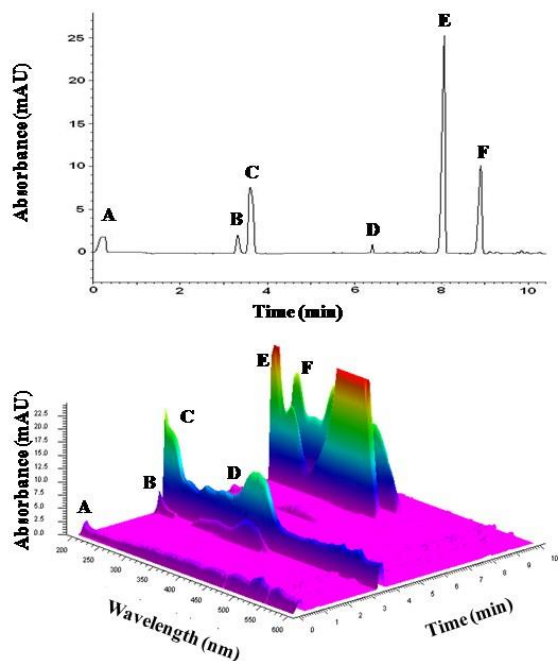


Figure 3. CE/DAD electropherogram showing separation of six fluorescent brighteners. Peak identity: (A) neutrals, (B) pyrazoline, (C) heterocycle, (D) thiopheneoxazole, (E) distyrylbiphenyl; and (F) stilbene.

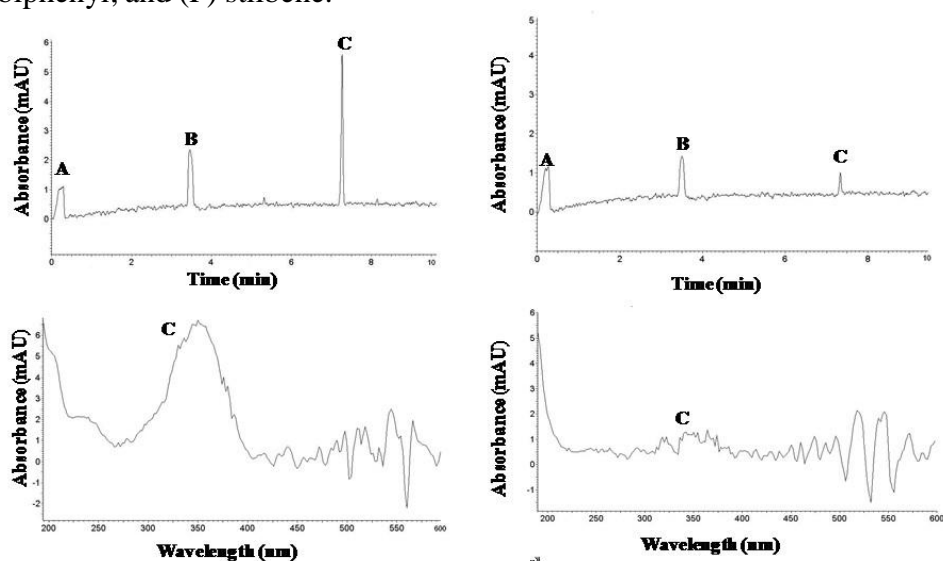


Figure 4. Capillary electrophoresis-UV/visible electropherogram of a commercial fluorescent brightener extracted from: (left) a 10-mm white cotton fiber thread; and, (right) a 1-mm white cotton fiber thread. Peak identity: (A) neutrals; (B) pyridine; and (C) distyrylbiphenyl.

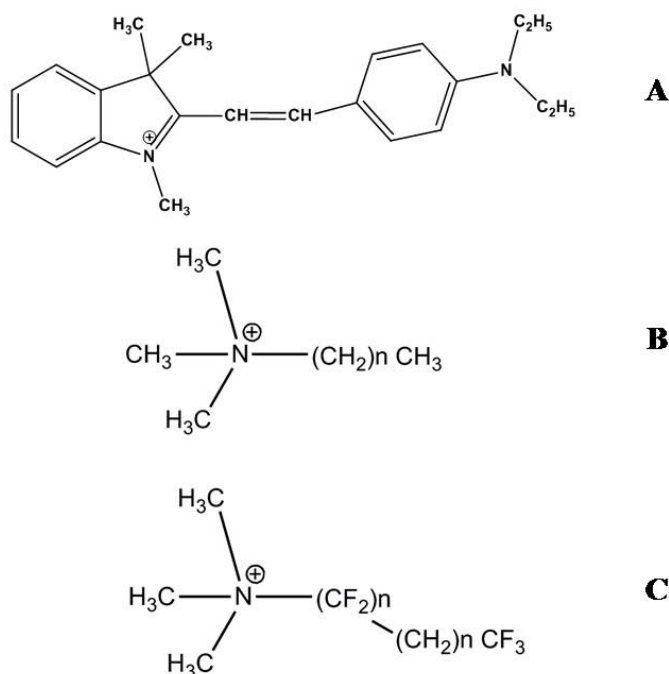


Figure 5. Chemical structures of colored dye and finishing agents on acrylic fiber: (A) C.I. Basic Violet 16; (B) finishing agent 1; and, (C) finishing agent 2.

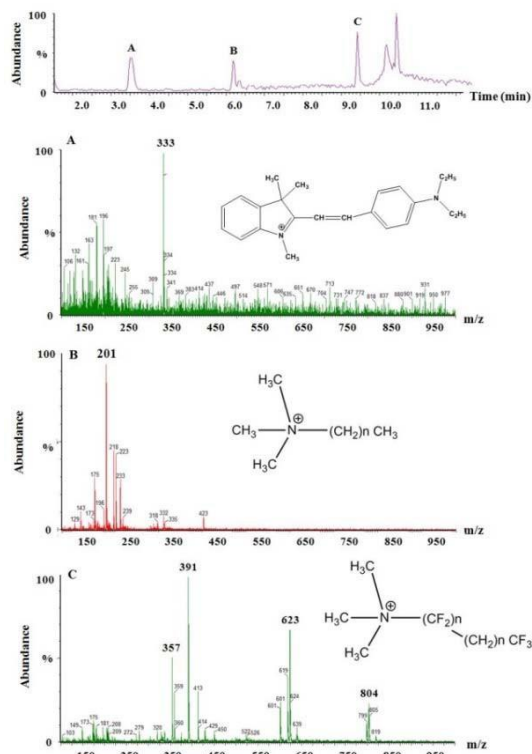


Figure 6. LC/MS total ion chromatogram (top) of an extract from an unweathered single 10-mm acrylic fiber and mass spectra of: (A) C.I. Basic Violet 16; (B) finishing agent 1; and, (C) finishing agent 2.

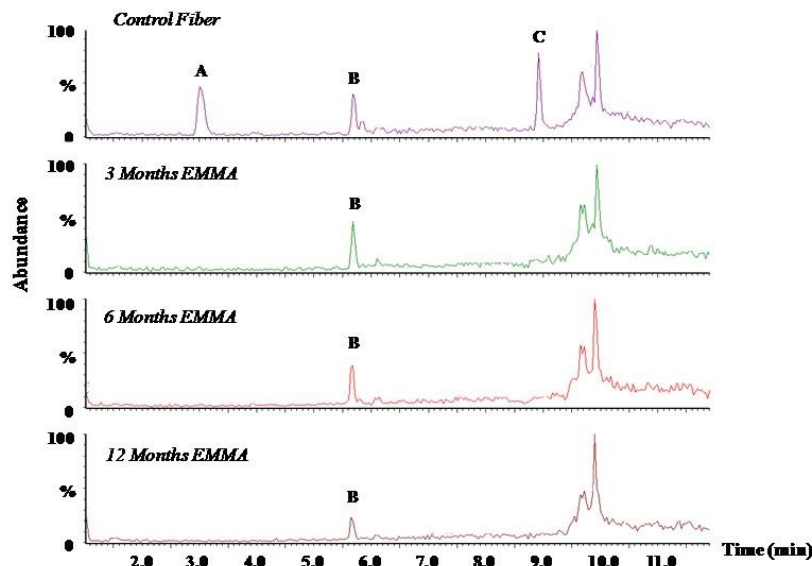


Figure 7. LC/MS total ion chromatogram of an extract from a single 10-mm acrylic fiber before and after outdoor hot and humid weathering of 3, 6, and 12 months in Miami. Peak identity: (A) C.I. Basic Violet 16; (B) finishing agent 1; and, (C) finishing agent 2.

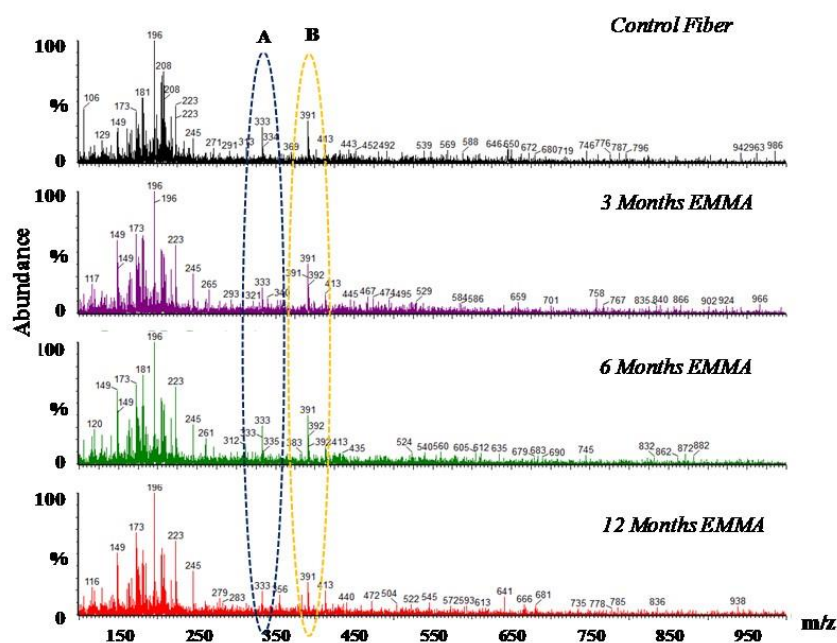


Figure 8. LC/MS total ion mass spectra from an extract of a single 10-mm acrylic fiber before and after outdoor hot and humid weathering of 3, 6, and 12 months in Miami. Ion identities: (A) C.I. Basic Violet 16; and, (B) finishing agent 2.

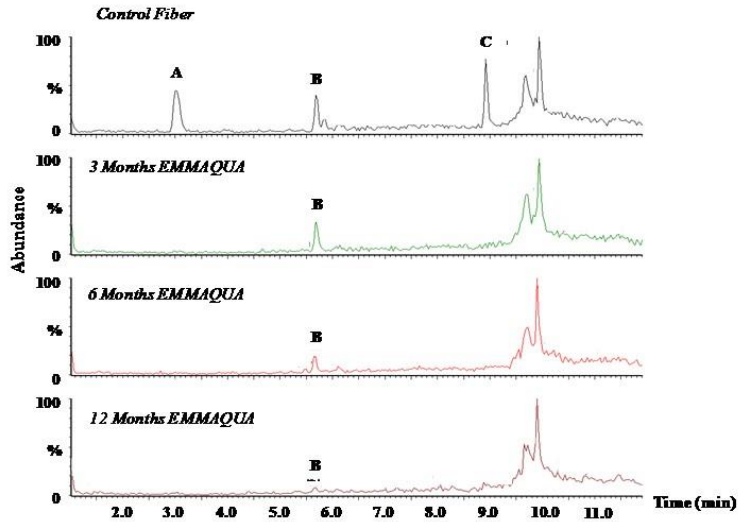


Figure 9. LC/MS total ion chromatogram of an extract from a single 10-mm acrylic fiber before and after accelerated hot and humid weathering of 3, 6, and 12 months in Miami. Peak identity: (A) C.I. Basic Violet 16; (B) finishing agent 1; and, (C) finishing agent 2.

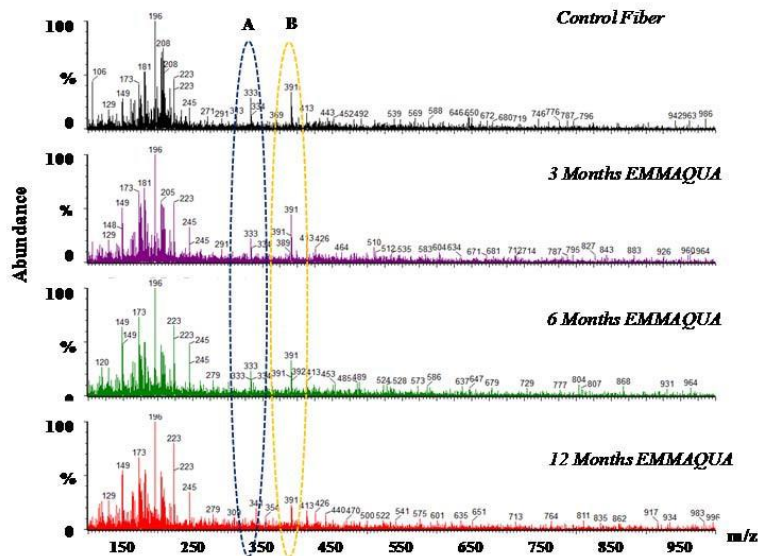


Figure 10. LC/MS total ion mass spectra from an extract of a single 10-mm acrylic fiber before and after accelerated hot and humid weathering of 3, 6, and 12 months in Miami. Peak identity: (A) C.I. Basic Violet 16; (B) finishing agent 1; and, (C) finishing agent 2.

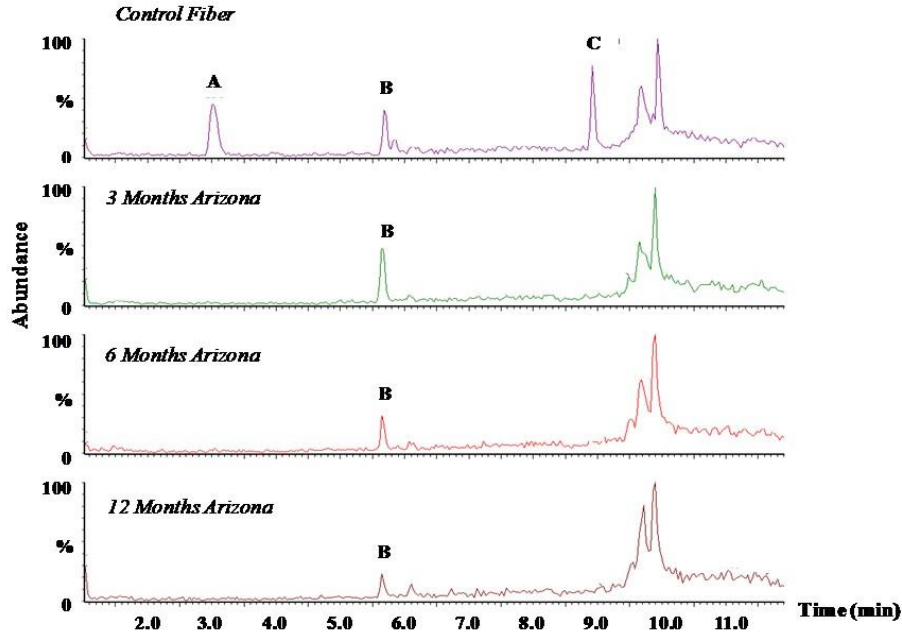


Figure 11. LC/MS total ion chromatogram of an extract from a single 10-mm acrylic fiber before and after hot and dry outdoor weathering of 3, 6, and 12 months in Phoenix. Peak identity: (A) C.I. Basic Violet 16; (B) finishing agent 1; and, (C) finishing agent 2.

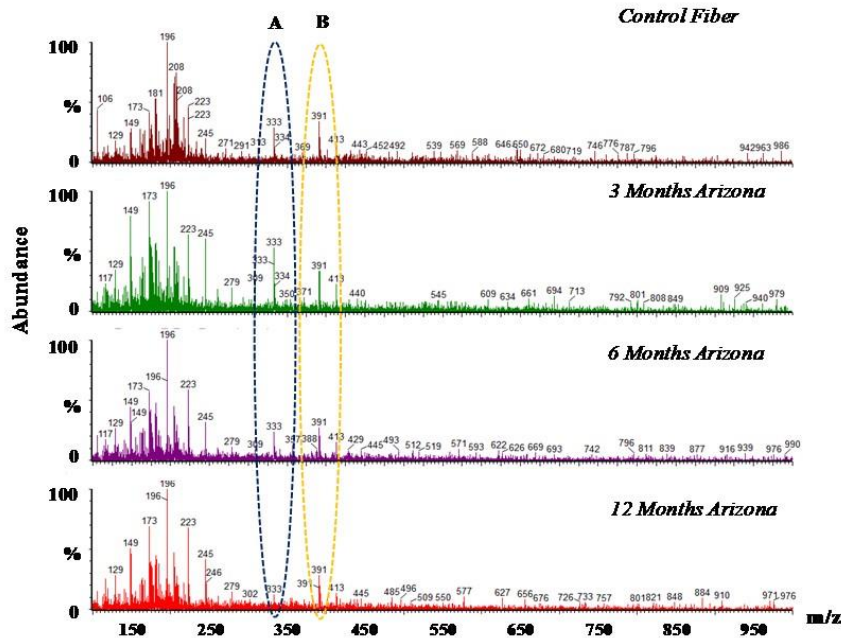


Figure 12. LC/MS total ion mass spectra from an extract of a single 10-mm acrylic fiber outdoor before and after hot and dry outdoor weathering of 3, 6, and 12 months in Phoenix. Peak identity: (A) C.I. Basic Violet 16; (B) finishing agent 1; and, (C) finishing agent 2.

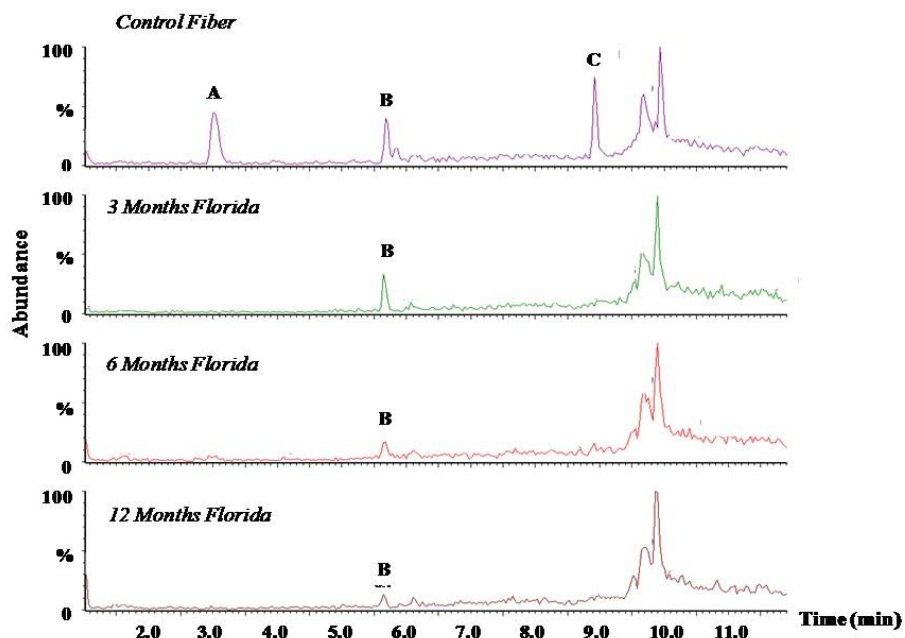


Figure 13. LC/MS ion chromatogram of an extract from a single 10-mm acrylic fiber before and after natural hot and humid weathering in Miami. Peak identity: (A) C.I. Basic Violet 16; (B) finishing agent 1; and (C) finishing agent 2.

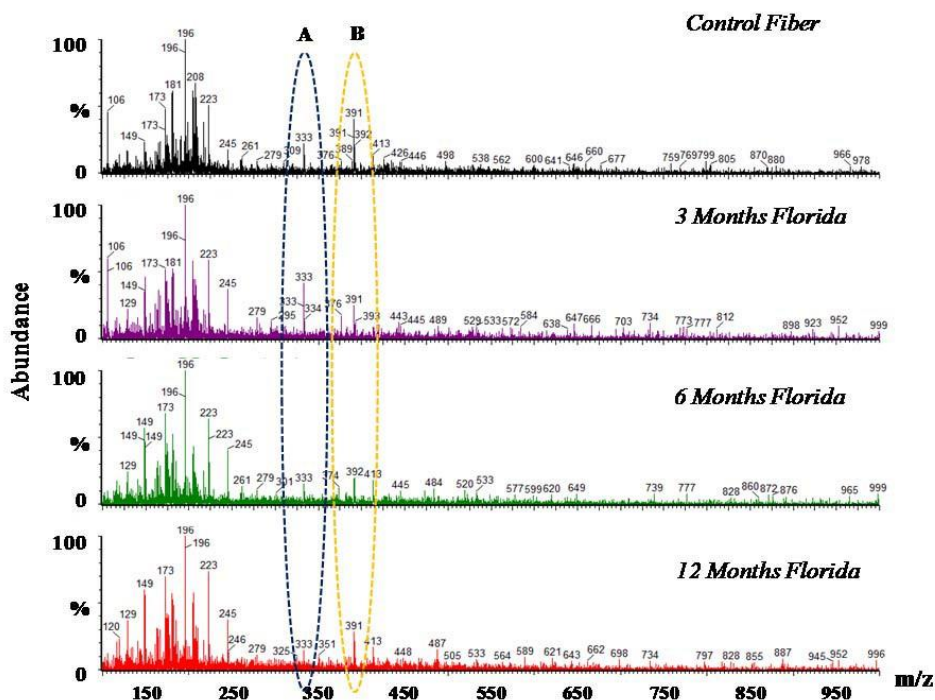


Figure 14. LC/MS total ion mass spectra from an extract of a single 10-mm acrylic fiber outdoor before and after natural hot and humid weathering in Arizona. Ion identity: (A) C.I. Basic Violet 16; and, (B) finishing agent 2.

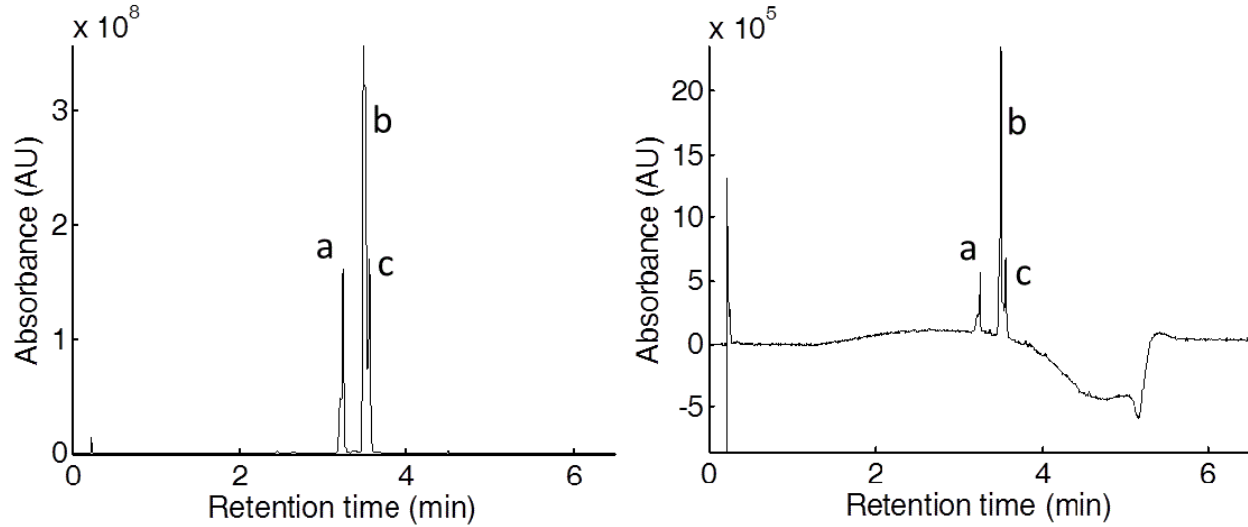


Figure 15. UPLC/diode array chromatograms of three basic dyes extracted from samples after exposure to hot and humid outdoor weather conditions in Miami, FL: (left) a 1 cm bundle of ~40 acrylic fibers from fabric ; and, (right) a single 1 cm acrylic fiber. Dye identity: (a) CI Basic Yellow 28; (b) CI Basic Violet 16; (c) CI Basic Blue 159.

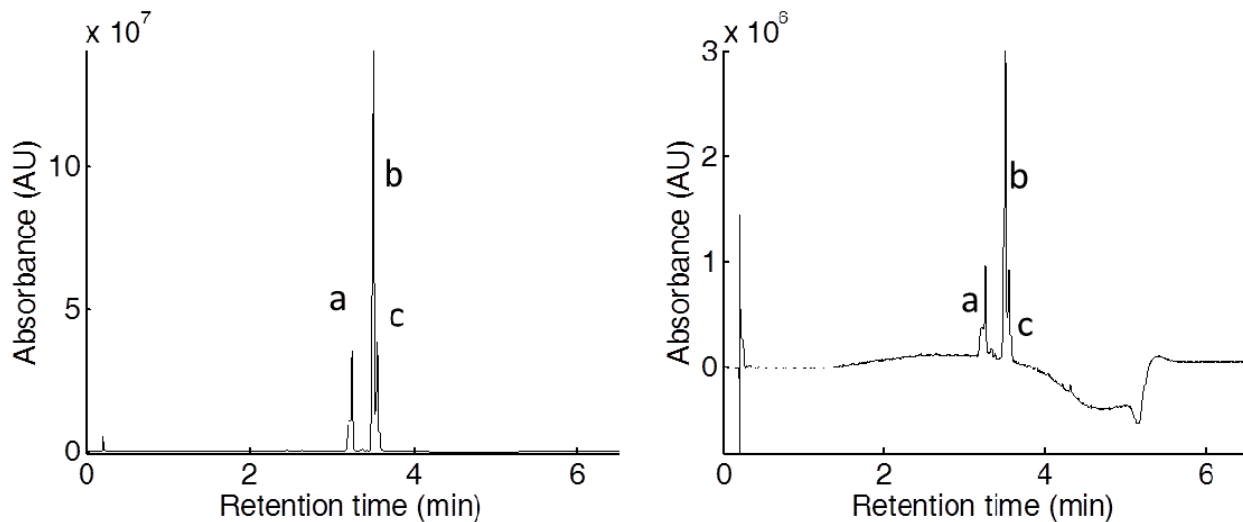


Figure 16. UPLC/diode array chromatograms of three basic dyes extracted from: (left) a 1 cm bundle of ~40 acrylic fibers from fabric exposed to hot and dry outdoor weather conditions in Phoenix, AZ, for 12 months; and, (right) a single 1 cm acrylic fiber. Dye identity: (a) CI Basic Yellow 28; (b) CI Basic Violet 16; (c) CI Basic Blue 159.

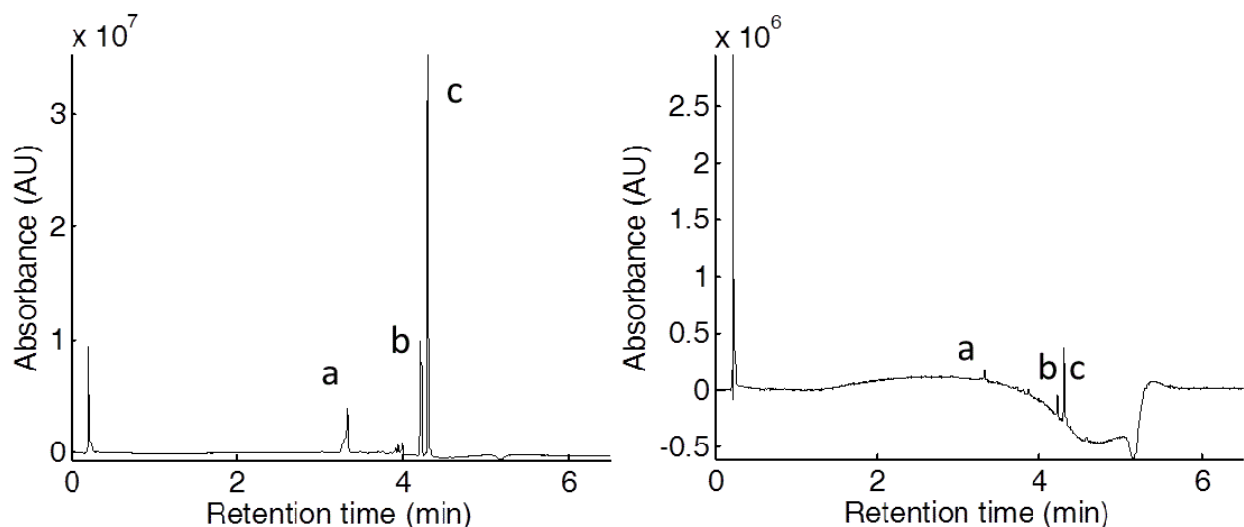


Figure 17. UPLC/diode array chromatograms of three disperse dyes extracted from: (left) a 1 cm bundle of ~40 nylon fibers from fabric exposed to hot and humid outdoor weather conditions in Miami, FL, for 12 months; and, (right) a single 1 cm nylon fiber. Dye identity: (a) CI Acid Blue 45; (b) CI Acid Yellow 49; (c) CI Acid Green 27.

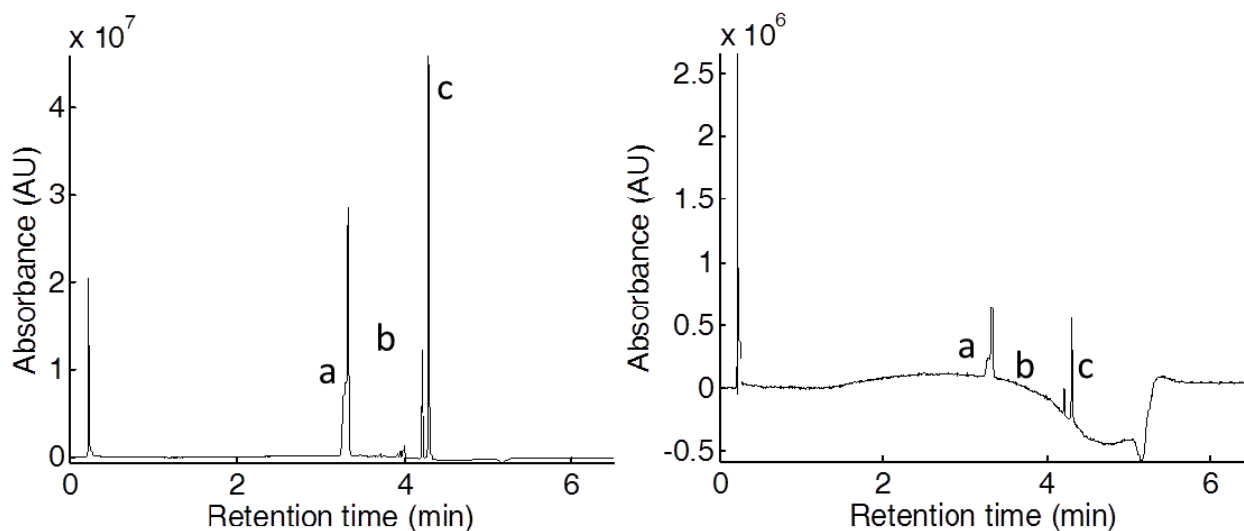


Figure 18. UPLC/diode array chromatograms of three disperse dyes extracted from: (left) a 1 cm bundle of ~40 nylon fibers from fabric exposed to hot and dry outdoor weather conditions in Phoenix, AZ, for 12 months; and, (right) a single 1 cm nylon fiber. Dye identity: (a) CI Acid Blue 45; (b) CI Acid Yellow 49; (c) CI Acid Green 27.

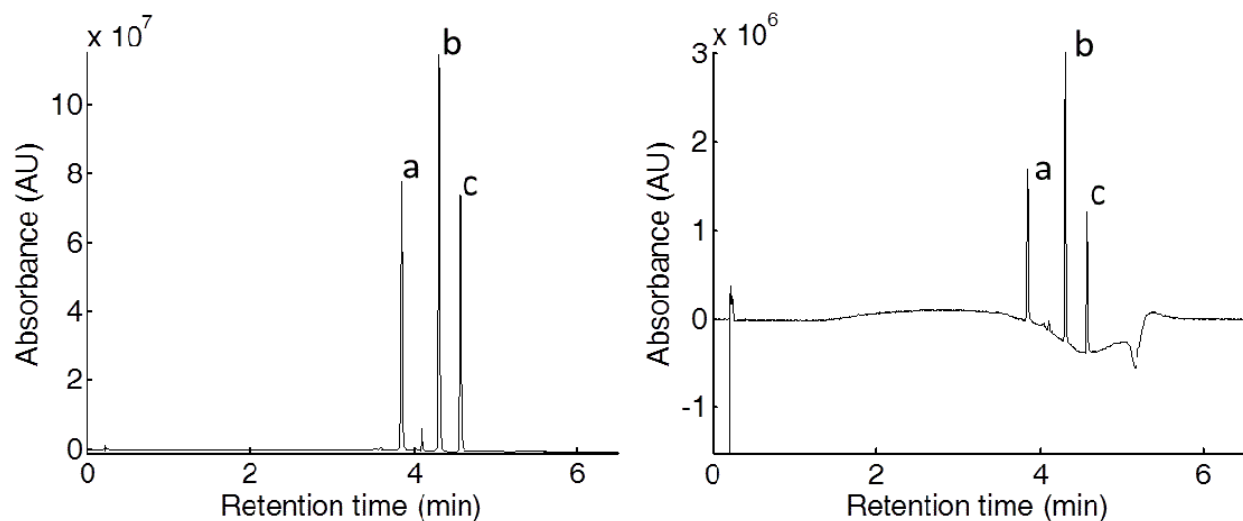


Figure 19. UPLC/diode array chromatograms of three disperse dyes extracted from: (left) a 1 cm bundle of ~40 polyester fibers from fabric exposed to hot and humid outdoor weather conditions in Miami, FL, for 12 months; and, (right) from a single 1 cm polyester fiber. Dye identity: (a) CI Disperse Yellow 114; (b) CI Disperse Violet 77; (c) CI Disperse Red 60.

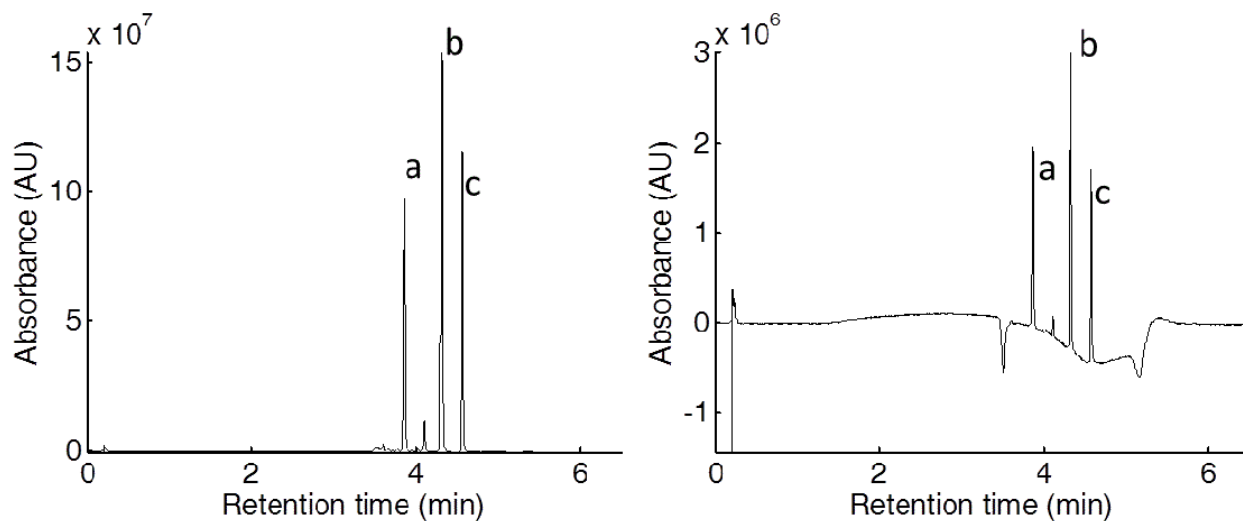


Figure 20. UPLC/diode array chromatograms of three disperse dyes extracted from: (left) a 1 cm bundle of ~40 polyester fibers from fabric exposed to hot and dry outdoor weather conditions in Phoenix, AZ, for 12 months; and, (right) from a single 1 cm polyester fiber. Dye identity: (a) CI Disperse Yellow 114; (b) CI Disperse Violet 77; (c) CI Disperse Red 60.

## **E. Mandel sensitivity applied to analytical method performance comparisons and limits of detection**

Scott J. Hoy, Molly R. Burnip, Stanley N. Deming and Stephen L. Morgan, Department of Chemistry and Biochemistry, University of South Carolina, Columbia, SC 29208

### **ABSTRACT**

The concept of the Mandel sensitivity ratio as an analytical performance characteristic was introduced by John Mandel of the National Bureau of Standards in 1954, but has been not been widely applied in analytical chemistry. The statistical basis for the Mandel sensitivity ratio is reviewed here, along with examples of its use. Because this sensitivity ratio is independent of the scale in which measurements are expressed, it is a useful tool for comparisons of variability between different measurement processes.

### **INTRODUCTION**

Validation of a chemical measurement process (CMP) typically involves the reporting of accuracy, precision, limit of detection, and other figures of merit. Such measures are often used to decide which approach should be employed in favor of another. Mandel points out that accuracy comparisons are usually not contingent on meeting just a few requirements: (a) a monotonic functional relation must exist between what is measured and the property to be determined; (b) reference materials having known values must be available over the target range of the property to be studied; and, (c) the calibration model must be sufficiently free of both random and systematic errors to establish a clear and unbiased relationship.<sup>1,2</sup> Further, statistical measures of calibration accuracy are available for assessing the accuracy performance of a calibration function established by regression.<sup>3,4</sup>

Comparing CMP performance based on estimates of variability from different measurement methods and assigning a level of technical merit to a relevant performance characteristic, however, can be problematic. The oft-recommended approach is to report relative standard deviations (RSDs) or, equivalently, coefficients of variation (CVs) for the two methods. Otto-Hanson, *et al.* provides an illustrative example for which the different measurement scales confound comparison.<sup>5</sup> With two measurements of daily temperature at certain different times and locations expressed in Celsius and Fahrenheit degrees, Assuming that one measurement has a mean of 50 °F with a standard deviation of 10 °F, and the other a mean of 10 °C with a standard deviation of 5.6 °C. With relative standard deviations of 20% and 56%, it might seem that Fahrenheit measurements are more reliable. This comparison is invalid because Fahrenheit and Celsius scales are not proportional to one another because they are interval scale measurements without a meaningful origin, or zero point.<sup>6</sup> In this case, the relationship between the two measurements is known and the numbers could be converted into the other. In general, the relationship between measurements having different scales may not be known.

Mandel sensitivity can be applied to comparisons of CMPs on different scales because it is a scale independent. The computations are trivial, depending only on the slope of the calibration lines and estimates of the variability of the measurement methods to be compared.

## BACKGROUND

**Conventional sensitivity.** The conventional sensitivity ( $S$ ) of a CMP is defined as the change in the measured signal ( $\Delta y$ ) divided by the change in the property being measured ( $\Delta x$ ), *i.e.*, the slope of the calibration relationship:

$$S = \Delta y / \Delta x \quad (1)$$

Figure 1 represents the calibration relationship for two different chromatographic methods of determining the same analyte. The first (upper blue line) method has a sensitivity of

$$\frac{\Delta y}{\Delta x} = \frac{100 \text{ counts}}{100 \mu\text{g}} = 1.0 \text{ counts } \mu\text{g}^{-1} \quad (2)$$

The second method (lower red line) has a sensitivity of

$$\frac{\Delta y}{\Delta x} = \frac{50 \text{ counts}}{100 \mu\text{g}} = 0.5 \text{ counts } \mu\text{g}^{-1} \quad (3)$$

Because of the steeper slope, it appears that the first method is better (more sensitive).

**Mandel response.** The straight-line calibration relationships represent idealized models of the real behavior of the chromatographic methods, idealized in the sense that they ignore noise or uncertainty in the measured data. A more realistic view of variation in the chromatographic results for these two methods is shown by the numerous individual data points in Figure 2. The calibration lines show what might be expected on the average; the dots show what might be obtained if many individual measurements were made on these two systems. Although the first method has the greater sensitivity ( $\Delta y/\Delta x = 1.0 \text{ count } \mu\text{g}^{-1}$  vs.  $0.5 \text{ count } \mu\text{g}^{-1}$ ), it also has greater noise ( $\sigma_b = 5 \text{ counts}$  vs.  $2 \text{ counts}$ ).

The noise associated with the first chromatographic method is illustrated in two ways in the Figure 3. The point at ( $25 \mu\text{g}$ ,  $25 \text{ counts}$ ) is shown with a window extending one standard deviation of the blank ( $\sigma_b = 5 \text{ counts}$ ) above, and one standard deviation below. The Gaussian curve to the left in the figure is another way of illustrating the uncertainty of the data point at ( $25 \mu\text{g}$ ,  $25 \text{ counts}$ ). It is a projection of the uncertainty onto the signal axis (chromatographic peak area). The Gaussian curve is centered at  $25 \text{ counts}$ , with marked lines drawn at  $\pm\sigma_b$  as "verticals" within the Gaussian. For the first chromatographic method,  $\sigma_b = 5.0 \text{ counts}$ , and the Mandel response for the data point above  $25 \mu\text{g}$  is

$$y_M = \frac{y}{\sigma_b} = \frac{25 \text{ counts}}{5.0 \text{ counts}} = 5.0 \quad (4)$$

The vertical scale at the right of the plot shows the Mandel response. Note that the conventional response of  $25 \text{ counts}$  corresponds to a Mandel response of  $5$ .

Similarly, the noise associated with the second chromatographic method is illustrated in two ways in Figure 4. The point at ( $50 \mu\text{g}$ ,  $25 \text{ counts}$ ) is shown with another window extending one

standard deviation of the blank ( $\sigma_b = 5$  counts) above, and one standard deviation below. As before, the Gaussian curve on the left axis in the figure is a projection of the uncertainty onto the signal axis. In this case, the Gaussian is centered at 25 counts, with marked lines drawn at  $\pm\sigma_b$  as "verticals" within the Gaussian.

**Mandel sensitivity.** Mandel defined sensitivity as the ability of a test method to detect a change in the amount of the property under study.<sup>1,2</sup> This ability depends (in part) on the precision of the CMP. Mandel suggested measuring the response as unitless multiples of the standard deviation of the blank ( $\sigma_b$ ):  $y_M = y / \sigma_b$ . The Mandel sensitivity,  $S_M$ , is defined in the same way as traditional sensitivity, however, for Mandel response,  $y_M$ , replaces  $\Delta y$  in the sensitivity calculation. Thus, the Mandel sensitivity ( $S_M$ ) is defined as the change in the Mandel response ( $\Delta y_M$ ) divided by the change in the property ( $\Delta x$ ):

$$S_M = \Delta y_M / \Delta x = \Delta(y / \sigma_b) / \Delta x = (\Delta y / \Delta x) / \sigma_b = S / \sigma_b \quad (5)$$

For the first method (with the steeper slope), the Mandel sensitivity is

$$S_M = S / \sigma_b = \frac{(1.0 \text{ counts } \mu\text{g}^{-1})}{5.0 \text{ counts}} = 0.20 \mu\text{g}^{-1} \quad (6)$$

The second (less sensitive) method, for which  $\sigma_b = 2.0$  counts, has a Mandel sensitivity ( $S_M$ ) of

$$S_M = S / \sigma_b = \frac{(1.0 \text{ counts } \mu\text{g}^{-1})}{5.0 \text{ counts}} = 0.20 \mu\text{g}^{-1} \quad (7)$$

The Mandel sensitivity is a slope. It can be interpreted as the number of standard deviations of the blank that the signal changes per unit change in analyte amount. The Mandel sensitivity removes the original response measurement units (peak area), and has units of reciprocal amount (in this case,  $\mu\text{g}^{-1}$ ).

Although the first method had a larger *conventional* sensitivity ( $1.0 \text{ counts } \mu\text{g}^{-1}$  vs.  $0.5 \text{ counts } \mu\text{g}^{-1}$ ), the second method has the larger *Mandel* sensitivity ( $0.25 \mu\text{g}^{-1}$  vs.  $0.20 \mu\text{g}^{-1}$ ). Because Mandel sensitivity is "the ability of a test method to detect a change in the amount of the property under study," the second method (with the shallower slope) will be better able to detect a change in the amount of analyte.

The Mandel response concept lends itself to depicting the performance of two CMPs on a common scale for comparison. When the two chromatographic methods are plotted in Figure 5 on the same vertical scale of Mandel response, it is clear that the second method, which had the smaller *conventional* sensitivity, has the larger *Mandel sensitivity* ( $0.25 \mu\text{g}^{-1}$ ). The first method, which had the larger *conventional* sensitivity, is seen to have the smaller *Mandel sensitivity* ( $0.20 \mu\text{g}^{-1}$ ). Note that the scaled noise in this plot is the same for both methods (as it should be on this common scale).

**Detection decision limits.** Mandel's original sensitivity was motivated by the concept of deciding whether two CMP responses close to one another can be discriminated—a decision process that is related to calculating decision levels associated with analyte detection. The

common Mandel response scale is an elegant path to calculate such decision limits, because these limits are all based on multiples of the standard deviation of the blank ( $\sigma_b$ ), the very quantity that is measured by the Mandel response. Before discussing the application of Mandel sensitivity to CMP detection limits, we review the basis for the common critical decisions limits for analyte detection.

The limit of detection (LOD) is specified by calculating the signal level above the mean of the blank at which the fraction risk of concluding that analyte is present, when it actually is not present, is acceptably small. Assuming a Gaussian distribution of noise for measurements of a sample containing no analyte (the 'blank'), an estimate of the standard deviation is obtained by replicate measurements of a blank, or by other statistical approaches, and assumed to have sufficient reliability to be considered a good estimate of the population standard deviation of the CMP. Because the variability of many CMPs is homoscedastic at low levels of analyte, the standard deviation of the blank,  $\sigma_b$ , is usually a good estimate of the uncertainty around the LOD. This decision limit is calculated by finding the number ( $k$ ) of standard deviations above the mean that provides an acceptably low upper-tailed area above that level. A common choice for this criterion is  $k = 3$ , which provides an upper-tailed area of  $\alpha = 0.0014$ . This probability can be interpreted as the false positive risk of obtaining a response as high as or higher than LOD from a sample that contains no analyte. Equivalently, the level of confidence associated with correct detection decision at this level is  $100\% \times (1 - \alpha)$ , or 99.86 %. No single value of  $k$  is appropriate for all situations. For example,  $k = 3.3$  provides higher detection reliability with a level of confidence for correct detection of 99.95 %, and a fractional false positive probability of  $\alpha = 0.0005$ . The amount of analyte equivalent to the limit of detection (on the signal axis) is the limit of detection amount ( $LDA$ ) and is found by inverting the calibration relationship. If a straight line calibration ( $y = mx + b$ , where  $y$  is detector response,  $x$  is analyte amount,  $m$  is the slope, and  $b$  is the  $y$ -intercept) is assumed and using  $k = 3.3$ ,

$$LDA = \frac{3.3 \times s_b}{m} \quad (8)$$

However, at  $k = 3$  or  $k = 3.3$  for the A, the false negative error rate ( $\beta$ ) is unacceptably high: 50% of time samples containing analyte present at that LDA will be falsely declared not detected. Remarkably, the  $\beta$  risk has historically been often ignored, even in standards documents from regulatory authorities.<sup>7,8</sup>

The recognition of false negative ( $\beta$ ) risk leads to another critical limit, the minimum consistently detectable amount (MCDA). The MCDA represents the amount at which analyte can be said to be consistently detected, *i.e.*, where the false negative error rate is reduced to be equivalent to the false positive error rate. With the signal domain measurement 6 standard deviations of the blank above the mean of the blank, the fractional risk of encountering a sample giving a signal below the LOD is 0.0014. At 6.6 standard deviations of the blank above the mean of the blank, the fractional risk of a false negative result occurring below the LDA is 0.0005. Thus, the MCDA might be calculated as:

$$MCDA = \frac{6.6 \times s_b}{m} \quad (9)$$

Analyte amounts above the LDA support the detection decision with high confidence, but do so without controlling the false negative risk. Analyte detected at or above the MCDA are associated with a detection confidence of at least 99.95 % and a false negative  $\beta$  risk of 0.0005. The low false negative error rate at the MCDA insures that analyte at or above this limit is *consistently* detected.

At an analyte concentration equal to the LDA, the expected % relative standard deviation (%RSD) of measurements can be calculated from the standard deviation of the blank  $\sigma_b$  projected to the amount axis as the standard deviation of predicted analyte amount,  $\sigma_a$ :

$$\%RSD = 100\% \left( \frac{\sigma_a}{6.6\sigma_a} \right) = 15.15\% \quad (10)$$

The %RSD at an analyte concentration equal to the MCDA is:

$$\%RSD = 100\% \left( \frac{\sigma_a}{3.3\sigma_a} \right) = 30.30\% \quad (11)$$

These %RSD values are too uncertain for the resulting measurements to be considered quantitative (no analytical chemist would boast of achieving a 30.30 %RSD). The generally accepted signal-to-noise ratio considered to be quantitative is 10:1, or equivalently and %RSD of 10 %. Thus, limit of quantitation (LOQ) is defined as the concentration of analyte that produces a signal 10 times the standard deviation of noise (defined by the standard deviation of the blank),

$$\%RSD = 100\% \left( \frac{\sigma_a}{10\sigma_n} \right) = 10\% \quad (12)$$

At analyte levels between the MCDA and the LOQ, analyte is consistently detected with high confidence and low false negative errors, but the %RSD is insufficiently to guarantee accurate quantitation unbiased by experimental uncertainty.

### MANDEL SENSITIVITY APPLIED TO DETECTION DECISION LIMITS

Calibrations from the two chromatographic methods discussed earlier are plotted on again on the same vertical scale of Mandel response in Figure 6. The LDA (with  $k = 3.3$ ) for both methods can be calculated from the Mandel sensitivity as

$$LDA = \frac{3.3}{S_m} \quad (13)$$

For the first chromatographic method, with  $S_M = 0.20 \mu\text{g}^{-1}$ ,

$$LDA = \frac{3.3}{0.20 \mu\text{g}^{-1}} = 16.5 \mu\text{g} \quad (14)$$

For the second chromatographic method, with  $S_M = 0.25 \mu\text{g}^{-1}$ ,

$$LDA = \frac{3.3}{0.25 \mu\text{g}^{-1}} = 13.2 \mu\text{g} \quad (15)$$

These LDA values are the analyte amounts (on the x-axis in Figure 6) at which the horizontal green line at height  $3.3\sigma_b$  intersects with the respective calibration lines.

The MCDA (with  $k = 6.6$ ) for both methods can be calculated from the Mandel sensitivity as

$$MCDA = \frac{6.6}{S_M} \quad (16)$$

For the first chromatographic method, with  $S_M = 0.20 \mu\text{g}^{-1}$ ,

$$MCDA = \frac{6.6}{0.20 \mu\text{g}^{-1}} = 33.0 \mu\text{g} \quad (17)$$

For the second chromatographic method, with  $S_M = 0.25 \mu\text{g}^{-1}$ ,

$$MCDA = \frac{6.6}{0.25 \mu\text{g}^{-1}} = 26.4 \mu\text{g} \quad (18)$$

These MCDA values occur in Figure 7 at the intersection of the horizontal green line at  $6.6\sigma_b$  with the Mandel response calibration lines.

Finally, the LOQ (with  $k = 10$ ) for both methods can be calculated from the Mandel sensitivity as:

$$LOQ = 10/S_M \quad (19)$$

For the first chromatographic method, with  $S_M = 0.20 \mu\text{g}^{-1}$ ,

$$LOQ = (10/0.20 \mu\text{g}^{-1}) = 50.0 \mu\text{g} \quad (20)$$

For the second chromatographic method, with  $S_M = 0.25 \mu\text{g}^{-1}$ ,

$$LOQ = (6.6 / 0.25 \mu\text{g}^{-1}) = 40.0 \mu\text{g} \quad (21)$$

These LOQ values occur in Figure 8 at the intersection of the horizontal line at  $10\sigma_b$  with the Mandel response calibration lines.

## CONCLUSIONS

Evaluating a CMP from the viewpoint of Mandel response and sensitivity offers an easy and rapid method for comparison of the calibration performance of analytical methods by use of scale independent approach. Mandel sensitivity offers an advantage over scale dependent approaches such as RSDs and CVs because it normalizes performance relative to the variability of the measurement method. This approach enables calculation of detection limit critical values in a universal way that also provides intuitive and visual understanding of the differences among limit of detection amount, minimal consistently detectable amount, and limit of quantitation.

## ACKNOWLEDGEMENTS

This research was supported by award 2010-DN-BX-K245 from the National Institute of Justice, Office of Justice Programs, U. S. Department of Justice. The opinions, findings, and conclusions or recommendations expressed in this publication are those of the author(s) and do not necessarily reflect those of the Department of Justice. Mention of commercial products does not imply endorsement on the part of the National Institute of Justice.

## REFERENCES

- (1) Mandel, J.; Stiehler, R. D. Sensitivity—A criterion for the comparison of methods of test, *Journal of Research of the National Bureau of Standards* **1954**, *53*, 155-159.
- (2) Mandel, J. *The Statistical Analysis of Experimental Data*, John Wiley & Sons, Inc., New York, 1964, pp. 363-389.
- (3) Draper, N. R.; Smith, S. *Applied Regression Analysis*, 3<sup>rd</sup> ed., John Wiley & Sons, Inc., New York, 1998.
- (4) Deming, S. N.; Morgan, S. L. The use of linear models and matrix least squares in clinical chemistry, *Clin. Chem.* **1979**, *25*, 840-855.
- (5) Otto-Hanson, L.; Eskridge, K. M.; Steadman, J. R.; Madisa, G. The sensitivity ratio: A superior method to compare plant and pathogen screening tests. *Crop Sci.* **2009**, *49*(1), 153-160.
- (6) Stevens, S. S. On the theory of scales of measurement. *Science* **1946**, 677-680.
- (7) Currie, L. A. Detection: Overview of historical, societal, and technical issues. Chapter 1 in: *Detection in Analytical Chemistry: Importance, Theory, and Practice*, L. A. Currie (ed.), American Chemical Society, Washington, DC, 1988.
- (8) Currie, L. A. Detection: International update, and some emerging dilemmas involving calibration, the blank, and multiple detection decisions. *Chemom, Intell. Lab. Sys.* **1997**, *37*, 151-181.

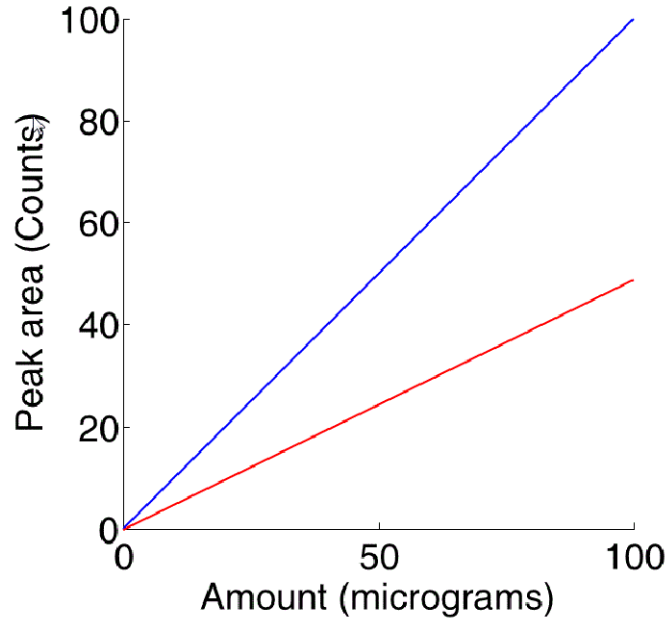


Figure 1. Calibration relationship for two different measurement processes.

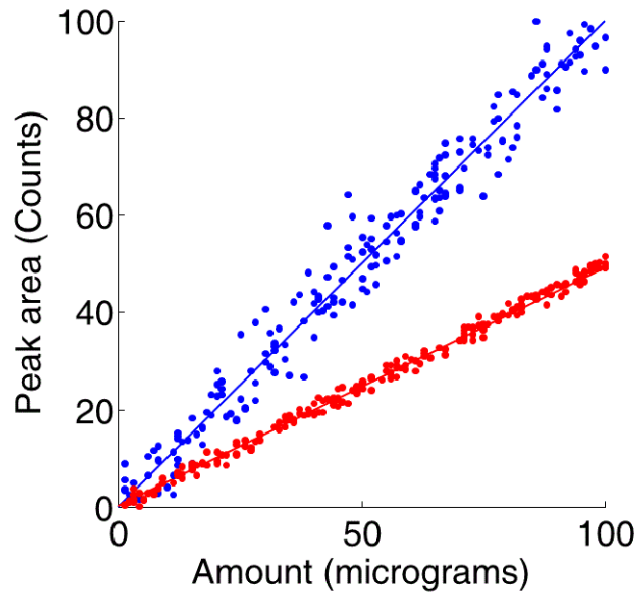


Figure 2. Calibration relationship for two different measurement processes with noise; standard deviation for upper (blue) calibration is 5 counts, and the standard deviation for the lower (red) calibration is 2 counts.

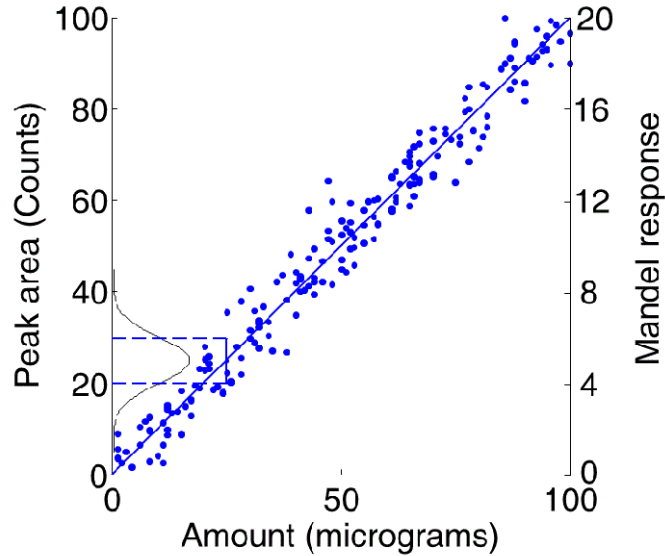


Figure 3. Calibration relationship for the first method with plus and minus one standard deviation window about the response of 25 peak counts for 25 micrograms. The right hand scale shows the Mandel response in unitless multiples of the standard deviation.

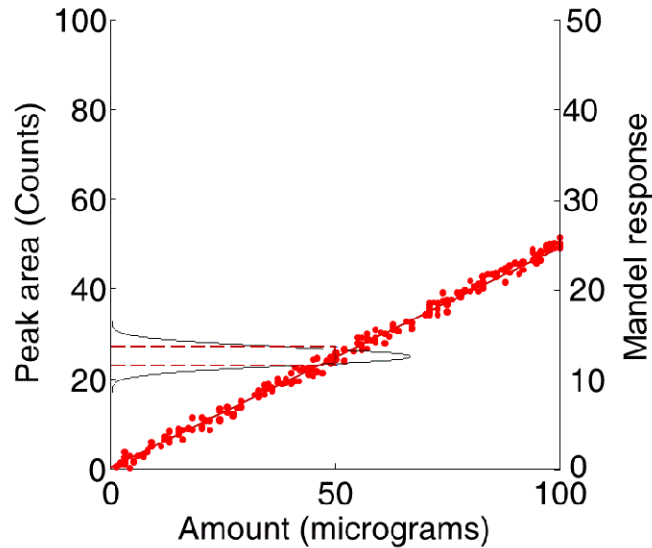


Figure 4. Calibration relationship for the second method with plus and minus one standard deviation window about the response at 25 peak counts for 50 micrograms. The right hand scale shows the Mandel response in unitless multiples of the standard deviation.

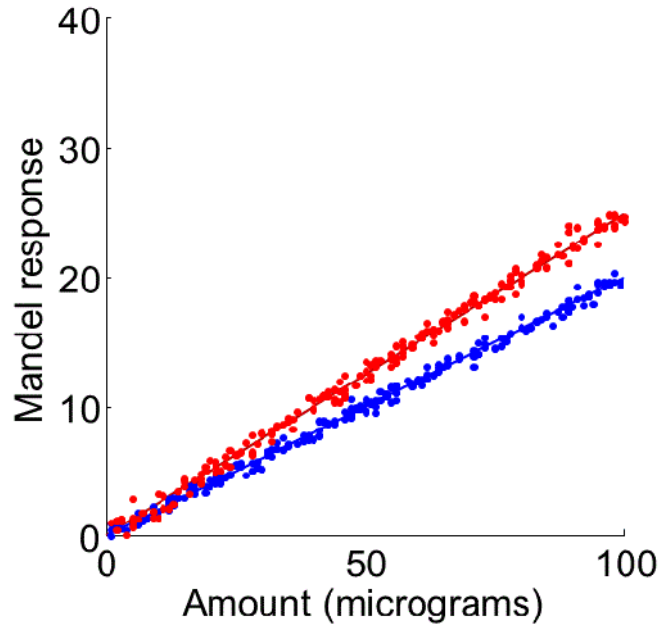


Figure 5. Common Mandel response scale for comparison of calibration performance. The second (red) method has larger Mandel sensitivity ( $0.25 \mu\text{g}^{-1}$ ) than the first (blue) method ( $0.20 \mu\text{g}^{-1}$ ).

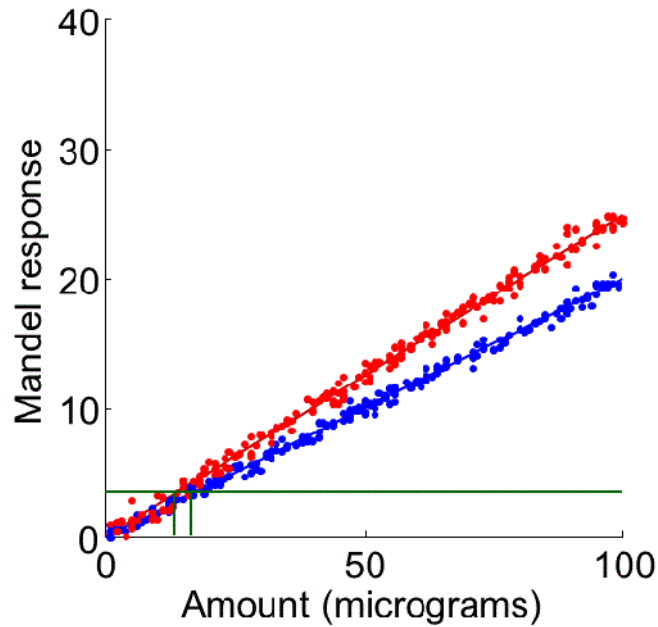


Figure 6. Common Mandel response scale for estimation of LDA. The second (red) method has a lower LDA ( $13.2 \mu\text{g}$ ) than the first (blue) method ( $16.5 \mu\text{g}$ ).

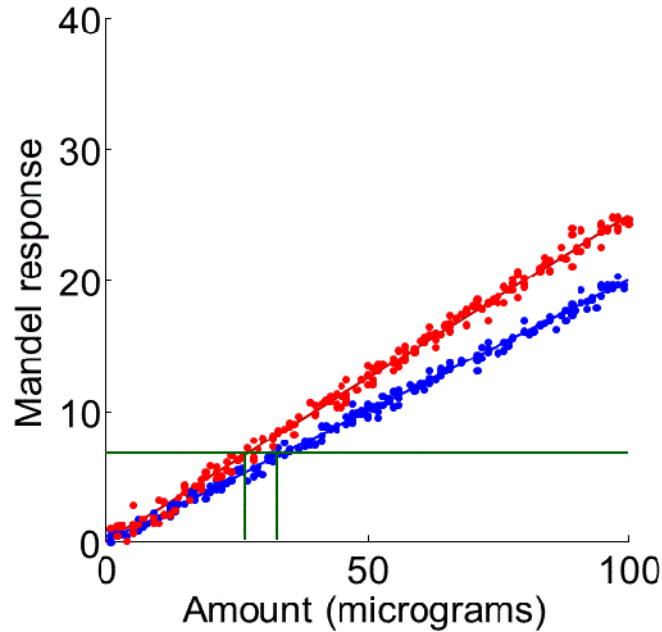


Figure 7. Common Mandel response scale for estimation of MCDA. The second (red) method has a lower MCDA (26.4  $\mu\text{g}$ ) than the first (blue) method (33.0  $\mu\text{g}$ ).

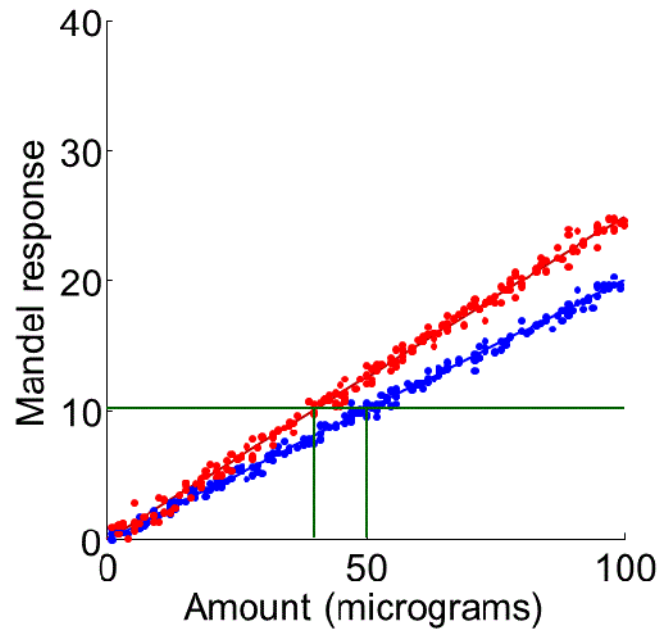


Figure 8. Common Mandel response scale for estimation of LOQ. The second (red) method has a lower LOQ (40.0  $\mu\text{g}$ ) than the first (blue) method (50.0  $\mu\text{g}$ ).

## F. Limits of detection from the viewpoint of statistical hypothesis testing

Kaylee R. McDonald, Molly R. Burnip, Scott J. Hoy, and Stephen L. Morgan, Department of Chemistry and Biochemistry, University of South Carolina, Columbia, SC 29208

### ABSTRACT

The limit of detection (LOD) is one of the most fundamental performance measures of an analytical chemical method; its impact extends also to numerous societal implications<sup>1</sup>. Typically, a detection threshold is defined in the signal domain and extrapolated to the equivalent amount or concentration domain. However, ambiguity often exists in the choice of measurement uncertainty as a basis for the LOD (replicate blank measurements, residuals from the calibration relationship, etc.). Few sources discuss assumptions made with different choices (normality of data distribution, homoscedasticity of variance, absence of outliers), and validation testing is rarely mentioned. The statistical basis for LOD variants is also often not clear to practitioners and the reporting of multiple types of decision limits, particularly in regard to false positive and negative detection probabilities can be confusing. We summarize these issues and present comparisons of alternative approaches for estimation of detection limits along with appropriate validation tests. Finally, we present the application of statistical tolerance intervals to LOD estimation to provide a statistical basis for uncertainty estimates related to LODs. Based on sample statistics rather than assumed known population parameters, a tolerance interval specifies the range of concentrations that include a specific proportion of the entire population of results around the estimated LOD. This approach allows for statements to be made concerning false positive and negative results with a stated level of confidence.

### INTRODUCTION

Although the concept of a limit of detection (LOD) has been under serious discussion in the analytical literature for over 20 years before the seminal text by Lloyd Currie was published in 1988,<sup>1</sup> there remains considerable confusion and inconsistency in definitions of throughout the literature. Even accreditation organizations and governing bodies vary in their 'suggestions' for how to calculate a limit of detection. Some organizations do not define the exact meaning of the limit of detection and even suggest multiple approaches for its calculation. As Table 1 below suggests, there is a lack of consistent definitions, as well as inconsistent notation and calculations.

The International Union of Pure and Applied Chemistry (IUPAC) originally defined detection limit as “the measure of the inherent Detection Capability of a Chemical Measurement Process”.<sup>1,2</sup> IUPAC defined the limit of detection, expressed as the concentration,  $c_L$ , or the quantity,  $q_L$ , derived from the smallest measure,  $x_{LOD}$ , that can be detected with reasonable certainty for a given analytical procedure.<sup>3</sup> The value of the limit of detection (defined on the signal axis) is given by the equation,  $x_{LOD} = \bar{x}_b + ks_b$ , where  $\bar{x}_b$  is the mean of the blank measurements,  $s_b$  is the standard deviation of the blank measurements, and  $k$  is a numerical factor chosen according to the confidence level desired.” IUPAC specified a value of  $k = 3$ , (associated with a false positive detection error rate of 0.014), but elsewhere in the literature,  $k$  ranges from 2 to 3.3. Inconsistency in the definition of the LOD forestalls forensic practitioners from understanding its interpretation, has the effect of confounding comparisons of LOD values between different methods, and impedes interlaboratory comparisons.

The International Conference on Harmonization (ICH) states that, “[t]he detection limit is determined by the analysis of samples with known concentrations of analyte and by establishing the minimum level at which the analyte can be reliably detected.” ICH then suggests that LOD can be determined by visual examination, signal-to-noise, and on the standard deviation of the response and the slope using the standard deviation of the blank or the calibration curve. Some organizations define the LOD concept, but do not provide well-defined procedures for its determination.<sup>3</sup> The only LOD citation found in SWGMAT documents is from SWGTOX, which roughly follows IUPAC, but suggests several different sources for estimating the standard deviation of the measurement uncertainty: the lowest non-zero calibrator, background noise based on three replicate blank measurements, replicate measurements of spiked reference materials, and from the standard deviation of the y-intercept.<sup>4</sup> Differences in validation documents for detection limits from four sources are summarized in Table 1. These issues are not new to the scientific community, but they are not well addressed by current standards.<sup>2,4-6</sup>

Guidelines	ICH (1996)	IUPAC (1997)	SWGTOX (2012)	AMC (1987)
<b>Precise Definition</b>	Not Specified.	The limit of detection, expressed as the concentration, $c_L$ , or the quantity, $q_L$ , is derived from the smallest measure, $x_L$ , that can be detected with reasonable certainty for a given analytical procedure.	Not Specified.	Uses IUPAC definition.
<b>Method for uncertainty estimation</b>	Based on visual examination, based on signal to noise (3 or 2:1 is acceptable), based on the standard deviation of the response and the slope (using the standard deviation of the blanks or the calibration curve), or based on recommended data	Not Specified.	Use lowest non-zero calibrator, use decision point concentration as LD, estimate LD using background noise (use reference materials or statistical analysis of background), or estimate LD using a linear calibration curve.	The detection limit of a system is estimated in principle by repeated measurements in the response domain of the field blank taken through the appropriate procedure.
<b>Calculation</b>	Based on standard deviation of the response and the slope: $LD = (3.3\sigma)/S$ , where $\sigma$ is the standard deviation of the response and S is the sensitivity.	$x_L = \bar{x}_{bl} + k s_{bl}$ where $\bar{x}_{bl}$ is the mean of the blank measures, $s_{bl}$ is the standard of the blank measures, and k is a numerical factor chosen according to the confidence level desired	LD using reference materials: $S/N = (\text{height of analyte})/(\text{amp. of noise})$ Estimating LD using statistical analysis of background: $LD = \bar{x} + 3.3\sigma$ , where $\bar{x}$ and $\sigma$ are the mean and standard deviation of the negative samples, respectively. Estimating LOD using a linear calibration curve: $LOD = (3.3\sigma_y)/m_{avg}$ where $\sigma_y$ is the standard deviation of the y-intercept and $m_{avg}$ is the average slope	The smallest measure of response ( $x_L$ ) that can be detected with reasonable certainty in a given analytical procedure, where $x_L = \bar{x}_B + k s_B$ and $\bar{x}_B$ is the mean of the blank measures, $s_B$ is the standard deviation of the blank measures, and k is a numerical constant. $c_L$ (or $q_L$ ) = $k s_B/S$ The detection limit is given by where S is the sensitivity of the method. A value of k = 3 is “strongly recommended” by IUPAC.

Table 1. Comparison of LOD definitions.

The lack of agreement or detail in procedures for calculation of the limit of detection is an impediment to validation for chemical measurement processes. Inter-laboratory comparisons may not be commensurable, although all organizations may think they talking about the same concept. Even if two laboratories use similar instruments and the same analytical procedure, comparisons will be invalidated if LOD is estimated by different approaches. Even if the equation used in both cases was the same, the interpretation of the variables employed might vary. Perhaps the largest variation in interpretation involves the source of uncertainty employed

in the LOD calculation: how should the estimate of the standard deviation of the measurement uncertainty be evaluated? The objective of the present discussion is to bring these issues to light in the forensic analytical community in the hopes that upcoming revisions in standards will acknowledge these difficulties.

## EXPERIMENTAL

Dye standards and extracts were separated and detected using a Waters Acquity™ Ultra-Performance Liquid Chromatography (UPLC) H-Class system equipped with a quaternary solvent pump system and a UV/visible photodiode array detector (PDA) eλ detector (Milford, MA). The column was a 2.1 × 50 mm I.D. 1.7 μm particle size Waters Acquity™ BEH C18 column with a 2.1 × 5 mm I.D. 1.7 μm particle size Waters Acquity UPLC® BEH C18 VanGuard precolumn. The mobile phase gradient for this was based on mixtures of 50 mM ammonium acetate in water and 0.15% formic acid in methanol, purchased at HPLC grade from Fisher Scientific (. The column temperature was set at 40 °C. The diode array detector scanned the wavelength range from 325 nm to 675 nm at a rate of 40 Hz and 1.2 nm resolution. The sample injection volumes were 10 μL.

Calibration designs were constructed for all nine dyes based on 5 replicate experiments at 6 levels of dye concentration (10 ppb, 20 ppb, 30 ppb, 40 ppb, and 50 ppb, in addition to 15 measurements of a blank). For each dye peak, QuanLynx™, data management software included with MassLynx™ (Waters, Milford, MA) was used to integrate peak areas above corrected baselines.

## RESULTS AND DISCUSSION

**Estimating measurement uncertainty.** To estimate the limit of detection for any analytical method, the analyst must have a valid estimate of the measurement uncertainty in the signal domain, and several options are available from a well-designed calibration. Specifically, the uncertainty of the chemical measurement process (CMP) can be estimated from different:

- the standard deviation,  $s_b$ , of replicate measurements of the blank;
- the standard deviation,  $s_{nz}$ , of the replicate measurements of the lowest non-zero concentration standard;
- the standard deviation,  $s_{b0}$ , of the estimated intercept parameter, based on the sum of squares of residuals for the fitted calibration line; and,
- the standard deviation,  $s_r$ , of the residuals for the fitted calibration line.

Table 2 shows the different estimates of standard deviation that might be calculated for the UPLC analysis of Acid Red 337, depending on the source for measurement uncertainty.

Calibration for Acid Red 337 dye		
$\sigma_b$	LOD basis	LOD
standard deviation of replicate measurements of blanks, df = 14		9.50
standard deviation of the lowest non-zero calibrator, df = 9	$3.3\sigma_b$	2.17
standard deviation of the residuals of the fitted line, df = 43		8.90

Table 2. Effects on limit of detection with estimating variability from different sources. The symbol 'df' represents degrees of freedom.

Validation statistics for calibration are also rarely generated by forensic practitioners. For example, for calibration models based on linear or polynomial relationships, a specific test for lack of fit exists that allows one to evaluate whether, e.g., the straight line relationship has statistically validity.<sup>7-9</sup> If the fitted model is not suitable for use as a predictor of concentration, and the third and fourth alternative sources of estimation of measurement variation will be biased in any LOD calculation.

**Defining and understanding the limit of detection.** The number of standard deviations,  $k$ , above the mean of the blank measurement that defines the limit of detection determines the probability of false positive detection. There is no single value for LOD that is appropriate for all situations and, ultimately, the analyst and the client should think about the consequences of false positives and set LOD accordingly. The values of  $\text{LOD} = \mu_b + 3\sigma_b$ , and  $\text{LOD} = \mu_b + 3.3\sigma_b$  are often seen.

If LOD is set  $\mu_b + 3\sigma_b$ , then the fractional risk of detecting analyte when, in fact, it is absent is  $\alpha = 0.0014$ . For LOD set at  $\mu_b + 3.3\sigma_b$ , the fractional risk of detecting analyte, when it is absent, is  $\alpha = 0.0005$  (“one-twentieth of one percent”), which is usually considered an acceptable level of risk (Figure 1, left and center panels). However, at any specified signal-to-noise ratio when analyte is actually present at the amount producing that signal level, the false negative error rate ( $\beta$ , the error of not detecting analyte when it is, in fact, present) is 50%. This concept is illustrated in the right panel of Figure 1.

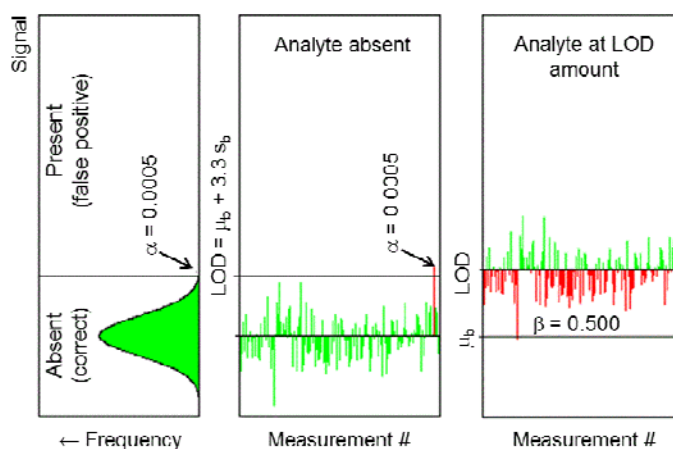


Figure 1. False positive and false negative risks for a sample containing analyte equivalent to the limit of detection amount of analyte, the LDA.

This false negative rate can only be reduced at a threshold of concentration higher than the limit of detection. If enough analyte is added to raise the mean signal to, say,  $3.3\sigma_b$  above LOD (equivalent to  $6.6\sigma_b$  above the mean of the blank, then the false negative rate can be reduced to  $\beta = 0.0005$  and the analyte will be detected consistently (Figure 3). The amount of analyte that gives sufficiently consistent detection can be called the “*minimum-consistently-detectable amount*,” or MCDA. This concept of “consistently detectable” is important. It means that if the sample that does contain analyte is measured repeatedly, most of the time (99.95% of the time, in this example) it will be concluded that analyte is present. If false negative results are of concern to a forensic laboratory, then the use MCDA should be considered.

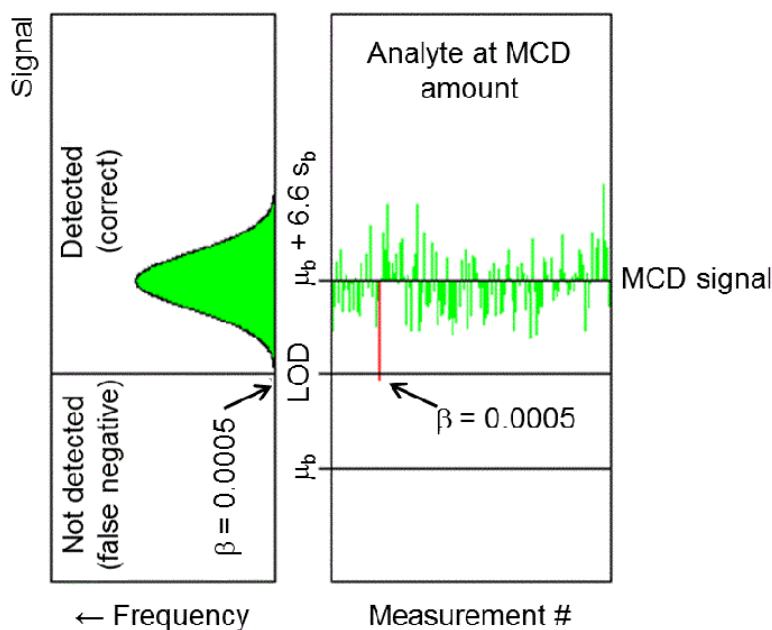


Figure 2. For a sample that contains an amount of analyte that gives a signal equal to the mean of the blank plus 6.6 standard deviations of the blank signal (twice that for LOD), it can be said that analyte has been confidently detected (at or above the LOD), and that the analyte is also consistently detected (at or above the MCDA).

**Statistical tolerance intervals.** If controlling both false positive *and* false negative error rates is of concern for a calibration, and if it is desired to know the expected number of individual such errors that might occur, then a *tolerance interval* is required. A tolerance interval is an interval that contains at least a defined portion,  $p$ , of the population with a defined degree of confidence,  $100(1 - \alpha)\%$ . As a result, there is  $100(1 - \alpha)\%$  confidence that the tolerance interval includes  $100p\%$  of the population. The confidence level associated with the tolerance interval takes into account the fact that samples do not perfectly reflect the true population.

For practical purposes, a tolerance interval also allows the experimenter to choose the values for false negative and false positive error rates. Control of these levels is critical when *either* result may have significant consequences (*e.g.*, forensic cases that end in trial based on laboratory results). The tolerance interval can also be adjusted to determine an upper or lower bound of a portion of the data. These upper limits can help generate more accurate limits of detection. A tolerance interval calculator requires a mean and standard deviation (can be taken from blank replicates) and the desired confidence and spread of the population. Tolerance intervals enable calculation of limits of detection based on a larger number of detection decisions with a specified level of confidence. Statistical tolerance intervals can be used with any of the LOD definitions cited. False positive and false negative error rates can both be set, which is important when both directions represent negative/unwanted outcomes. Upper/lower one-sided tolerance intervals for limit of detection applications can be calculated, so that the specified population lies below/above the given value. Statistical tolerance intervals have not been easily applied in practice, partly because of the paucity of statistical tables for the asymmetric functions needed, and the complex calculations required.<sup>6</sup> However, resources in the form of online calculators and sample calculations are readily available.<sup>10-11</sup>

Statistical tolerance intervals typically produce LODs higher than estimated using other approaches. However, the additional information on future behavior of the measurement process can be useful for decision-making. For example, a tolerance interval can be based on a specified proportion of samples at the LOD concentration that could be expected to be within the calculated interval at a given confidence level.

Figure 3 illustrates calculation of an LOD using specified false positive and negative error rates. Table 3 shows estimated LOD values for textile dyes analyzed by microextraction/UPLC/UV-visible detection. Results using four different approaches over high (0-400 ppb) and low (0-100 ppb) concentration ranges.

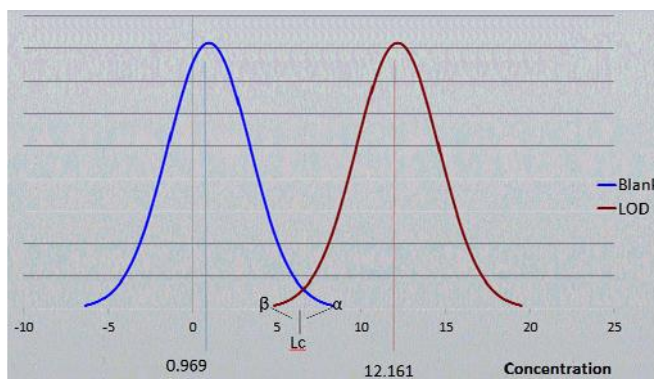


Figure 3. False positive and false negative risks for LOD calculations using  $3\sigma$  and the statistical tolerance interval approach.

3.3s and the statistical tolerance interval approach.

DYE	LOD <sub>1</sub> (High)	LOD <sub>2</sub> (High)	LOD <sub>3</sub> (High)	LOD <sub>4</sub> (High)
Basic Red 46	4.77	5.41	11.80	13.81
Basic Violet 16	3.62	1.69	6.32	6.05
Basic Yellow 28	6.97	1.07	14.10	19.04
Acid Red 337	9.50	2.17	8.90	12.23
Acid Yellow 49	3.22	1.96	10.40	12.24
Acid Blue 281	4.87	1.56	6.79	7.56
Disperse Violet 77	10.10	0.37	9.42	14.94
Disperse Blue 60	37.00	13.50	16.80	30.99
Disperse Yellow 114	11.30	4.68	7.60	10.90
DYE	LOD <sub>1</sub> (Low)	LOD <sub>2</sub> (Low)	LOD <sub>3</sub> (Low)	LOD <sub>4</sub> (Low)
Basic Red 46	2.37	3.12	1.21	2.75
Basic Violet 16	1.84	2.09	0.91	1.55
Basic Yellow 28	2.69	0.93	0.77	2.39
Acid Red 337	3.07	1.89	0.86	2.39
Acid Yellow 49	4.26	2.59	1.01	3.90
Acid Blue 281	4.38	0.41	1.22	4.39
Disperse Violet 77	2.23	1.28	0.99	2.21
Disperse Blue 60	-	-	-	-
Disperse Yellow 114	12.60	12.60	2.34	12.16

Table 3. Comparison of UPLC-UV/visible detection LODs for textile dyes (in ppb) (3.3s) based on: (1)  $s_b$ ; (2)  $s$  of the lowest non-zero concentration replicates; (3)  $s$  of the y-intercept of the calibration line; and (4) a statistical tolerance interval.

## CONCLUSION

This document is a work in progress which will be supplemented by additional examples and discussion. To facilitate analysis of calibration data, we have designed a program for Microsoft Windows that carries on a complete regression analysis, residual analysis, analysis of variance, and limit of detection estimation by several optional approaches. The program includes everything required for validation work in a routine forensic laboratory and more. For example, replicate measurements of response at several analyte concentrations can be used in statistical hypothesis tests for the presence of non-constant variability as a function of analyte concentration. Such heteroscedasticity is common when noise increases with analyte signal (e.g., in most measurements involving counts). The SLED toxicology laboratory often encounters heteroscedastic data, for which the oft-cited remedy is to use weighted least squares (with measurements assigned weights inversely proportional to variance at the different concentration levels), instead of ordinary least squares. We have added the appropriate statistical hypothesis tests for non-constant variance and have implemented the option of weighted least square for calibrations. The program is continually undergoing modifications to introduce protocols that can be automated, such as limit of detection calculations from calibration data. For another example, forensic scientists at SLED also routinely inspect data for the presence of unrepresentative measurements (outliers); an outlier module will be added to the program soon. We have also validated program code by running test data sets on commercially available programs such as Minitab and JMP for comparison. The program has the appearance of an 'app' with buttons that run procedures when pressed. Most importantly, the forensic chemist does not have to worry about complex computations, and time can be spent productively on interpreting understandable calibrations. Appendix 1 shows sample output and diagnostic plots for one of our data sets from the program. We expect that this program will be the subject of a research manuscript and that the permutations on statistical approaches for calibration it offers may also result in other publications. We plan to make the program freely available as a download from a USC web site and to solicit user feedback for further improvements. Output examples are shown in the following appendix to this section.

A poster based on this work generated interest at the SCIX 2013 meeting in Minneapolis in October 2013 and received the a Best Student Poster Award. Our AAFS poster in February 2014 covered some of the same material.

## REFERENCES

1. Currie, L. A. (Ed.) *Detection in Analytical Chemistry: Importance, Theory, and Practice*, ACS Symp. Series 361, American Chemical Society, Washington, DC, 1988.
2. Currie, Lloyd A. "Detection and Quantification Limits: Origins and Historical Overview". *Anal. Chim. Acta*. **1999**. 391, 127-134
3. International Union of Pure and Applied Chemistry (IUPAC). *Compendium of Chemical Terminology*, 2nd ed. (the "Gold Book"). Compiled by A. D. McNaught and A. Wilkinson. Blackwell Scientific Publications, Oxford (1997).

4. Scientific Working Group for Forensic Toxicology (SWGTOX), *Standard Practices for Method Validation in Forensic Toxicology*, SWGTOX Doc 0003 Revision Draft, 18 June 2012.
5. Analytical Methods Committee. "Recommendations for the Definition, Estimation and Use of the Detection Limit". *Analyst* **1987**, *112*, 199-204
6. Gibbons, R. D.; Coleman, D. E. *Statistical Methods for Detection and Quantification of Environmental Contaminants*, John Wiley, New York, 2001.
7. Draper, N. R.; Smith, H. *Applied Regression Analysis*, 3<sup>rd</sup> ed., John Wiley & Sons, New York, 1998.
8. Deming, S. N.; Morgan, S. L. "The use of linear models and matrix least squares in clinical chemistry," *Clin. Chem.* **1979**, *25*(6), 840-855.
9. Deming, S. N.; Morgan, S. L. *Experimental Design: A Chemometric Approach*, 2nd ed., Elsevier Science Publishers, Amsterdam, 1993.
10. Hahn G. J.; Meeker, W. Q. *Statistical Intervals: A Guide for Practitioners*, John Wiley & Sons, Inc., New York, 1991.
11. *Engineering Statistics Handbook*, National Institute of Standards, Washington, DC [URL: <http://www.itl.nist.gov/div898/handbook/index.htm>].

## APPENDIX 1: CALIBRATE, A PROGRAM FOR CALIBRATION STATISTICS AND LIMITS OF DETECTION

Calibration of the response from an analytical chemical measurement system as a function of analyte concentration or amount is one of the most important tasks for both practical use of a measurement and validation of its performance. Calibration models that are linear in the parameters to be estimated (e.g., first-order models with intercept and slope parameters, or second-order models with intercept, slope, and curvature parameters). The least squares approach to fitting linear models using matrix algebra is described by many sources, including Draper and Smith (1), Neter, *et al.* (2), Rawlings (3), and Deming and Morgan (4, 5). The software described here was developed to provide an easy to use calibration tool for forensic analytical that satisfies formal guidelines for calibration-based limit of detection computations.

### References

1. Draper, N. R.; Smith, H. *Applied Regression Analysis*, 3<sup>rd</sup> ed., John Wiley & Sons, New York, 1998.
2. Neter, J.; Wasserman, W., Kutner, M. H. *Applied Linear Statistical Models*, 3<sup>rd</sup> ed., Richard D. Irwin, Inc., 1990.
3. Rawlings, J. O. *Applied Regression Analysis: A Research Tool*, Wadsworth & Brooks/Cole, Belmont, CA, 1988.
4. Deming, S. N.; Morgan, S. L. The use of linear models and matrix least squares in clinical chemistry, *Clin. Chem.* **1979**, 25(6), 840-855.
5. S. N. Deming and S. L. Morgan, *Experimental Design: A Chemometric Approach*, 2nd ed., Elsevier Science Publishers, Amsterdam, 1993.

## PROGRAM DESCRIPTION

### DATA INPUT

```
Calibrate Version 14.0125
Date: 06-Feb-2014 09:06:08
Data set created: 06-Feb-2014 09:06:04
Directory path: C:\Users\Morgan\Documents\_cal
File name: BasicRed46.xls
```

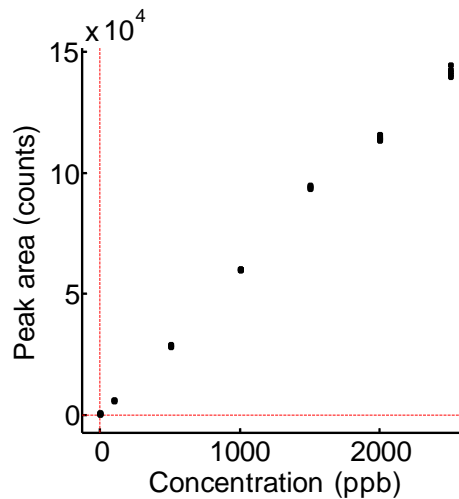
The calibration design has 45 total data points, 7 design points. There are 38 replicate experiments at the same location of previous experiments; 15 of these are blank experiments at zero analyte concentration.

X-axis: Concentration, range of x values: 0 to 2500 ppb

Y-axis: Peak area, range of y values: 94.839 to 144702.328 counts

	Concentration (ppb)	Peak area (counts)
1	0	600.9940
2	0	103.2470
3	0	109.7140
4	0	316.0390
5	0	1008.4650
6	0	542.6480
7	0	234.5230
8	0	94.8390
9	0	273.5380

10		0		852.5950
11		0		471.5820
12		0		151.6910
13		0		136.7900
14		0		517.4370
15		0		142.0550
16		100		6214.4410
17		100		5810.6950
18		100		6167.4390
19		100		6261.3500
20		100		6055.8260
21		500		29086.1540
22		500		28979.4860
23		500		28671.7010
24		500		28760.1190
25		500		28351.7520
26		1000		60547.1760
27		1000		59907.1840
28		1000		60329.4340
29		1000		59979.5470
30		1000		60340.4650
31		1500		95059.3750
32		1500		95123.2970
33		1500		94623.5700
34		1500		93923.6020
35		1500		93795.9140
36		2000		115979.1640
37		2000		114853.1560
38		2000		114346.9380
39		2000		113448.6950
40		2000		113890.6020
41		2500		144702.3280
42		2500		142966.5000
43		2500		142144.0310
44		2500		140925.0000
45		2500		140143.6410



## 1. REPLICATE GROUP STATISTICS AND HETEROSCEDASTICITY TESTING

Replicate group statistics

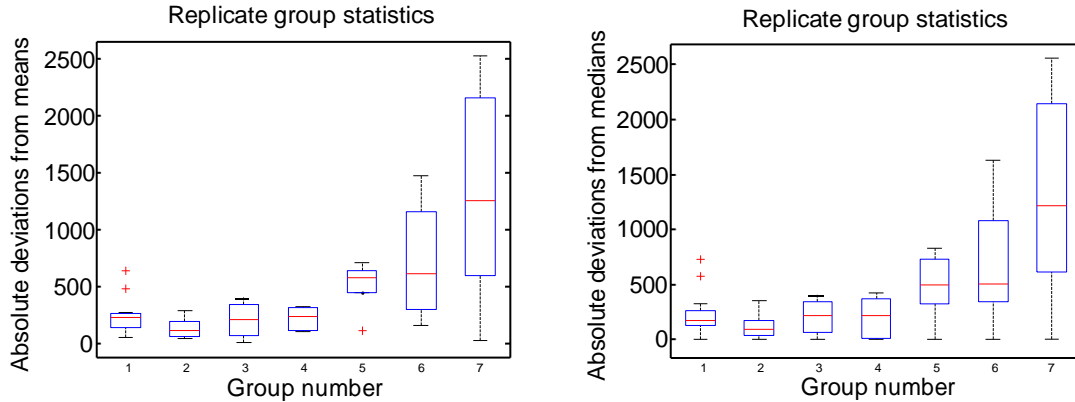
	Concentration (ppb)	Mean (count)	Std. deviation (counts)	n
1	0.00000	370.4105	287.2219	15
2	100.0000	6101.9502	179.7973	5
3	500.0000	28769.8424	286.5874	5
4	1000.0000	60220.7612	268.8868	5
5	1500.0000	94505.1516	621.3912	5
6	2000.0000	114503.7110	976.2956	5
7	2500.0000	142176.3000	1782.1146	5

Pooled standard deviation = 724.801928, based on 38 degrees of freedom

Levene's hypothesis test for the equality of multiple variances is based on absolute deviations from group means. This test is sensitive to departures from normality in the data. The calculated F-statistic is 6.5409, with 6 numerator and 38 denominator degrees of freedom, based on the analysis of variance F-statistic. The critical value of F-statistic is 2.3490 at the 95% level of confidence. The probability that this outcome occurred by chance is 0.0001 (8.3606e-05). The null hypothesis that the variances are equal can be rejected at or above the 99.99 % level of confidence. This outcome strongly indicates that ordinary least squares calibration is inappropriate, and that weighted least square should be performed.

The Brown-Forsythe hypothesis test for the equality of multiple variances is based on absolute deviations from group medians. This test is robust against even serious departures from normality in the data. The calculated F-statistic is 5.5627, with 6 numerator and 38 denominator degrees of freedom, based on the analysis of variance F-statistic. The critical value of F-statistic is 2.3490 at the 95% level of confidence. The probability that this outcome occurred by chance is 0.0003 (0.00032327). The null hypothesis that the variances are equal can be rejected at or above the 99.97 % level of confidence. This outcome strongly indicates that ordinary least squares calibration is inappropriate, and that weighted least square should be performed.

Bartlett's hypothesis tests for the equality of multiple variances compares the pooled variance and the group variances with a Chi-squared statistic. Bartlett's test is sensitive to non-normality. The calculated Chi-squared statistic is 40.5931, with 6 degrees of freedom. The probability that this outcome occurred by chance is 3.4823e-07). The critical value of Chi-squared is 12.5916 at the 95% level of confidence. The null hypothesis that the variances are equal can be rejected at or above the 99.99 % level of confidence. This outcome strongly indicates that ordinary least squares calibration is inappropriate, and that weighted least square should be performed.



## 2. ORDINARY LEAST SQUARES MODELLING

Regression parameters for ordinary least squares model:

	Estimate	Standard error	Lower 95% CI	Upper 95% CI
Intercept	987.6879	584.3942	-190.8553	2166.2312
Slope	57.6973	0.4726	56.7442	58.6505

Single-parameter hypothesis tests (based on the standard deviation of residuals):

	t-statistic	p-value
Intercept	1.690	0.0982
Slope	122.078	0.0000

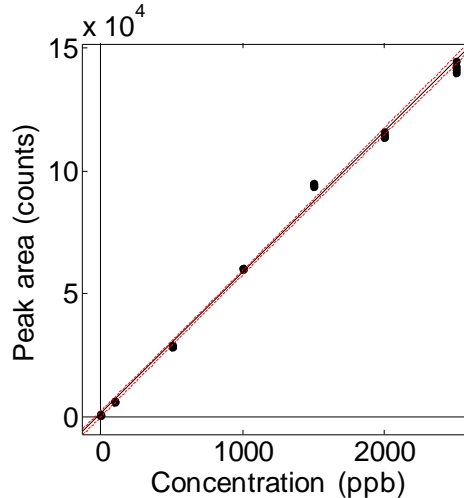
For the null hypothesis that the intercept or slope parameter is equal to zero, versus the alternative hypothesis of not equal to zero, the critical value of Student's t at the 95% level of confidence with 43 degrees of freedom is 4.0670.

The confidence interval for the intercept includes the value of zero, and the calculated t-statistic does not exceed the critical value of Student's t. Thus, the null hypothesis that the intercept is equal to zero cannot be rejected at the 95% level of confidence. The exact level of confidence at which the null hypothesis of zero intercept can be rejected is only 90.18 %.

The confidence interval for the slope does not include the value of zero, and the calculated t-statistic exceeds the critical value of Student's t. Thus, the null hypothesis that the slope is equal to zero can be rejected at or above the 95% level of confidence. The exact level of confidence at which the null hypothesis of zero slope can be rejected is >99.99 %.

Coefficient of determination,  $R^2 = 0.9971$   
 Coefficient of correlation,  $R = 0.9986$

The factor effect (slope) in the calibration model explains 99.71 % of the variability in the data about the mean.



### 3. WEIGHTED LEAST SQUARES MODELLING

Regression parameters for weighted least squares model:

	Estimate	Standard error	Lower 95% CI	Upper 95% CI
Intercept	0.0016	0.0015	-0.0014	0.0047
Slope	9.7816	0.2825	59.2119	60.3513

Single-parameter hypothesis tests:

(based on the standard deviation of residuals/n)

	t-statistic	p-value
Intercept	1.076	0.2881
Slope	211.634	0.0000

For the null hypothesis that the intercept or slope parameter is equal to zero, versus the alternative hypothesis of not equal to zero, the critical value of Student's t at the 95% level of confidence with 43 degrees of freedom is 4.0670

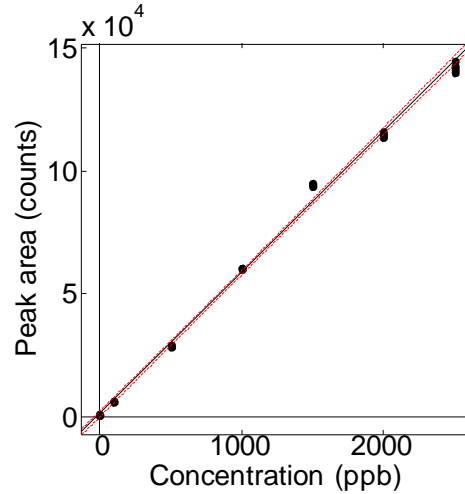
The confidence interval for the intercept includes the value of zero, and the calculated t-statistic does not exceed the critical value of Student's t. Thus, the null hypothesis that the intercept is equal to zero cannot be rejected at the 95% level of confidence. The exact level of confidence at which the null hypothesis of zero intercept can be rejected is only 71.19 %.

The confidence interval for the slope does not include the value of zero, and the calculated t-statistic exceeds the critical value of Student's t. Thus, the null hypothesis that the slope is equal to zero can be rejected at or above the 95% level of confidence. The exact level of confidence at which the null hypothesis of zero slope can be rejected is 100.00 %

Coefficient of determination,  $R^2 = 0.9990$

Coefficient of correlation,  $R = 0.9995$

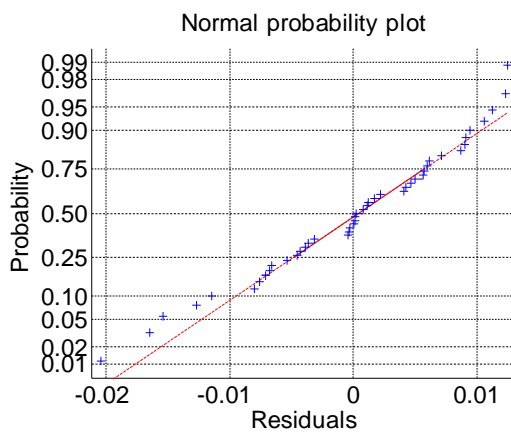
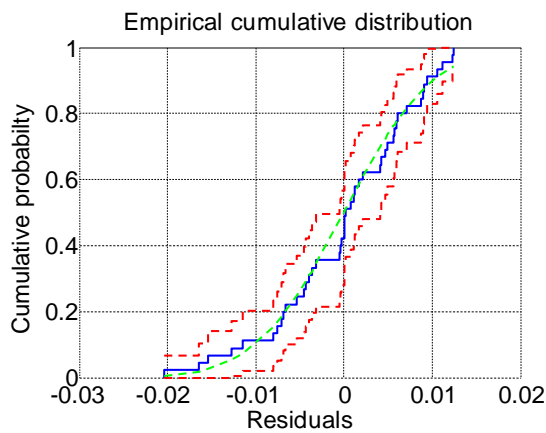
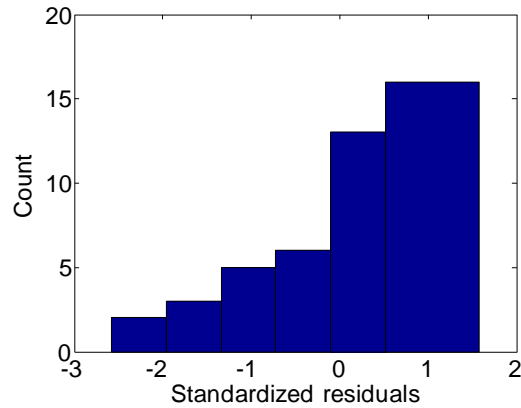
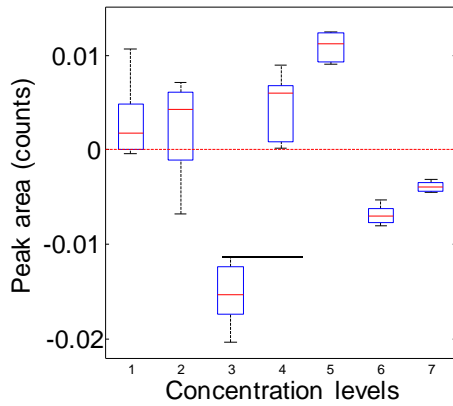
The factor effect (slope) in the calibration model explains 99.90 % of the variability in the data about the mean.



**4. RESIDUAL ANALYSIS**

	Concentration (ppb)	Peak area (counts)	Residual (counts)	Predicted y (counts)
1	0	0.0073	0.0016	0.0057
2	0	0.0013	0.0016	-0.0004
3	0	0.0013	0.0016	-0.0003
4	0	0.0038	0.0016	0.0022
5	0	0.0122	0.0016	0.0106
6	0	0.0066	0.0016	0.0050
7	0	0.0028	0.0016	0.0012
8	0	0.0011	0.0016	-0.0005
9	0	0.0033	0.0016	0.0017
10	0	0.0103	0.0016	0.0087
11	0	0.0057	0.0016	0.0041
12	0	0.0018	0.0016	0.0002
13	0	0.0017	0.0016	0.0000
14	0	0.0063	0.0016	0.0046
15	0	0.0017	0.0016	0.0001
16	3.093382e-03	0.1922	0.1866	0.0057
17	3.093382e-03	0.1797	0.1866	-0.0068
18	3.093382e-03	0.1908	0.1866	0.0042
19	3.093382e-03	0.1937	0.1866	0.0071
20	3.093382e-03	0.1873	0.1866	0.0008
21	6.087737e-03	0.3541	0.3656	-0.0114
22	6.087737e-03	0.3528	0.3656	-0.0127
23	6.087737e-03	0.3491	0.3656	-0.0165
24	6.087737e-03	0.3502	0.3656	-0.0154
25	6.087737e-03	0.3452	0.3656	-0.0204
26	1.383124e-02	0.8374	0.8285	0.0090
27	1.383124e-02	0.8286	0.8285	0.0001
28	1.383124e-02	0.8344	0.8285	0.0060
29	1.383124e-02	0.8296	0.8285	0.0011
30	1.383124e-02	0.8346	0.8285	0.0061
31	3.884732e-03	0.2462	0.2339	0.0123
32	3.884732e-03	0.2464	0.2339	0.0125
33	3.884732e-03	0.2451	0.2339	0.0112
34	3.884732e-03	0.2432	0.2339	0.0094
35	3.884732e-03	0.2429	0.2339	0.0091
36	2.098299e-03	0.1217	0.1271	-0.0054
37	2.098299e-03	0.1205	0.1271	-0.0066
38	2.098299e-03	0.1200	0.1271	-0.0071
39	2.098299e-03	0.1190	0.1271	-0.0080
40	2.098299e-03	0.1195	0.1271	-0.0076
41	7.871704e-04	0.0456	0.0487	-0.0031
42	7.871704e-04	0.0450	0.0487	-0.0037
43	7.871704e-04	0.0448	0.0487	-0.0039
44	7.871704e-04	0.0444	0.0487	-0.0043
45	7.871704e-04	0.0441	0.0487	-0.0046

Standard deviation of residuals = 7.97690e-03 counts, with 43 df



### 5. ANALYSIS OF VARIANCE

Source	Sum of squares	df	Mean square
Total	4.6429	45.0000	NaN
Mean	1.7902	1.0000	NaN
Corrected	2.8527	44.0000	NaN
Regression	2.8500	1.0000	2.8500
Residuals	0.0027	43.0000	0.0001
Lack of fit	0.0023	5.0000	0.0005
Pure error	0.0004	38.0000	0.0000

Hypothesis test for the significance of the regression: The calculated F-statistic is 44789.0707, with 1 numerator and 43 denominator degrees of freedom, based on the variance of the residuals. The critical value of F-statistic is 4.0670 at the 95% level of confidence. The probability that this outcome occurred by chance is 0.0000 (0). The null hypothesis that the slope is equal to zero can be rejected at or above the 99.99 % level of confidence.

Hypothesis test for lack of fit: The calculated F-statistic is 42.7158, with 5 numerator df and 38 denominator df. The critical value of F-statistic is 2.4625 at the 95% level of confidence. The probability that this outcome occurred by chance is 0.0000 (1.3767e-14). The lack of fit of the model is significant at or above the 99.99 % level of confidence, indicating that a better model might be found.

## 6. LIMIT OF DETECTION

Replicate group statistics:

	Concentration (ppb)	Mean (counts)	Std. deviation (counts)	n
1	0.0000	370.4105	287.2219	15
2	100.0000	6101.9502	179.7973	5
3	500.0000	28769.8424	286.5874	5
4	1000.0000	60220.7612	268.8868	5
5	1500.0000	94505.1516	621.3912	5
6	2000.0000	114503.7110	976.2956	5
7	2500.0000	142176.3000	1782.1146	5

Pooled standard deviation = 724.801928, based on 38 degrees of freedom

Limit of detection calculations (based on  $3.3*s/slope$ ):

Using the standard deviation of the blanks = 287.221916

(with 14 degrees of freedom), LOD =  $1.58549e+01$  ppb

Using the standard deviation of replicates at lowest non-zero concentration =

179.797311 (with 4 degrees of freedom), LOD =  $9.92498e+00$  ppb

Using the standard deviation of the intercept from the calibration = 0.001513

counts, (with 43 degrees of freedom), LOD =  $8.34941e-05$  ppb

Using the pooled standard deviation of replicate measurements = 724.801928

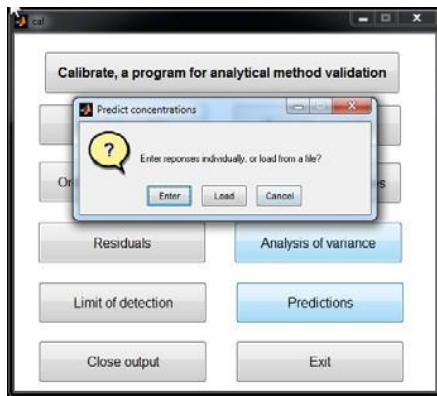
counts, (with 38 degrees of freedom), LOD =  $4.00097e+01$  ppb

Using the standard deviation of calibration residuals = 0.007977 counts,

(with 43 degrees of freedom), LOD =  $4.40332e-04$  ppb

LOD estimates based on information from more than one level may be biased if the variance of replicate measurements is not constant, or if the calibration model exhibits lack of fit.

## 7. PREDICTION OF UNKNOWN SAMPLES



Predicted Concentration for unknown samples:

	Peak area	Concentration
1	23245.0000	388.8320
2	3245.0000	54.2809

## Appendix 2. SOFTWARE VALIDATION

*Purpose:* to validate regression analysis, residual analysis and analysis of variance functions.

*Test data source:* Draper, N. R.; Smith, H. *Applied Regression Analysis*, 3<sup>rd</sup> ed., John Wiley & Sons, New York, 1998, Table 1.1, page 21. The fitting of a straight line with intercept and slope parameters to this data, the residual analysis, and the analysis of variance are shown on pages 20-40. The required data format is a Microsoft Excel file with a file extension of \*.xls, or \*.xlsx. The file contains one (x,y) data pair per row (with x-values in the first column, and y-values in the second column) without column headers.

### PROGRAM OUTPUT

CALX, Version 14.0801

Date: 26-Sep-2014 20:00:12

Data set created: 26-Sep-2014 15:35:32

Directory path: C:\Users\morgan\Documents\\_cal

File name: Draper\_Smith\_p21.xlsx

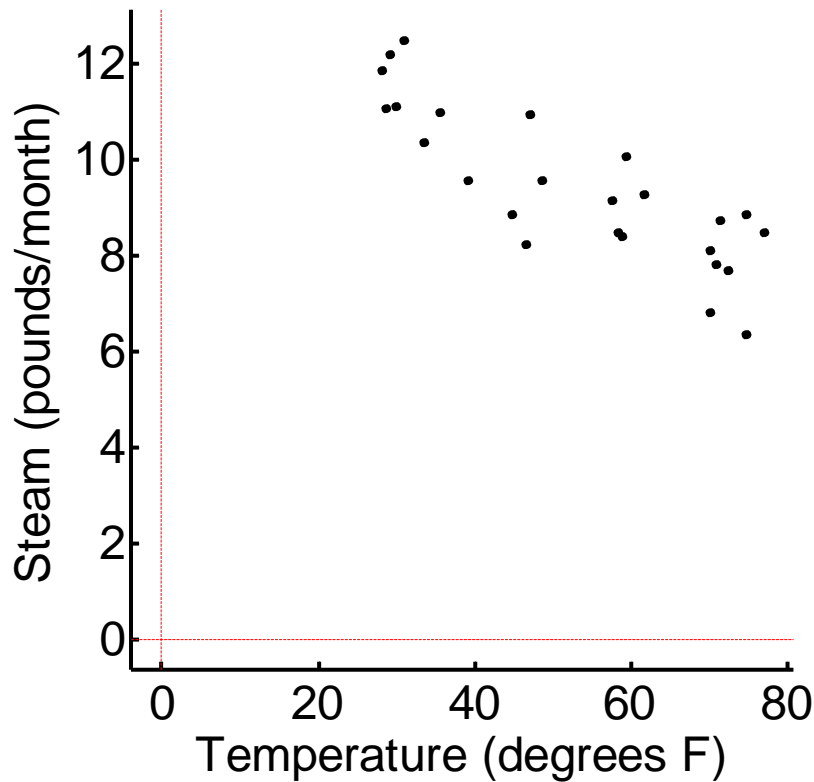
#### Data summary:

The calibration design has 25 total data points, and 24 design points. There is only one replicate experiment at the same location of a previous experiment. There are no blank experiments at zero analyte concentration. Data are sorted in order of increasing values for the independent x-variable.

X-axis: Temperature, range of x values: 28.1 to 76.7 degrees F

Y-axis: Steam, range of y values: 6.36 to 12.51 pounds/month

	Temperature (degrees	Steam (pounds/month)
1	2.810000e+01	11.8800
2	2.860000e+01	11.0800
3	2.890000e+01	12.1900
4	2.970000e+01	11.1300
5	3.080000e+01	12.5100
6	3.340000e+01	10.3600
7	3.530000e+01	10.9800
8	3.910000e+01	9.5700
9	4.460000e+01	8.8600
10	4.640000e+01	8.2400
11	4.680000e+01	10.9400
12	4.850000e+01	9.5800
13	5.750000e+01	9.1400
14	5.810000e+01	8.4700
15	5.880000e+01	8.4000
16	5.930000e+01	10.0900
17	6.140000e+01	9.2700
18	7.000000e+01	8.1100
19	7.000000e+01	6.8300
20	7.070000e+01	7.8200
21	7.130000e+01	8.7300
22	7.210000e+01	7.6800
23	7.440000e+01	6.3600
24	7.450000e+01	8.8800
25	7.670000e+01	8.5000



**Replicate group statistics:**

	Temperature (degrees F)	Mean (pounds/month)	Std. deviation (pounds/mo	n
1	28.1000	11.8800	0.0000	1
2	28.6000	11.0800	0.0000	1
3	28.9000	12.1900	0.0000	1
4	29.7000	11.1300	0.0000	1
5	30.8000	12.5100	0.0000	1
6	33.4000	10.3600	0.0000	1
7	35.3000	10.9800	0.0000	1
8	39.1000	9.5700	0.0000	1
9	44.6000	8.8600	0.0000	1
10	46.4000	8.2400	0.0000	1
11	46.8000	10.9400	0.0000	1
12	48.5000	9.5800	0.0000	1
13	57.5000	9.1400	0.0000	1
14	58.1000	8.4700	0.0000	1
15	58.8000	8.4000	0.0000	1
16	59.3000	10.0900	0.0000	1
17	61.4000	9.2700	0.0000	1
18	70.0000	7.4700	0.9051	2
19	70.7000	7.8200	0.0000	1
20	71.3000	8.7300	0.0000	1
21	72.1000	7.6800	0.0000	1
22	74.4000	6.3600	0.0000	1
23	74.5000	8.8800	0.0000	1
24	76.7000	8.5000	0.0000	1

Pooled standard deviation = 0.905097, based on 1 degree of freedom.

Because the variability cannot be estimated at all levels of the independent variable, whether the data is homoscedastic or heteroscedastic cannot be assessed.

---

**Regression parameter estimates using ordinary least squares:**

	Estimate	Standard error	Lower 95% CI	Upper 95% CI
Intercept	13.6230	0.5815	12.4201	14.8258
Slope	-0.0798	0.0105	-0.1016	-0.0581

Single-parameter hypothesis tests based on the standard deviation of residuals:

	t-statistic	p-value
Intercept	23.429	0.0000
Slope	7.586	0.0000

For the null hypothesis that any model parameter is equal to zero, versus the alternative hypothesis of not equal to zero, the critical value of Student's t at the 95% level of confidence with 23 degrees of freedom is 4.2793.

The confidence interval for the intercept does not include the value of zero, and the calculated t-statistic exceeds the critical value of Student's t. Thus, the null hypothesis that the intercept is equal to zero can be rejected at or above the 95% level of confidence. The exact level of confidence at which the null hypothesis of zero intercept can be rejected is 100.00 %

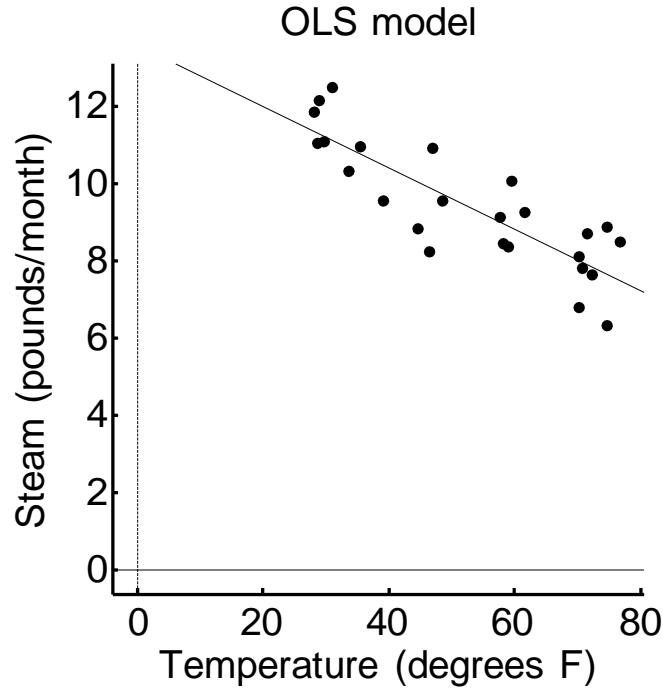
The confidence interval for the slope does not include the value of zero, and the calculated t-statistic exceeds the critical value of Student's t. Thus, the null hypothesis that the slope is equal to zero can be rejected at or above the 95% level of confidence. The exact level of confidence at which the null hypothesis of zero slope can be rejected is 100.00 %

Coefficient of determination,  $R^2 = 0.7144$

The factor effect (slope) in the calibration model explains 71.44 % of the variability in the data about the mean.

Coefficient of correlation,  $R = -0.8452$

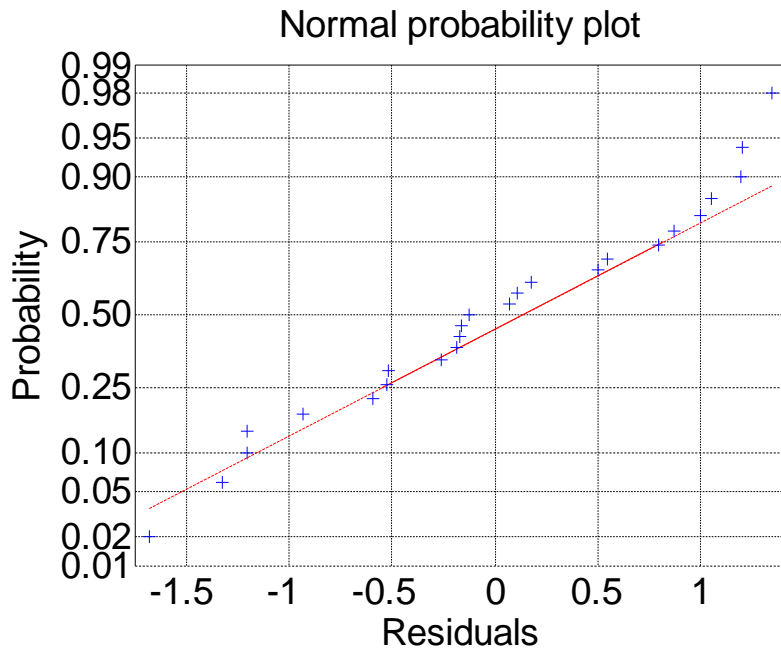
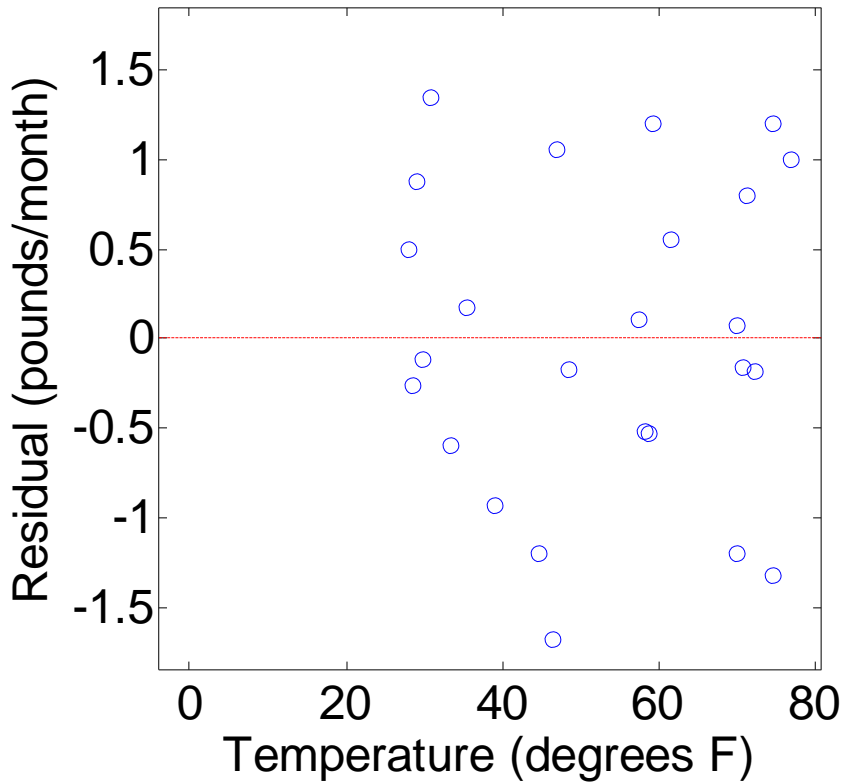
---



**Residual analysis using ordinary least squares:**

	Temperature (degrees	Steam (pounds/month)	Residual (pounds/mon	Predicted y (pounds/
1	2.810000e+01	11.8800	11.3798	0.5002
2	2.860000e+01	11.0800	11.3399	-0.2599
3	2.890000e+01	12.1900	11.3159	0.8741
4	2.970000e+01	11.1300	11.2521	-0.1221
5	3.080000e+01	12.5100	11.1643	1.3457
6	3.340000e+01	10.3600	10.9567	-0.5967
7	3.530000e+01	10.9800	10.8050	0.1750
8	3.910000e+01	9.5700	10.5017	-0.9317
9	4.460000e+01	8.8600	10.0626	-1.2026
10	4.640000e+01	8.2400	9.9189	-1.6789
11	4.680000e+01	10.9400	9.8870	1.0530
12	4.850000e+01	9.5800	9.7513	-0.1713
13	5.750000e+01	9.1400	9.0328	0.1072
14	5.810000e+01	8.4700	8.9849	-0.5149
15	5.880000e+01	8.4000	8.9291	-0.5291
16	5.930000e+01	10.0900	8.8891	1.2009
17	6.140000e+01	9.2700	8.7215	0.5485
18	7.000000e+01	8.1100	8.0350	0.0750
19	7.000000e+01	6.8300	8.0350	-1.2050
20	7.070000e+01	7.8200	7.9791	-0.1591
21	7.130000e+01	8.7300	7.9312	0.7988
22	7.210000e+01	7.6800	7.8673	-0.1873
23	7.440000e+01	6.3600	7.6837	-1.3237
24	7.450000e+01	8.8800	7.6758	1.2042
25	7.670000e+01	8.5000	7.5001	0.9999

Standard deviation of residuals = 8.90125e-01 pounds/month, with 23 df.



The residual plot (top) exhibits no obvious patterns and the Normal probability plot of standardized residuals (bottom) shows residuals falling close to the red line (representing a standard normal distribution).

### Asymmetry measures for distribution of residuals:

Skewness, g1: -0.1591

Skewness is related to asymmetry in the horizontal direction (x-axis). A standard normal distribution of data will have a skewness of zero, and any symmetric distribution should have a skewness close to zero. Positive values indicate the distribution is skewed towards lower values (to the left, a tailing peak). Negative values indicate the distribution is skewed towards higher values (to the right, a fronting peak).

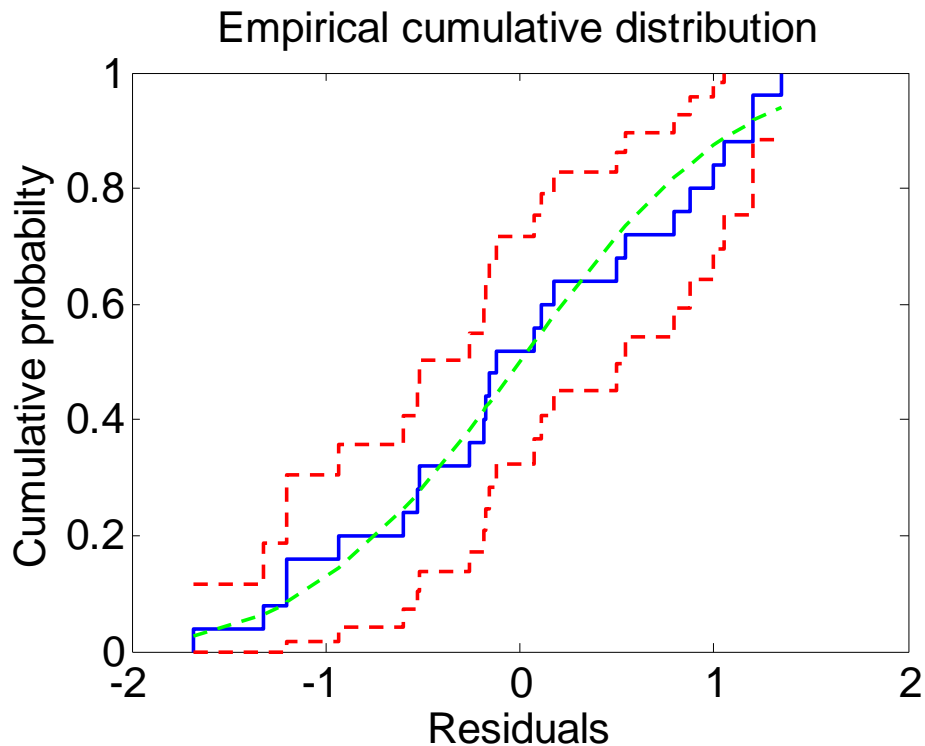
Kurtosis ('standard'), g2: -0.9002

Kurtosis ('excess'), g2-3: -3.9002

Kurtosis is related to asymmetry in the vertical direction. The standard definition of kurtosis produces a value of 3 for a standard normal distribution. Some sources subtract the value of 3 from g2 so that the kurtosis for a standard normal distribution is zero. With this modified definition, distributions that exhibit positive kurtosis are termed leptokurtic and are more peaked (with more area in the center). Distributions that exhibit negative kurtosis are termed platykurtic and are more spread out (with more area in the tails).

Conclusion: These distribution asymmetry results that the residuals are slightly skewed to higher values (perhaps seen in the deviations of residuals from the straight line at higher values), and that the distribution of residuals tend to be more spread out than a normal distribution.

### Empirical cumulative distribution plot



The empirical cumulative probability distribution (ECPD) plot shows: (blue) the cumulative probability distribution of the residuals; red) 95% confidence intervals for the ECPD based on the residuals; and, (green) the expected cumulative probability distribution of a standardized normal distribution with the same mean and standard deviation. The green curve is within the 95% confidence bounds, indicating the null hypothesis that the residuals follow a normal distribution cannot be rejected at the 95% level of confidence.

**Analysis of variance using ordinary least squares:**

Source	Sum of squares	df	Mean square
Total	2284.1102	25.0000	
Mean	2220.2944	1.0000	
Corrected	63.8158	24.0000	
Regression	45.5924	1.0000	45.5924
Residuals	18.2234	23.0000	0.7923
Lack of fit	17.4042	22.0000	0.7911
Pure error	0.8192	1.0000	0.8192

Hypothesis test for the significance of the regression:

The calculated F-statistic is 57.5428, with 1 numerator and 23 denominator degrees of freedom, based on the variance of the residuals. The probability that this outcome occurred by chance is 0.0000. The critical value of F-statistic is 4.2793 at the 95% level of confidence.

The null hypothesis that the slope is equal to zero can be rejected at the 100.00 % level of confidence.

Hypothesis test for lack of fit:

The calculated F-statistic is 0.9657, with 22 numerator df and 1 denominator degrees of freedom. The probability that this outcome occurred by chance = 0.6801. The critical value of F-statistic is 248.5791 at the 95% level of confidence.

The lack of fit of the model is not significant at the 95% level of confidence, indicating that there is no reason to doubt the adequacy of the model. The exact confidence at which the null hypothesis of no lack of fit might be rejected is only 31.99 %.

**Software validation summary:**

All regression analysis results produced by CALX match exactly those shown on pages 20-40 of the Draper and Smith text.

## CALX SOFTWARE VALIDATION TEST 2.

*Purpose:* to validate hypothesis tests for homoscedasticity of data.

*Test data source:* Draper, N. R.; Smith, H. *Applied Regression Analysis*, 3<sup>rd</sup> ed., John Wiley & Sons, New York, 1998, Table 2.1, page 51. The outcome of variability testing is shown on pages 56-59. The required data format is a Microsoft Excel file with a file extension of \*.xls, or \*.xlsx. The file contains one (x,y) data pair per row (with x-values in the first column, and y-values in the second column) without column headers.

### PROGRAM OUTPUT

CALX, Version 14.0801

Date: 27-Sep-2014 13:04:28

Data set created: 27-Sep-2014 13:03:52

Directory path: C:\Users\morgan\Documents\\_cal

File name: Draper\_Smith\_p51\_variability test.xlsx

Data summary:

The calibration design has 18 total data points, and 8 design points. There are 10 replicate experiment at locations of previous experiments; There are no blank experiments at zero analyte concentration. Data are sorted in order of increasing values for the independent x-variable.

X-axis: X, range of x values: 1.3 to 6 measured

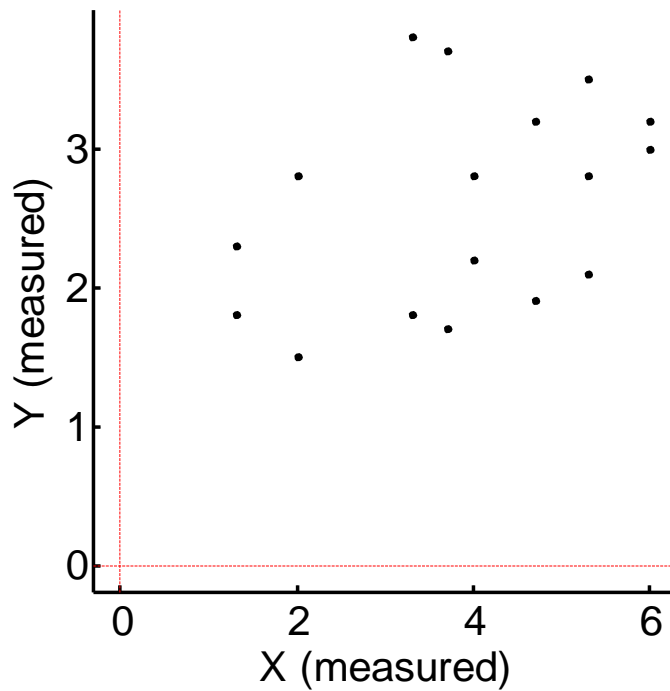
Y-axis: Y, range of y values: 1.5 to 3.8 measured

	X (measured)	Y (measured)
1	1.30	2.30
2	1.30	1.80
3	2.00	2.80
4	2.00	1.50
5	3.30	3.80
6	3.30	1.80
7	3.70	3.70
8	3.70	1.70
9	4.00	2.80
10	4.00	2.80
11	4.00	2.20
12	4.70	3.20
13	4.70	1.90
14	5.30	3.50
15	5.30	2.80
16	5.30	2.10
17	6.00	3.20
18	6.00	3.00

Replicate group statistics:

	X (measured)	Mean (measured)	Std. deviation (measured)	n
1	1.3000	2.0500	0.3536	2
2	2.0000	2.1500	0.9192	2
3	3.3000	2.8000	1.4142	2
4	3.7000	2.7000	1.4142	2
5	4.0000	2.6000	0.3464	3
6	4.7000	2.5500	0.9192	2
7	5.3000	2.8000	0.7000	3
8	6.0000	3.1000	0.1414	2

Pooled standard deviation = 0.839940, based on 10 degrees of freedom.



**(a) Hypothesis testing for equality of multiple variances using Levene's test:** Levene's test is based on absolute deviations from group means. To distinguish it from the next test, this test is often referred to as "Levene's test using means." Levine's test is sensitive to departures from normality in the data.

The calculated F-statistic is 6.8239, with 7 numerator and 10 denominator degrees of freedom. Critical values of the F statistic for these degrees of freedom are:

Level of confidence	Critical value of F
0.9500	3.1355
0.9750	3.9498
0.9900	5.2001
0.9999	16.3189

The null hypothesis that the variances are equal can be rejected at or above the 99.99% level of confidence, and the probability that this outcome occurred by chance is less than 0.0001 (0.0037115).

This outcome strongly indicates that ordinary least squares calibration is inappropriate, and that weighted least squares should be performed.

**Software validation summary:** The above outcome for Levene's test using means is identical to the result shown in Draper and Smith, page 57-58.

**(b) Hypothesis testing for equality of multiple variances using the Brown-Forsythe test:** The Brown-Forsythe test is based on absolute deviations from group medians. Since this test differs from Levene's test only in that absolute deviations from the mean are replaced by absolute deviations from the median, this test is often referred to as "Levene's test using medians." This test is robust against even serious departures from normality in the data.

The calculated F-statistic is 4.5462, with 7 numerator and 10 denominator degrees of freedom. Critical values of the F statistic for these degrees of freedom are:

Level of confidence	Critical value of F
0.9500	3.1355
0.9750	3.9498
0.9900	5.2001
0.9999	16.3189

The null hypothesis that the variances are equal can be rejected at or above the 95% level of confidence. The exact level of confidence at which the null hypothesis of equality can be rejected is 98.42%. The probability that this result occurred by chance is less than 0.0001 (0.015832).

This outcome indicates that ordinary least squares calibration is inappropriate, and that weighted least squares should be performed.

**Software validation summary:** The above outcome for the Brown-Forsythe test is identical to the result shown in Draper and Smith, page 58. Note that this test is not as significant an outcome as the previous test with means; however the final conclusion (reject the null hypothesis) is the same as before. As explained by Draper and Smith, when only two measurements are in a group, the median and mean are the same. For the Brown-Forsythe test, only groups of 3 or more replicates can produce different results than Levene's test with means. For the two groups with 3 measurements, medians cause the F-statistic to be slightly less significant than previously. Such disagreement is not atypical when different tests based on slightly different criteria for the same hypothesis. Naturally, one feels more comfortable with the outcome of an hypothesis test that agrees with the result from other tests that look at the data differently. There is a human temptation to try them all and present only the results of the method that give the desired outcome. Don't do this — it's unethical. Instead, choose one method and stick with it.

**(c) Hypothesis testing for equality of multiple variances using Bartlett's test:** Bartlett's test compares the pooled variance and the group variances with a Chi-squared statistic. This test is sensitive to non-normality of the data.

The calculated Chi-squared statistic is 5.3597, with 7 degrees of freedom. Critical values of the Chi-squared statistic for various degrees of freedom are:

Level of confidence	Critical value Chi2
0.9500	14.0671
0.9750	16.0128
0.9900	18.4753
0.9999	29.8775

The null hypothesis that the variances are equal cannot be rejected at the 95% level of confidence. The exact level of confidence at which the null hypothesis of equality can be rejected is only 38.38%.

This outcome indicates that ordinary least squares calibration is appropriate, and that ordinary least squares should be performed.

**Software validation summary:** The above outcome for the Brown-Forsythe test is not the same as the results shown in Draper and Smith, page 56-57. However, both this result and the Draper and Smith result agree in their hypothesis test conclusion to fail to reject the null hypothesis if equal variance

There are several versions of the Bartlett's test. We suspect that the version implemented in the MATLAB Statistics Toolbox that we use is a more recent version of the test than the version in the 1998 edition of Draper and Smith. As stated previously, such disagreement is not atypical when different tests based on slightly different criteria for the same hypothesis.

## OVERALL RESULTS

The objective of this project was to validate analytical methods for the forensic chemical characterization of dyes extracted from trace evidence fibers, thereby enhancing discrimination for comparison of known and questioned casework fibers. Previous work in our laboratory with microextraction techniques coupled with capillary electrophoresis (CE) and mass spectrometry (MS) demonstrated discriminating and sensitive forensic analysis of fiber dyes.

We have focused on improving the extraction efficiency and ease of application of extraction protocols for (basic) dyes on acrylic, (direct, reactive, and vat) dyes on cotton, (acid) dyes on nylon, and disperse dyes on polyester.

All extractions were carried out under the prescribed solvent conditions at 100 °C for one hour to achieve extraction completeness, although shorter extraction times were not investigated. Extracts aliquots (100 µL) are dried and reconstituted in 50 µL of 50:50 methanol and 50 mM ammonium acetate buffered at pH 4.5. These samples were vortex-mixed to ensure complete solvation of extracted dye prior to direct injection to UPLC analysis. As we have previously reported, basic dyes were extracted from acrylic fibers with a 50:50 mixture of formic acid and water. Extraction of acid dyes from nylon was performed with equal amounts of pyridine, ammonium hydroxide, and water to improve robustness according to prior experimentation. Extractions of disperse dyes from polyester carried with chlorobenzene as we previously reported. The remaining fiber sample (if visible) was observed to be colorless for all fibers. UPLC analysis is done using a gradient-based ultra performance liquid chromatography UPLC method for separation of basic dyes on acrylic fibers, acidic dyes on nylon fibers, and disperse dyes on polyester fibers.

Validation outcomes for extraction/UPLC analysis of extracted dyes from acrylic, nylon, and polyester are excellent. With UPLC-UV/visible detection, calibration models typically produced coefficients of determination ( $R^2$ ) of 0.9993 or higher for wide range calibrations. At 100 ppb concentration levels, signal-to-noise ratios were 100 or higher. UPLC-UV/visible limits of detection (LOD) from wide concentration calibrations were 10 ppb or lower, which represents the detection of 100 pg of extracted dye. Extractions from two disperse dyes yielded less reproducible results and higher LODs, most likely because of low dye loading. Specifically, Disperse Blue 60 had the lowest absorbance response of all dyes, and a corresponding higher LOD (13.50 ppb to 16.80 ppb, depending on the estimation method). In general, UPLC with UV/visible detection yielded lower detection limits than UPLC-MS-MS. However, the MS instrument used for this work was a shared-use instrument and optimization of MS ionization conditions may improve the mass spectrometric performance.

The analysis of cotton fibers is challenging because they can be dyed with three different classes of dye, each requiring a different method for extraction and analysis. We have focused on direct, reactive, and indigo dyes and optimized extraction conditions and chromatographic methods. Direct dyes have been successfully extracted from cotton fibers as small as 1 mm in length and dye amounts have been quantitated by UPLC with UV/visible detection. For direct dyes, optimum extraction was at 51.5% water, 20.6% pyridine, and 27.9% acetone. Because the region around this optimum is relatively flat, this outcome is relatively robust and for ease of use, 50% water, 25% pyridine, and 25% acetone is recommended for direct dye extractions. Extractions using 100% DMSO were found to be optimal for extraction of indigo dye from cotton. UPLC with UV/visible detection detected dyes in extracts from single 1-mm length cotton fibers with

RMS signal-to-noise ratios of 118.05 and 62.80 for Direct Blue 71 and Indigo, respectively. Limits of detection and quantification of 2.1 pg and 6.2 pg for Direct Blue 721 and Indigo, respectively, support the potential for analysis of even sub-mm length cotton fibers. UPLC-DAD produced detection limits as low as 0.33-1.42 ppb and quantitation limits as low as 1.00-4.30 ppb. Detection and quantification extracts from single of 1-10 mm cotton fibers dyes with Reactive Yellow 160 were also confirmed.

We have also developed methods based on capillary electrophoresis and LC/MS for analysis of fluorescent brighteners and other finishing agents extracted from textile fibers. Trace analysis of dyes and fluorescent brighteners on short single fibers of 1-10 mm length has been accomplished by capillary electrophoresis with diode array detection. These analyses have been done on unweathered and weathered fibers out to one year of environmental exposure.

## CONCLUSIONS

### 1. Discussion of findings

The design of a guillotine for cutting reproducible lengths of fibers down to 5 mm in length has improved reproducibility of fiber analysis results compared to variation seen in previous work. Fibers of 0.5 mm and 1 mm still have to be cut by hand using a table-mounted magnifying glass and scalpel, although we are looking at the design of a cutting system for very small fiber lengths. Another minor improvement resulted from use of sample vials designed for high recovery with low solvent volumes (< 50  $\mu$ L) to enable concentration of dyes in the extract.

The development of a single UPLC method capable of analyzing three dye classes of fibers (acrylic, nylon, and polyester) avoids having to use different columns with multiple chromatographic conditions, and increases sample throughput. The gradient program for UV/visible detection employed mixtures of 50 mM ammonium acetate in water and 0.15% formic acid in methanol. For MS detection, the mobile phase consisted of 50 mM ammonium acetate in water and 0.15% formic acid in methanol, with a gradient that compensates for the slower flow rate required for MS. These experimental conditions are familiar to forensic analysts that perform liquid chromatography and do not require departure from normal protocols.

Reactive dyes are chemically bonded to cotton fiber, and their extraction from cotton is problematic. However, these fiber dyes are important to forensic fiber examiners because they account for approximately 82% of all dyes used in the dyeing of cotton. For reactive dyes, the fiber-dye bond must be broken under stringent hydrolysis conditions that are destructive to the fiber and can cause dye degradation products to be produced. However, despite chemical degradation of the original dye, separation of the resulting product mixture and (ultimately, identification of components by mass spectrometry) can provide forensic profiling to discriminate reactive dyes from one another. Improved understanding of reactive dye degradation can also assist interpretation of extracted components and enable identification of the parent reactive dye.

Analyses of fluorescent brighteners extracted from white fibers offer exciting opportunities for forensic investigators to discriminate essentially colorless fibers. Based on weathering of textile samples acquired under previous funding from the FBI Laboratory, we have characterized using CE and LC/MS changes that occur in detected amounts of C.I Basic violet 16 and two finishing agents from acrylic fabric weathered by environmental exposure in a hot humid climate

and a hot dry climate for up to one year. Detection of dyes has also been demonstrated on acrylic, nylon, and polyester weathered for one year. This work is ongoing at this time and we expect that paper to be supplemented with more data.

An observation from our prior work is that the microspectrophotometry data may not be sufficient for confident identification of dyes extracted from weathered fibers because of weak UV/visible or fluorescence spectra. Matching of questioned (weathered) samples to known samples may be better enabled from UPLC data; certainly mass spectral analysis can identify dyes even on 12 month-weathered samples. The ability to detect dyestuffs on environmentally weathered fibers adds value for investigators attempting interpretation of environmental effects on fiber evidence and determination of their forensic relevance. We hope that this work will provide trace evidence examiners with greater insight into the possible perturbations observed in casework samples by providing both qualitative and quantitative insights into the effects of environmental exposure. Explanations by trace evidence examiners for observed differences in textile fibers as a result of environmental exposure will be more convincing if accompanied by awareness of possible chemical or physical changes.

As noted in the paper on Mandel sensitivity, this concept offers an advantage over scale dependent approaches such as RSDs and CVs because it normalizes performance relative to the variability of the measurement method. This approach enables calculation of detection limit critical values in a universal way that also provides intuitive and visual understanding of the differences among limit of detection amount, minimal consistently detectable amount, and limit of quantitation. In revising the paper in this report for publication, we will look for potential applications of these ideas for comparison of results from the different analytical methods that we have used.

The chapter on statistical concepts concerning limits of detection, a short summary of our in-house calibration software was provided. This program was written to automate chromatographic data processing with validation in mind at all times. Over the next months we will make further improvements to include; (a) in the case of a straight line model exhibiting lack of fit, the program will be designed to automatically generate the statistical analysis for the next higher-order model, a quadratic equation. This modification is in response to the need of the LC/MS laboratory at the SC State Law Enforcement Division Forensic Laboratory, where non-straight line calibrations are apparently often needed. (b) Analysis of false positive and false negatives outcomes displayed for decision using a receiver operator characteristic curve; (b) a statistical tolerance interval calculation for LOD estimation. (c) estimated uncertainties (e.g., 95% confidence intervals in predicted amount of analyte. (d) a user preference menu that defines critical choices in LOD parameters and other settings to be retained in a profile file for future use, A major driving force for our development of this software was to automate limits of detection calculations in this NIJ project.

## **2. Implications for policy and practice**

It has been observed that use of trace evidence and testimony of examiners has decreased in recent years, perhaps due to “over-reliance on nuclear DNA, latent print, and mitochondrial DNA evidence.”<sup>1</sup> Fiber evidence is also maligned in popular forensic books with phrases such as “hanging by a thread” and “an inexact science,” implying fiber comparisons are entirely “subjective.”<sup>2,3</sup> Other significant questions raised in the 2009 National Academy of Sciences report<sup>4</sup> include the following:

- (a) The Scientific Working Group for Materials Analysis (SWGMAAT) has produced guidelines, but no set standards, for the number and quality of characteristics that must correspond in order to conclude that two fibers came from the same manufacturing batch. There have been no studies of fibers (*e.g.*, the variability of their characteristics before and after manufacturing) on which to base such a threshold.
- (b) There have been no studies that characterize either reliability or error rates in procedures.
- (c) There have been no studies to inform judgments about whether environmentally related changes discerned in particular fibers are distinctive enough to reliably individualize their source.

The goal of the forensic fiber examination is comparison of questioned fibers found at a crime scene with one or more known fibers to determine possible associations between victims, suspects, and crime scenes. If a match of questioned to known fibers is not excluded, the possibility of associations between suspect individuals and the crime may provide probative value or investigative leads. Visual comparison of fiber morphology by optical microscopy can provide discriminating information quickly in the early stages of a fiber examination. For example, acrylic is a synthetic fibers that is manufactured by dissolving polyacrylamide in organic solvent. After extruding the polymer into water and drying, the fiber collapses to a shriveled appearance with crinkled cross-sections ranging from circular to dogbone shapes. Synthetic fibers are often crimped to make them hold together better and to impart bulkiness when made into yarn; the number of crimps per inch might itself be a distinctive signature of such fibers from their manufacturing process. Cotton, a cellulosic natural fiber, has a distinct twisted and non-uniform appearance characteristic of its biological origin.<sup>5</sup> Physical measurements of fiber diameter, and cross-sectional shape, can also contribute to decision-making. Finally, polarized light microscopy can be used to determine optical characteristics such as refractive index, birefringence, and sign of elongation, which can be sufficiently discriminating for rapid identification of generic fiber type.<sup>5,6</sup> Fibers with different If these methods fail to exclude a match between questioned and known fibers, fluorescence microscopy, UV/visible and/or fluorescence microspectrophotometry, and infrared (IR) spectroscopy are used for chemical structural information, color characterization, and more specific polymer identification. All of these techniques are fast, nondestructive, and enable discrimination of fibers by different and increasingly specific characteristics. Fiber size, shape, color, and polymer identity differentiates most fibers. However, these techniques do not identify dyes. For example, two textile fibers dyed with mixtures of several, possibly different, dyes might be formulated by different manufacturers to achieve a particular (common) color. These fibers could be visually indistinguishable. Visual comparison of shapes of peak, valleys, and rising or falling portions of the UV/visible or fluorescence spectra might reveal subtle differences. However, judgment of the practical significance of these differences is often subjective, and the spectra usually represent unresolved mixtures of several unidentified dyes. Infrared spectra are dominated by the polymer and cannot be used for dye identification. *Modern instrumental analysis of separated dye components can increase the reliability of fiber examinations by providing discriminating information on dye characterization and possibly identification of dyes at the molecular level from trace evidence fibers as small as 0.5 mm.*

Extraction methods developed for basic dyes on acrylic, acid dyes on nylon, and disperse dyes on polyester fibers involve extraction with solvents that do not affect the chemical composition of the polymer, and thus do not impose limitations on use of the fiber for further examinations. With these fibers, IR can be conducted on previously extracted samples if needed. Reactive dye

extraction from cotton requires base hydrolysis with sodium hydroxide which can change the chemical form of the dye and modify the fiber polymer chemistry; strongly alkaline solutions are also not compatible with C18 stationary phases for liquid chromatography. Previous research employed 1.5% NaOH which does cause damage. In this work, 0.1875 M sodium hydroxide was employed and the resulting chromatograms showed no evidence of chemical products from cellulose.

The second issue mentioned in the NAS report requires consistent attention to validation.<sup>7</sup> "Validate" is an active verb that demands due diligence to sources of measurement uncertainty during validation and monitoring of measurement process to identify the inevitable rise of entropy during routine applications. Validated measurements judged by fitness for use and based on good science are the answer to Daubert issues such as scientific validity and error rate. *The research we have conducted is targeted at understanding the scientific basis, establishing the validity, and translating new discriminating methods for forensic fiber examinations into forensic laboratory practice.*

### References:

1. Oien, C. T. *Case management issues from crime scene to courtroom*. Trace Evidence Symposium, Clearwater, FL, 2007 [URL: <http://nfstc.org/projects/trace/>].
2. Fisher, J. *Forensics under Fire: Are Bad Science and Dueling Experts Corrupting Criminal Justice?* Rutgers University Press: New Brunswick, NJ, 2008.
3. Kelly, J. F.; Wearner, P. K. *Tainting Evidence: Inside the Scandals at the FBI Crime Lab*, The Free Press: New York, 1998.
4. National Research Council of the National Academies. *Strengthening Forensic Science in the United States: A Path Forward*, The National Academies Press: Washington, DC, 2009.
5. Palenik, S. In: Robertson J, Grieve M (eds) *Forensic examination of fibres*, 2nd ed., Taylor & Francis, London, 1999, 364-378.
6. Stoeffler, S. F. *J. Forensic Sci.* **1996**, *41*: 297-299.
7. Houck, M. "Statistics and trace evidence: the tyranny of numbers," *Forensic Science Communications*, 1 January 1999.

### Implications for further research

We have begun to address the issue (c) cited on p. 136. Our laboratory previously created a large and representative collection of environmentally weathered fabrics that we have analyzed, and for which initial fiber dye analysis results are included in the Accomplishments section of this report. We will collect the UV/visible and mass spectra from this project into suitable databases that can be made publicly available.

A third year graduate, Molly Burnip, is currently working as an intern with Dr. Wendy Bell (Capt., SLED, Toxicology) and Jennifer Stoner (Lt., SLED Trace Dept.) at the SC State Law Enforcement Division Forensic laboratory. Our difficulties in working with SLED have been documented in previous reports. This work is ongoing at this time, and we now have access to a new SLED LC/MS instrument and Molly is working with the trace lab on sample preparation and with examiner in the toxicology laboratory to implement LC/MS analysis of dye extracts and to conduct validation experiments meeting the laboratory accreditation standards. When not working at SLED, Molly is continuing to analyze weathered fiber samples in an effort to perform LC/MS analysis of weathered samples from SLED inventory. We will also be completing our

work on statistical tolerance intervals, preparing talks, and editing the papers in this report for publication.

## **Dissemination of research findings**

### **Progress reports**

Six-monthly progress reports to the National Institute of Justice are up-to-date and approved. A final six-month project report from 1 January 2014-30 June 2014 will complete these progress reports.

### **Scientific meeting presentations**

The following oral presentations have been made at scientific meetings and workshops during this current project, for which NIJ was acknowledged for full support. Abstracts in meeting proceedings were published for all of these presentation.

1. Oscar Cabrices, Anthony R. Trimboli, James E. Hendrix, and Stephen L. Morgan, "Liquid chromatography/mass spectrometry investigations of dye and fiber degradation resulting from environmental exposure," paper A181, Criminalistics section, American Academy of Forensic Sciences, Annual Meeting, Chicago, IL, 24 February 2011.
2. Stephen L. Morgan, Oscar G. Cabrices, Scott J. Hoy, and James E. Hendrix, "Forensic discrimination of dyed textile fibers using UV/visible microspectrophotometry and micro-extraction/liquid chromatography/mass spectrometry," paper submitted to the California Association of Criminalist spring meeting 2011, Long Beach, CA, 18 May 2011.
3. Stephen L. Morgan, Oscar G. Cabrices, and Scott J. Hoy, "Forensic Characterization and Chemical Identification of Dyes Extracted from Millimeter-length Fibers," invited poster, FBI/NIJ Trace Evidence Symposium: Science, Significance, and Impact, Kansas City, KS, 10 August 2011.
4. Stephen L. Morgan, Oscar G. Cabrices, Scott J. Hoy, James E. Hendrix, "Forensic analysis of dyes on trace evidence fibers by liquid chromatography, paper presented at the Federation of Analytical Chemistry and Spectroscopy Societies, Annual Meeting, 4 October 2011.
5. Stephen L. Morgan, Oscar G. Cabrices, Scott J. Hoy, Andrei Kovaltshuk, Molly R. Burnip, and Nicholas M. Riley, "Forensic Characterization and Identification of Dyes Extracted from Millimeter-length Fibers using Ultra-Performance Liquid Chromatography/Mass Spectrometry," paper A151 presented at the American Academy of Forensic Sciences, Annual Meeting, Atlanta, GA, 20-25 February 2012.
6. Scott J. Hoy, Molly R. Burnip, Stephen L. Morgan, "Microextraction and ultra performance liquid chromatography for dye profile analysis from millimeter-length trace evidence cotton fibers," poster presented at the 2012 Graduate Student Poster Competition, Department of Chemistry and Biochemistry, Columbia, SC, 3 March 2012.
7. Scott J. Hoy, Molly R. Burnip, and Stephen L. Morgan, "Validation of Forensic Characterization and Chemical Identification of Dyes from Millimeter-length Fibers," poster presented at The NIJ Conference 2012, Arlington, VA, 19 June 2012.
8. Scott J. Hoy, Molly R. Burnip, and Stephen L. Morgan, poster to be presented at the American Chemical Society POLY/PMSE Student Chapter Poster Competition and Industrial Networking Event, University of South Carolina, Columbia, SC 10 August 2012
9. Stephen L. Morgan, Scott J. Hoy, Molly R. Burnip, and Oscar G. Cabrices, "Ultra Performance Liquid Chromatography and Mass Spectrometry for Forensic Characterization

- of Dyes Extracted from Millimeter-length Textile Fibers," invited paper in forensic session chaired by Charles Wilkins, SCIX 2012, sponsored by the Federation of Analytical Chemistry and Spectroscopy Societies, Kansas City, MO, 2 October 2012.
10. Scott J. Hoy, Molly R. Burnip, and Stephen L Morgan, "Forensic profiling of dye extracts from millimeter-length cotton fibers using ultra performance liquid chromatography and mass spectrometry," poster at SCIX 2012, sponsored by the Federation of Analytical Chemistry and Spectroscopy Societies, FACSS, Kansas City, MO, 30 September-5 October 2012.
  11. Scott J. Hoy, Molly R. Burnip, Stephen L. Morgan, Wendy C. Bell, Tracy A. McKinnon, and Jennifer M. Stoner, "Microextraction and analysis of direct and reactive dye formulations from cotton fibers using ultra-performance liquid chromatography and mass spectrometry," paper 2190-18P at the Pittsburgh Conference on Analytical Chemistry and Applied Spectroscopy, Philadelphia, PA, 20 March 2013.
  12. Molly R. Burnip, Kaylee R. McDonald, Scott J. Hoy, Stephen L. Morgan, Validation of UPLC/MS methods for trace analysis of dyes extracted from acrylic, nylon and polyester fibers, oral paper at SCIX 2013 (sponsored by FACSS), Milwaukee, WI, 30 Sept.-4 Oct. 2013.
  13. Kaylee R. McDonald, Molly R. Burnip, Scott J. Hoy, and Stephen L. Morgan, Limits of detection from the viewpoint of statistical hypothesis testing, poster at SCIX 2013 (sponsored by FACSS), Milwaukee, WI, 2 Oct. 2013.
  14. Kaylee R. McDonald, Molly R. Burnip, Scott J. Hoy, and Stephen L. Morgan, Validation of liquid chromatography methods for trace analysis of dyes extracted from acrylic, cotton, nylon, and polyester fibers using UV/visible and mass spectrometric detection," poster at paper A142 presented at the American Academy of Forensic Sciences, Annual Meeting, Seattle, WA, 21 February 2014.

Dr. Morgan organized and is chairing a session on "Data Analysis in Forensics" at the 2014 SCIX meeting (Reno, NV), and is speaking on validation statistics work. A proposal for a full-day Forensic Analytical Chemistry Symposium to be held next March at PittCon 2015 (New Orleans) has also been approved, organized by Dr. Jose Almirall, Dr. Morgan, and Dr. Igor Lednev. These venues for formal scientific presentations offer prime-time recognition for forensic analysis chemistry research funded by NIJ.

#### **Presentations at other venues (universities, high schools, organizations, etc.)**

15. Stephen L. Morgan, "Every contact leaves a trace: Forensic analytical chemistry and CSI" invited talk at the Gamma Sigma Chemistry Club, spring induction ceremonies, Catawba College, Salisbury, NC, 27 April 2011.
16. Stephen L. Morgan, "Every contact leaves a trace: Forensic analytical chemistry and CSI" invited talk at Strom Thurmond High School, Johnston, SC, 25 May 2011.
17. Graduate student Oscar Cabrices gave a presentation, "UPLC diode array and mass spectrometric analysis of extracted textile dyes," to members of the Trace Evidence and Forensic Toxicology Sections of the Forensic Services Laboratory, State Law Enforcement Division (SLED), Columbia, SC, 15 June 2011.
18. Andrei Kovaltshuk and Nicholas M. Riley (with Molly R. Burnip and Stephen L. Morgan), "Forensic characterization and chemical identification of dyes extracted from millimeter-

length fibers," poster presented at the University of South Carolina Undergraduate Discovery Day poster competition, 20 April 2012.

19. Stephen L. Morgan, Michael L. Myrick, Eric M. Breitung, "Analytical Chemistry Research for Forensic and Cultural Heritage Decision-Making," invited seminar, Department of Chemistry, University of South Carolina, Columbia, SC 18 January 2013.
20. Stephen L. Morgan, Analytical Chemistry for Forensic Trace Analysis and Crime Scene Blood Imaging, invited seminar at the University of Mississippi, Oxford, MI, 28 March 2013.
21. Stephen L. Morgan, Analytical Chemistry for Forensic Trace Analysis of Fibers and Imaging Blood at Scene Crimes, invited seminar at the University of Albany (SUNY), Albany, NY, 30 April 2013.

### **Publications in print**

None at this time.

### **Publications accepted or submitted for publication**

None at this time, the manuscripts presented in the Accomplishments section are being prepared for submission.

### **Manuscripts in preparation for publication**

- (a) Scott J. Hoy, Molly R. Burnip, Kaylee R. McDonald, Oscar G. Cabrices, and Stephen L. Morgan, Comprehensive screening of acid, basic, and disperse dyes extracted from millimeter-length trace evidence fibers by ultra-performance liquid chromatography: methodology and figures of merit.
- (b) Scott J. Hoy, Molly R. Burnip, Kaylee R. McDonald, and Stephen L. Morgan, Extraction of direct dyes and indigo vat dye from trace cotton fibers for forensic characterization by ultra-performance liquid chromatography.
- (c) Scott J. Hoy, Molly R. Burnip, and Stephen L. Morgan, Extraction and characterization of reactive dyes and their hydrolysis products from trace cotton fibers by ultra-performance liquid chromatography.
- (d) Molly R. Burnip, Oscar G. Cabrices, Anthony R. Trimboli, Micheline Goulart, James E. Hendrix, and Stephen L. Morgan, Forensic Analysis of Fluorescent Brighteners, Dyes and Textile Fiber Degradation by Capillary Electrophoresis, Liquid Chromatography/Mass Spectrometry, and Ultra Performance Liquid Chromatography.
- (e) Scott J. Hoy, Molly R. Burnip, Stanley N. Deming and Stephen L. Morgan, Mandel sensitivity applied to analytical method performance comparisons and limits of detection.
- (f) Kaylee R. McDonald, Molly R. Burnip, Scott J. Hoy, and Stephen L. Morgan, Limits of detection from the viewpoint of statistical hypothesis testing.

### **Graduate and undergraduate research students supported by this grant**

Four graduate students have been supported by this project. Two of these graduate students have completed Ph.D. degrees in Chemistry as a result of working on this project:

Oscar G. Cabrices, Ph.D., Analytical Chemistry, University of South Carolina, August 2011, Forensic analysis of trace evidence fibers and drugs of abuse in biological matrices using chromatographic and mass spectrometric methods." Oscar is presently technical applications scientist at Gerstel, Inc, Baltimore, MD.

Scott J. Hoy Ph. D., Analytical Chemistry, University of South Carolina, August 2013,

"Development and Figures of Merit of Microextraction and Ultra-Performance Liquid Chromatography for Forensic Characterization of Dye Profiles on Trace Acrylic, Nylon, Polyester, and Cotton Textile Fibers." 10 August 2013. Scott is presently Senior Chemist at ExxonMobil, Baytown, TX.

Two graduate students have worked on the project during the last year:

Molly R. Burnip, is currently a third year graduate student at USC, and has worked on method development and validation.

Kaylee R. McDonald, is currently a third year graduate student at USC, and has worked on method validation issues.

Undergraduate research students working on this project include:

Molly R. Burnip (B. S., Chemistry, 2012) worked as an undergraduate researcher, 2011-2012. She graduated with Phi Beta Kappa honors in Chemistry. Molly is currently a second year graduate student at USC who has continued to work on the project for her Ph. D. dissertation research.

Nicholas M. Riley (B.S. Chemistry, 2012), was a Fulbright Scholar finalist, partially based on LC/MS dye analysis research. Nick won the highest student leadership award at USC (Algernon Sydney Sullivan Award, 2012), and graduated with Phi Beta Kappa honors in Chemistry. Nick is a second year chemistry graduate student at the University of Wisconsin, Madison, WI, working on mass spectrometry, proteomics, and quantitative systems biology in the laboratory of Professor Joshua J. Coon.

Andrei Kovaltshuk (now Andrew Green) won a USC Magellan Scholar Award of \$3,000 that paid him to work in my laboratory on "Forensic Characterization of Dye Extracts from Millimeter-Length Textile Fibers," during 2011. Andrei graduated with Magna cum Laude honors in Chemistry. Andrei is a second year graduate student in chemistry at the University of California-Riverside, Riverside, CA, working on mass spectrometric instrumentation design.